VOL. 11 NO. 6 JUNE 1966
PUBLISHED MONTHLY
Completing Vol. 11

Journal of

ELECTROANALYTICAL CHEMISTRY

International Journal Dealing with all Aspects of Electroanalytical Chemistry, Including Fundamental Electrochemistry

ELSEVIER

GENERAL INFORMATION

See also Suggestions and Instructions to Authors which will be sent free, on request to the Publishers.

Types of contributions

(a) Original research work not previously published in other periodicals.
(b) Reviews on recent developments in various fields.
(c) Short communications.
(d) Bibliographical notes and book reviews.

Languages

Papers will be published in English, French or German.

Submission of papers

Papers should be sent to one of the following Editors:

Professor J. O'M. Bockris, John Harrison Laboratory of Chemistry, University of Pennsylvania, Philadelphia 4, Pa. 19104, U.S.A.
Dr. R. Parsons, Department of Chemistry, The University, Bristol 8, England.
Professor C. N. Reilley, Department of Chemistry, University of North Carolina, Chapel Hill, N.C. 27515, U.S.A.

Authors should preferably submit two copies in double-spaced typing on pages of uniform size. Legends for figures should be typed on a separate page. The figures should be in a form suitable for reproduction, drawn in Indian ink on drawing paper or tracing paper, with lettering etc. in thin pencil. The sheets of drawing or tracing paper should preferably be of the same dimensions as those on which the article is typed. Photographs should be submitted as clear black and white prints on glossy paper.
All references should be given at the end of the paper. They should be numbered and the numbers should appear in the text at the appropriate places.
A summary of 50 to 200 words should be included.

Reprints

Twenty-five reprints will be supplied free of charge. Additional reprints can be ordered at quoted prices. They must be ordered on order forms which are sent together with the proofs.

Publication

The *Journal of Electroanalytical Chemistry* appears monthly and has six issues per volume and two volumes per year.

Subscription price: £ 12.12.0 or $ 35.00 or Dfl. 126.00 per year; £ 6.6.0 or $ 17.50 or Dfl. 63.00 per volume plus postage (per year): 8s. 6d. or $1.25 or Dfl. 4.20.
Additional cost for copies by air mail available on request.
For advertising rates apply to the publishers.

Subscriptions

Subscriptions should be sent to:

ELSEVIER PUBLISHING COMPANY, P.O. Box 211, Amsterdam, The Netherlands.

ON THE DETERMINATION OF KINETIC PARAMETERS FROM POTENTIAL-STEP AND VOLTAGE-STEP MEASUREMENTS

K. B. OLDHAM* AND R. A. OSTERYOUNG
North American Aviation Science Center, Thousand Oaks, California (U.S.A.)
(Received July 23rd, 1965)

Two techniques by which rate constants of fast electrode reactions have been measured are the potential-step method and the voltage-step method[1]. In both methods an initial equilibrium state of the electron-transfer reaction

$$\mathrm{Ox} + ne^- \rightleftarrows \mathrm{Rd} \tag{1}$$

is perturbed at time $t=0$ by a sudden change $E_1 \rightarrow E_2$ in the applied potential. The current resulting from this perturbation is then followed as a function of time and from the characteristics of this changing current, the standard rate constant k_s can be determined. The two methods differ in the magnitude of the step $(E_1 - E_2)$ and in its point of application.

In the potential-step method, the change $E_1 \rightarrow E_2$ is applied directly across the electrode by means of an electronic potentiostat. Assuming that the current is determined solely by semi-infinite linear diffusion and by the first-order kinetics of reaction (1), the current–time relationship may be shown[2] to be

$$i = nAFk_s \exp\left\{\frac{-\alpha nF(E_2-E_s)}{RT}\right\}\left[\bar{C} - \bar{C}' \exp\left\{\frac{nF(E_2-E_s)}{RT}\right\}\right] \exp\{\lambda_1^2 t\} \operatorname{erfc}\{\lambda_1\sqrt{t}\} \tag{2}$$

where

$$\lambda_1 = \frac{k_s}{\sqrt{D}} \exp\left\{\frac{-\alpha nF(E_2-E_s)}{RT}\right\}\left[1 + \sqrt{\frac{D}{D'}} \exp\left\{\frac{nF(E_2-E_s)}{RT}\right\}\right] \tag{3}$$

and where other symbols have been defined. Note that since E_2 is invariant, λ_1 is constant, as are all the terms on the right-hand side of (2) other than the two final factors.

In the voltage-step method, the change $E_1 \rightarrow E_2$ is applied, not to the electrode, but across the series combination of the cell and its current-measuring resistor. Moreover, the step has a magnitude equal to a small fraction of RT/nF, *i.e.*, of only a few millivolts. Under these conditions, the current is given, to a good approximation, by[3]

$$i = \frac{(E_1 - E_2) \exp\{\lambda_2^2 t\} \operatorname{erfc}\{\lambda_2\sqrt{t}\}}{\varrho + \dfrac{RT}{n^2 A F^2 k_s \bar{C}^{1-\alpha}\bar{C}'^{\alpha}}} \tag{4}$$

* Permanent address: University of Newcastle upon Tyne, England.

where ϱ is the total resistance and

$$\lambda_2 = \left[\frac{1}{\frac{1}{k_s \bar{C}^{1-\alpha} \bar{C}'^{\alpha}} + \frac{n^2 A F^2 \varrho}{RT}}\right]\left[\frac{1}{\bar{C}\sqrt{D}} + \frac{1}{\bar{C}'\sqrt{D'}}\right] \tag{5}$$

Again, all terms in eqn. (4) are constant apart from the exp and erfc factors, and λ_2 is also invariant.

The chronoamperometric equation for both methods is seen to be basically

$$i = i_0 \exp\{\lambda^2 t\} \operatorname{erfc}\{\lambda\sqrt{t}\} \tag{6}$$

where i_0 is the initial current. Since k_s enters into the expressions for both i_0 and λ, measurement of either of these parameters will enable the rate constant to be determined. However, as will be shown below, the content of kinetic information is greatest at short times and therefore more accurate k_s values are to be expected from i_0 than from λ. In practice, k_s has usually been determined from i_0, although both parameters have been studied in some similar investigations[4].

It may be shown that i contains appreciable kinetic information only at sufficiently short times. This is evident by noting that for either method an alternative form for eqn. (6) is

$$i = \varphi\lambda \exp\{\lambda^2 t\} \operatorname{erfc}\{\lambda\sqrt{t}\} \tag{7}$$

where φ is independent of k_s and α. Thus since

$$\lim_{\xi\to\infty}[\xi \exp \xi^2 \operatorname{erfc} \xi] = \frac{1}{\sqrt{\pi}} \tag{8}$$

we see that

$$\lim_{\lambda\sqrt{t}\to\infty}[i] = \frac{\varphi}{\sqrt{\pi t}} = i_{\text{lim}} \tag{9}$$

and is independent of the kinetics. We can regard the ratio

$$S = \frac{i_{\text{lim}} - i}{i_{\text{lim}}} = 1 - \lambda\sqrt{\pi t} \exp\{\lambda^2 t\} \operatorname{erfc}\{\lambda\sqrt{t}\} \tag{10}$$

TABLE 1

Certain important functions of ξ, *viz.*: Column 2 = $\exp \xi^2 \operatorname{erfc} \xi$; Column 3 = $1 - \sqrt{\pi}\, \xi \exp \xi^2 \operatorname{erfc} \xi$, *i.e.*, the value of S (eqn. 10) for $\xi = \lambda\sqrt{t}$; Column 4 = $100\left[1 - \frac{(\sqrt{\pi} - 2\xi) \exp\{-\xi^2\}}{\sqrt{\pi} \operatorname{erfc} \xi}\right]$, *i.e.*, the % difference between column 2 and the approximation given by eqn. (11).

ξ	*Column 2*	*Column 3*	*Column 4*	ξ	*Column 2*	*Column 3*	*Column 4*
0	1.000000	1.00000	0.00	0.70	0.525931	0.34736	60.05
0.05	0.945990	0.91616	0.25	1.00	0.427585	0.24219	130.02
0.10	0.896457	0.84111	1.04	1.50	0.321584	0.14501	315.37
0.15	0.850936	0.77376	2.37	2.00	0.255396	0.09465	592.30
0.20	0.809019	0.71321	4.29	3.00	0.179001	0.04819	1432.48
0.25	0.770347	0.65865	6.48	4.00	0.136999	0.02870	
0.30	0.734599	0.60939	9.95	5.00	0.110705	0.01890	
0.40	0.670788	0.52442	18.21	7.00	0.079800	0.00991	
0.50	0.615690	0.45436	29.22	10.00	0.056141	0.00493	

as defining the fraction of the current which is kinetically determined. Table 1 incorporates a column enabling S to be found for representative values of $\lambda\sqrt{t}$.

Direct observation of i_0 is prevented by experimental difficulties and by the double-layer charging current which was ignored in the derivation of the above equations. This current is additive to the faradaic current i, but decays more rapidly than does i, becoming negligible at times longer than a few times the product of the double layer capacitance and the resistance with which it is in series. If we denote by τ_φ the time after which charging current may be ignored, data collected during $t \geqslant \tau_\varphi$ may be used to obtain i_0 by a back extrapolation of a plot of i *versus* some convenient function of time. This extrapolation is made to $t=0$, or, better, to some positive time $t=\tau_e$ so as to correct for non-faradaic current[5,6].

Since for small values of its argument ξ,

$$\exp \xi^2 \operatorname{erfc} \xi \approx 1 - \frac{2\xi}{\sqrt{\pi}} \tag{11}$$

the most convenient function of time against which to plot i for extrapolation purposes is its square root. This is the basis of the standard procedure of graphing i *vs.* $\sqrt{t}$, selecting the near-linear initial section and extrapolating it to find i_0. The purpose of the present communication is to show that these extrapolations have not always been wisely made and to suggest methods of avoiding this difficulty.

Table 1 shows that the expression

$$i = i_0(1 - 2\lambda\sqrt{\frac{t}{\pi}}) \tag{12}$$

yields i-values differing from those generated by eqn. (6) by 1% or less, only if

$$\lambda\sqrt{t} \leqslant 0.1 \tag{13}$$

In other words, a plot of i *vs.* $\sqrt{t}$ is linear to better than 1% provided inequality (13) is satisfied. The necessity for satisfying this inequality, or one similar (*e.g.*, $\lambda\sqrt{t} \leqslant 0.2$ suggested by OKINAKA, TOSHIMA AND OKANIWA[7], corresponding to a departure from linearity of about 5%) has been appreciated by all workers in the field, but not all have realized that (13) also implies

$$\frac{i}{i_0} \geq 0.9 \tag{14}$$

(or $i/i_0 \geqslant 0.8$, taking the less stringent alternative of OKINAKA, TOSHIMA AND OKANIWA) as is evident from Table 1 and as was clearly stated by GERISCHER[8].

Let us consider that the results of a step-method experiment are plotted as points on an i *vs.* $\sqrt{t}$ graph (see Fig. 1). The first few points may be exalted on account of a non-faradaic contribution to the current. Following these, there may be a number of points which are considered to adequately delineate a straight line. Let i_y be the last such point and let a straight line be drawn through the colinear points and extrapolated back to give i_x (Fig. 1). Now, from inequality (14) it may be shown that only if

$$\frac{i_x - i_y}{i_y} \leq 0.11 \tag{15}$$

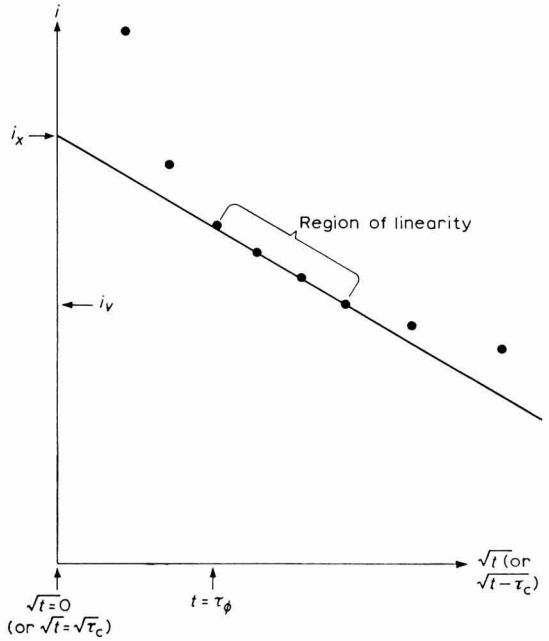

Fig. 1. Typical chronoamperometric data points; i_r is the current at the last colinear point.

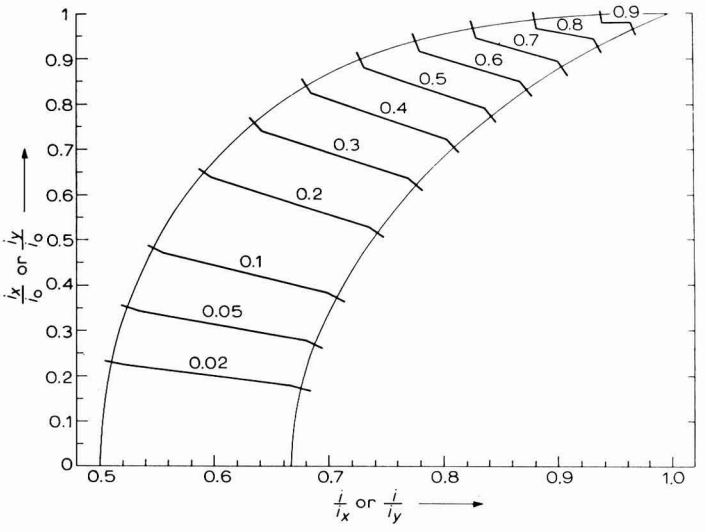

Fig. 2. The upper curve shows i_x/i_0 as a function of i/i_x. The lower curve shows i_y/i_0 as a function of i/i_y. The upper curve has the lines $i_x/i_0 = 1$ and $i/i_x = \frac{1}{2}$ as tangents at its limits. The corresponding tangential lines for the lower curve are $i_y/i_0 = i/i_y$ and $i/i_x = \frac{2}{3}$. The markers shown along each line indicate the points at which S acquires the stated values. S has the values of unity and zero at the ends of each curve. Interestingly, S is almost a linear function of i/i_x or i/i_y, so that interpolation along this axis is very accurate.

(or $i_x - i_\nu \leqslant 0.25\, i_\nu$ using the less stringent condition) is i_x a valid approximation to i_0, *i.e.*, the extrapolation should traverse a current span not exceeding 11% (or 25%) of the lowest datum encompassed by the straight line. We know of no published extrapolations in which this 11% criterion has even been approached; more usually[5,9] extrapolations traverse about 100% of i_ν and in one extreme case[7], a 300% extrapolation was employed. In these cases the values of i_x and i_0 are not even approximately equal.

We strongly urge that criterion (14) be used in place of (13). Inequality (13) is extremely treacherous in that λ is not known *a priori*. Reliance on an unsound extrapolation will lead to an underestimation of i_0 and hence of k_s. The use of this false k_s to calculate λ may produce a value of the latter which deceptively satisfies (13) and so apparently validates the extrapolation. We believe OKINAKA, TOSHIMA AND OKANIWA to have been victims of this insidious circumstance.

The function $\exp \xi^2 \operatorname{erfc} \xi$ never displays more than slight curvature *versus* ξ in the domain $0 > \xi > \infty$ and therefore values of i determined over a short range of $\sqrt{t}$ appear approximately linear and may be extrapolated without difficulty to find i_x. If we identify the extrapolation with the tangent to the curve at the ordinate value i, it is easily demonstrated that

$$\frac{i_x}{i_0} = (1 - 2\lambda^2 t)\,\frac{i}{i_0} + 2\lambda\sqrt{\frac{t}{\pi}} \tag{16}$$

Equations (6) and (16) may be regarded as defining a unique relationship between the two ratios i_x/i_0 and i/i_x; Fig. 2 includes a graph of this relationship. The figure also shows how, as i/i_x declines S decreases to zero, *i.e.*, the kinetic content eventually vanishes.

Notice that provided $i/i_x \geqslant 0.75$, i_x will be within 10% of i_0. For a longer extrapolation, Fig. 2 can be used to find i_0 from known values of i and i_x. This provides a powerful method for the determination of i_0 since, in principle, it may be applied at any point along the i *vs.* $\sqrt{t}$ graph. In practice, very short times are excluded because of the double-layer charging interference and very long times are affected by the decreasing value of S which accompanies increasing time. A decrease in S does not invalidate the method, but does demand increased precision in the data. Thus, a

TABLE 2

APPLICATION OF THE FIRST METHOD TO THE DATA OF VIELSTICH AND GERISCHER[9]

i/A (mA cm^{-2})	i_x/A	i/i_x	i_x/i_0	i_0/A (mA cm^{-2})	
1.40	1.96	0.714	0.870	2.25	
1.30	1.89	0.688	0.851	2.22	
1.20	1.78	0.674	0.831	2.14	Mean
1.10	1.68	0.655	0.800	2.10	=
1.00	1.60	0.625	0.740	2.16	2.20
0.90	1.50	0.600	0.678	2.21	
0.80	1.39	0.576	0.602	2.31	
0.70	1.28	0.547	0.482	2.65	
0.60	1.13	0.531	0.400	2.82	
0.50	0.97	0.515	0.276	3.52	
0.40	0.68	0.588	0.644	1.06	

value of i_0 determined by an extrapolation from $i/i_x = 0.73$, where $S = 0.5$, will be ten times as accurate as an i_0-value from a tangent at $i/i_x = 0.525$, where $S = 0.05$ only.

In Table 2 we show the application of this method to the potential-step data of VIELSTICH AND GERISCHER[9] for the reaction

$$Zn^{2+} + 2\,e \rightleftarrows Zn(Hg)$$

in molar aqueous sodium perchlorate. The tabulated values relate to $E_1 - E_2 = 0.020$ V and $\bar{C} = 2.1 \times 10^{-6}$ mole cm^{-3}. i_x-values were determined by drawing tangents at current values, i, to a smooth curve of the published experimental points on an i *vs.* $\sqrt{t}$ plot and extrapolating to $t = 0$. Knowing i/i_x, values of i_x/i_0 were read off from Fig. 2 and hence i_0 was computed from each of eleven tangents. Except at long times (currents less than one-third of i_0 and hence S less than 0.1) the method is seen to yield i_0-values which are highly reproducible (possibly fortuitously more reproducible than might be expected). We believe the value 2.2 mA cm^{-2} to be much more accurate and reliable than is possible from a single extrapolation technique. The extrapolation shown in the published graph[9] yields $i_0 = 1.67$ mA cm^{-2}. Notice that the data in Table 2 show no evidence of interference from charging current; no such interference is to be expected on the time scale of the experiment.

Figure 2 shows that

$$\frac{i}{i_x} \not< \frac{1}{2} \tag{17}$$

i.e., the extrapolation can never traverse a current range greater than the current at which the tangent was drawn. It therefore appears that the data for copper and cadmium deposition presented[7] by OKINAKA, TOSHIMA AND OKANIWA, and which violate inequality (17), are invalid, notwithstanding the agreement with established k_s-values which these authors find.

One drawback to the method described above—we shall term it the "first method"—is that, before it can be applied, the experimental i *vs.* t data must be replotted as i *vs.* $\sqrt{t}$. Not only is this inconvenient, but precision is lost in transcribing the data. We now describe a "second method" to obviate these difficulties. We wish to stress that our second method does not differ in basis from the technique described by GERISCHER[8], although we believe the application of our method to be more straightforward.

If tangents are drawn to an i *vs.* t graph and extrapolated to $t = 0$ (or to $t = \tau_c$), the intercept i_y may be shown to be given by

$$\frac{i_y}{i_0} = (1 - \lambda^2 t)\frac{i}{i_0} + \lambda\sqrt{\frac{t}{\pi}} \tag{18}$$

where (t,i) are the coordinates of the point at which the tangent was drawn. Notice that this expression for i_y differs from that for i_x (eqn. (16)) only by the presence of factors of 2 in the latter. The relationship between i_y/i_0 and i/i_y may be depicted graphically as was done for the first method; Fig. 2 shows the results. Notice that, whereas i/i_x can take values between $\frac{1}{2}$ and 1,

$$\frac{2}{3} \leq \frac{i}{i_y} \leq 1 \tag{19}$$

We have attempted to apply this method to the published data of LAITINEN, TISCHER AND ROE[5] on the application of the voltage-step method to the reaction

$$V(III) + e^- \rightleftarrows V(II)$$

in fused KCl–LiCl eutectic. Tangents to the experimental i *vs.* t curve[11] were drawn and extrapolated to $t = 9$ μsec, to give the values listed as i_y in Table 3. The value $\tau_c = 9$ μsec is that established by the authors[5] as the appropriate correction for double-layer charging. Notice that for $i < 45$ μA the ratio i/i_y lies within the range $0.667 \leqslant i/i_y \leqslant 0.700$. For this range, as Fig. 2 shows, $0 \leqslant S \leqslant 0.08$, so that for these data to

TABLE 3

APPLICATION OF THE SECOND METHOD TO THE DATA OF LAITINEN, TISCHER AND ROE[5]

i (μA)	i_y	i/i_y	i (μA)	i_y	i/i_y
70.0	79.3	0.883	37.5	54.8	0.684
65.0	76.6	0.848	35.0	50.2	0.698
60.0	74.8	0.802	32.5	48.1	0.676
55.0	71.1	0.773	30.0	43.4	0.691
50.0	67.1	0.745	27.5	39.8	0.692
45.0	62.6	0.718	25.0	37.2	0.673
40.0	57.0	0.702	22.5	33.9	0.665

TABLE 4*

APPLICATION OF THE SECOND METHOD TO THE DATA OF GERISCHER[8]

i	i_y	i/i_y	i_y/i_0	i_0
32.81	37.9	0.866	0.818	46.3
30.07	35.7	0.842	0.763	46.8
27.34	34.0	0.804	0.691	49.2
24.61	30.8	0.799	0.678	45.4
21.87	28.8	0.759	0.570	50.6
19.14	25.4	0.754	0.553	45.9
16.40	22.6	0.726	0.455	49.6
			Mean =	47.7
			σ =	2.1

* Currents in arbitrary units

contain significant kinetic information would demand a precision beyond that obtainable by the method. The scatter observed in i/i_y at this end of Table 3 is further evidence that these data are not significantly different from the 0.667 limit. For $i > 40$ μA, the ratio i/i_y does shift in the expected direction in a regular fashion. However, in this region the current contains a non-faradaic component which is far from negligible[5,10], so that none of the foregoing relationships is applicable. We are forced to the conclusion that the data of these authors cannot be used to determine kinetic parameters in the absence of a quantitative treatment of the effect of simultaneous faradaic and non-faradaic currents in the voltage-step method. It should be mentioned that changing the value of τ_c does not affect our conclusion on the validity of this experimental determination of k_s.

Finally, we show in Table 4 the result of applying the second method to the data

of GERISCHER[8] for the reaction

$$Cd(CN)_3^- + 2\,e^- \rightleftarrows Cd(Hg) + 3\,CN^-$$

We have analyzed the curve for a cyanide concentration of $2 \cdot 10^{-5}$ mole cm^{-3} published in Fig. 6 in GERISCHER's article. Our results are in Table 4 and show how, with suitable data, the method can yield an i_0-value with a standard deviation of only 4%.

NOTATION

A	surface area of working electrode (cm^2)
$\bar{C}$	bulk concentration of Ox (mole cm^{-3})
$\bar{C}'$	bulk concentration of Rd (mole cm^{-3})
D	diffusion coefficient of Ox (cm^2 sec^{-1})
D'	diffusion coefficient of Rd (cm^2 sec^{-1})
E_s	standard potential of the Ox/Rd system (V)
E_1	applied potential at $t < 0$ (V)
E_2	applied potential at $t > 0$ (V)
F	Faraday's constant (9.65×10^4 C equiv.$^{-1}$)
Ox	an electroreducible species
R	gas constant (8.31 J mole^{-1} deg^{-1})
Rd	reduction product of Ox
S	a ratio defined by eqn. (10)
T	absolute temperature (°K)
e^-	an electron
exp	exponential operator, $\exp \xi \equiv (2.718\ldots)^{\xi}$
erfc	error function complement operator, $\operatorname{erfc} \xi \equiv \frac{2}{\sqrt{\pi}} \int_{\xi}^{\infty} \exp\{-u^2\}\, du$
i	faradaic current (A)
$i_{\lim}$	value of i were k_s infinite (A)
i_0	initial value of i (A)
i_x	intercept determined by extrapolation of an i *vs.* $\sqrt{t}$ graph (A)
i_y	intercept determined by extrapolation of an i *vs.* t graph (A)
i_r	current corresponding to the last linear i *vs.* $\sqrt{t}$ datum (A)
k_s	electron transfer rate constant for reduction of Ox and oxidation of Rd at potential E_s (cm sec^{-1})
n	number of faradays to reduce one mole of Ox (equiv. mole^{-1})
t	duration of electrolysis at applied potential E_2 (sec)
u	an integration variable
α	cathodic transfer coefficient
λ	represents either λ_1 or λ_2 (sec$^{-\frac{1}{2}}$)
λ_1	characteristic parameter of the potential-step method (sec$^{-\frac{1}{2}}$)
λ_2	characteristic parameter of the voltage-step method (sec$^{-\frac{1}{2}}$)
ξ	an arbitrary variable
ϱ	resistance (ohm)
τ_c	effective time-delay to correct for non-faradaic current (sec)
τ_φ	time after which non-faradaic current has decayed to a negligible fraction (sec)
φ	a parameter independent of kinetics (A sec$^{\frac{1}{2}}$)

SUMMARY

An analysis of published data shows that in the determination of rate constants from experimental potential-step and voltage-step measurements, extrapolations have not always been wisely made. Two methods of avoiding the difficulties are proposed and each has been applied to various data.

REFERENCES

1 P. DELAHAY, *Advances in Electrochemistry and Electrochemical Engineering*, Vol. I, Interscience Publishers, N.Y., 1961, chap. 5.
2 H. GERISCHER AND W. VIELSTICH, *Z. Physik. Chem. (Frankfurt)*, 3 (1955) 16.
3 W. VIELSTICH AND P. DELAHAY, *J. Am. Chem. Soc.*, 79 (1957) 1874.
4 J. H. CHRISTIE, G. LAUER AND R. A. OSTERYOUNG, *J. Electroanal. Chem.*, 7 (1964) 60.
5 H. A. LAITINEN, R. P. TISCHER AND D. K. ROE, *J. Electrochem. Soc.*, 107 (1960) 546.
6 K. B. OLDHAM, submitted for publication in *J. Electroanal. Chem.*
7 U. OKINAKA, S. TOSHIMA AND H. OKANIWA, *Talanta*, 11 (1964) 203.
8 H. GERISCHER, *Z. Electrokhem.*, 64 (1960) 29.
9 W. VIELSTICH AND H. GERISCHER, *Z. Physik. Chem. (Frankfurt)*, 4 (1955) 10.
10 D. K. ROE, *Transactions of the Philadelphia Symposium on Electrode Processes*, edited by E. YEAGER, Wiley and Sons, New York, 1961, p. 217.
11 D. K. ROE, Thesis, University of Illinois, 1959.

POLAROGRAPHY OF NEODYMIUM, SAMARIUM, YTTERBIUM AND EUROPIUM IN ACETONITRILE

E. J. COKAL* AND E. N. WISE
Chemistry Department, The University of Arizona, Tucson, Arizona (U.S.A.)
(Received August 23rd, 1965)

INTRODUCTION

In an earlier paper[1] we described the controlled-potential coulometric determination of europium and ytterbium in methanolic solutions. At that time, we noticed that methanol was not a suitable solvent for the coulometry of any of the other lanthanide elements, and was difficult to use even in the case of ytterbium, because of hydrogen evolution from the solvent as the reduction proceeded. Furthermore, the use of methanolic solutions was further complicated by the unexpected phenomenon of co-reduction of ytterbium(III) at the potential required for the reduction of europium(III). Such behavior would not be predicted from the observed half-wave potentials of these ions in methanolic solution. For these reasons, our attention shifted to the use of other non-aqueous solvents as possible media for the coulometric determination of the rare-earth elements, and we wished also to see whether or not the co-reduction occurred in solvents other than methanol.

This paper is mainly concerned with the polarography of the rare earths which are capable of existence as divalent ions in acetonitrile solution. It is the antecedent to a paper in which we describe an extension of the controlled-potential coulometric reduction method to the determination of europium, ytterbium, and samarium in their mixtures which can be accomplished without difficulties arising from co-reductive behavior. KOLTHOFF AND COETZEE[2] have previously described the polarographic behavior of a number of metal ions, including the rare earths, in anhydrous acetonitrile under research-laboratory conditions. The material which we present is a description of the polarography of the latter elements in the analytical laboratory. Accordingly, we have avoided the use of special apparatus such as the dry box and elaborate solution-handling equipment.

The half-wave potentials determined in this work are not as well-defined as those usually found in aqueous-solution polarography because of the irregularity of the current–potential curves. As will be seen later, the effect of added water on the shape of the polarograms is of particular interest in connection with the determination of the half-wave potentials.

APPARATUS

Polarograph

The polarograph used in all investigations is of conventional circuitry. The

* Present address: Chemistry Dept., University of Puget Sound, Tacoma, Washington.

polarizing circuit consists of a motor-driven 10-turn, 200-Ω helipot with scan voltage supplied by dry cells.

The electrolysis current passes through a 500-Ω helipot and a fraction of the voltage drop produced across its terminals is taken as the input to a Hewlett-Packard Model 425-A microvolt-ammeter used as a high impedance d.c. amplifier. The output of this instrument, after suitable attenuation, is recorded by a Sargent Model MR recorder.

Provision is made for measuring the scanning and initial potentials with the Fluke differential voltmeter.

Electrolysis cell

The cell shown in Fig. 1, used in all work described here, is a slightly modified version of that previously used in the authors' work with methanolic solutions[1]. The working anode and cathode compartments are separated by a salt bridge. This change was incorporated to eliminate diffusion and migration of silver ions from the anode into the cathode compartment. The working anode, which is also used as the polarographic counter electrode, is made from a spiral of 16-gauge silver wire. The small anode used as the cathode potential reference electrode is separated from the cathode compartment only by a single sintered-glass disc, since the small current in the reference electrode circuit results in negligible production of silver ions. The electrolyte used in all compartments of the cell is a solution of 0.100 *M* tetraethylammoni-

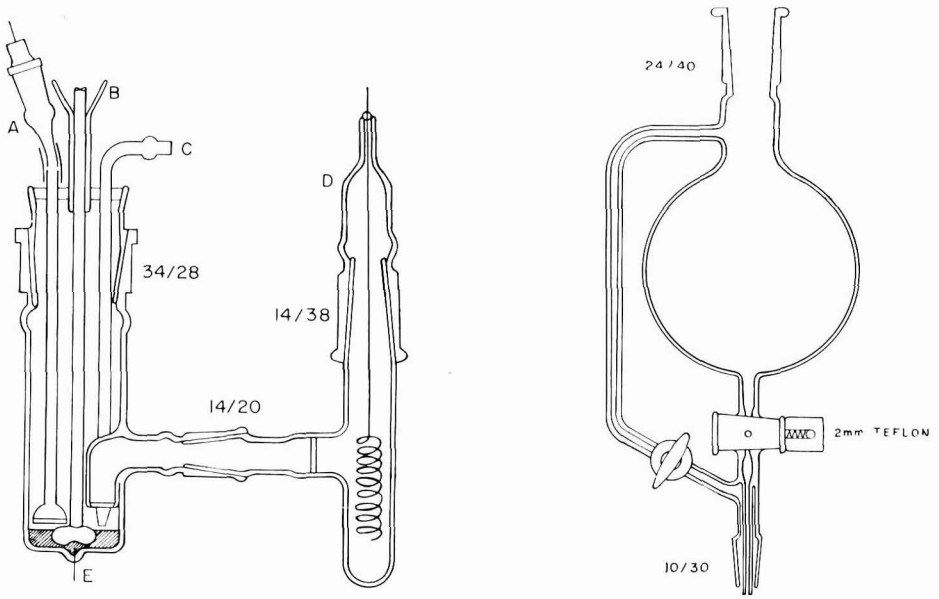

Fig. 1. Cell used for polarography and coulometry in acetonitrile solns. (A), Reference electrode assembly; the silver electrode wire is cemented to the inner part of the 10/18 joint with epoxy-resin cement; the outer part of the joint is connected to the lower tube with Tygon tubing. (B), Bottom part of a mercury seal stirrer. (C), Nitrogen inlet. (D), Counter electrode assembly. (E), Mercury pool electrode.

Fig. 2. Container for anhydrous solvent.

um perchlorate ($TEAClO_4$) in acetonitrile. A dropping mercury capillary (not shown in Fig. 1) is included in the complement of the cell's electrodes.

An external aqueous saturated calomel electrode was used as the ultimate reference potential throughout the investigation.

Thermostat

All the polarographic measurements were made at a constant temperature, usually 25°. This was accomplished by circulation of water from a Sargent "Thermonitor"-controlled constant-temperature water bath which maintained the bath temperature within $\pm 0.01°$ of the desired value.

PREPARATION OF REAGENTS

Acetonitrile

No commercially-available acetonitrile, including two brands of the spectrograde chemical, was found to be of adequate purity for coulometric work. The following purification method was found to give an 85–90% yield of suitable material from any available grade of acetonitrile. Consequently, the industrial or commercial-grade material was generally used for reasons of economy. This purification procedure is a modification of one published by COETZEE *et al.*[3] while our investigation was in progress. The acetonitrile used in our early work was purified by a slightly different procedure, the difference being that the cyanoethylation step described[3] was not included. Substantially lower residual currents resulted when the cyanoethylation step was used in the purification procedure.

A 500-ml separatory funnel containing 10 ml of saturated sodium hydroxide solution was almost filled with impure acetonitrile. After extraction of the acidic impurities, the aqueous phase was discarded and the acetonitrile placed in a distilling flask with 10 ml of half-saturated sodium hydroxide solution. This mixture was refluxed for 3–8 h and then fractionally distilled, leaving the residue of sodium hydroxide and high-boiling materials in the flask. The product was placed in another distilling flask, warmed, and phosphorus pentoxide added until all water present had been removed, as indicated by the white appearance imparted to the acetonitrile by suspended particles of P_2O_5. This suspension was refluxed for 30 min, with addition of phosphorus pentoxide, as required, to keep the suspension milky white. The dry acetonitrile was then distilled from the residue of basic impurities, polyphosphoric acids, and polymerized acetonitrile. Two or three grams of P_2O_5 were added to the product, which was then carefully fractionated on a 12 mm × 55 cm column packed with 3/32'' glass helices. The product was collected in the container shown in Fig. 2. It was protected from atmospheric moisture by a drying tube charged with successive layers of anhydrous calcium sulfate and phosphorus pentoxide; the calcium sulfate being used to prevent direct exposure of the phosphorus pentoxide to moist laboratory air. The water content of the purified acetonitrile was determined by a constant-current coulometric Karl Fischer titration. Acetonitrile prepared and stored as described above typically contains less than $5 \cdot 10^{-4}$ % water.

Tetraethylammonium perchlorate ($TEAClO_4$)

The salt was prepared by adding perchloric acid dropwise, from a burette, to a

warm, stirred solution of tetraethylammonium bromide or hydroxide until a permanent precipitate formed. The precipitation of $TEAClO_4$ was completed by addition of 0.2 *M* perchloric acid until no additional precipitation occurred. This point was found by interrupting the stirring to allow the precipitate to settle, then adding acid to the supernatant liquid. The contents of the beaker were cooled in an ice bath, transferred to a sintered-glass filter funnel, and washed with ice-cold water until nearly free of bromide ions. The product was dissolved in the minimum amount of hot water and recrystallized by allowing the solution to cool to room temperature.

The crystals were collected and air-dried on a sintered-glass filter, dried in an oven at 50°, and stored in a desiccator over P_2O_5. The supernatant layers from successive batches were retained, concentrated by evaporation over a hot plate, and successive crops collected until nearly all the $TEAClO_4$ had been recovered.

Nitrogen

A continuous nitrogen flow of approximately 0.5 cu. ft./h was necessary for rapid de-aeration of the catholyte and to prevent diffusion of atmospheric oxygen into the cell. This gas flow was provided by the use of Matheson pre-purified nitrogen of nominally 99.998% purity. The gas was passed over copper turnings in a tube furnace to remove a trace of oxygen, then through a moisture absorption bulb containing anhydrous calcium sulfate, and finally to the electrolysis cell.

Rare-earth materials

All the rare earths used in this investigation, except europium, were obtained as the oxides from the Ames Laboratory of Iowa State University. The stated purity was 99.8% or better in all cases. Europium oxide of 99.9% purity was obtained from Research Chemicals, Inc. Neodymium, europium, and samarium oxides were ignited at 900° for several hours, then cooled and stored in a nitrogen-filled desiccator until weighed. The remaining rare earths were weighed after a few minutes drying at 110° to remove surface moisture.

Miscellaneous chemicals

In all cases where purity is not specifically stated, analytical reagent-grade chemicals were used without further purification.

PROCEDURE

Preparation of rare-earth samples

Rare-earth perchlorate samples were sometimes prepared by solution of the oxide in perchloric acid, but the usual technique involved evaporation of an aqueous rare-earth chloride stock solution with perchloric acid. The oxides were weighed into the tube of the apparatus shown in Fig. 3, covered with 60% perchloric acid, and heated in a nitrogen stream to speed the dissolution of the oxides. The sample was first heated on a water bath until only a syrupy liquid remained in the sample tube. The water bath was then replaced by a mineral-oil bath and heating was continued until fumes of perchloric acid ceased to be evolved from the outlet tube. The sample tube was allowed to cool and was stored in a desiccator over phosphorus pentoxide. An acetonitrile solution of the sample was prepared by partially filling a 10-ml

volumetric flask from the acetonitrile storage vessel, and then transferring the sample to the flask with a micro transfer pipette, using small portions of this solvent.

Aliquots of the aqueous chloride stock solution, prepared by dissolving weighed portions of the oxide in excess 6 *M* hydrochloric acid, were evaporated to dryness on the water bath before addition of the perchloric acid. The procedure for this type of sample was otherwise the same. Only a thin film of lubricant on the lower 1/4 of the ground joint of the drying apparatus was used, because stopcock grease is readily oxidized by hot perchloric acid fumes. The temperature of the oil bath should not be allowed to exceed 250°, as extensive decomposition of the rare-earth perchlorates occurs above this temperature.

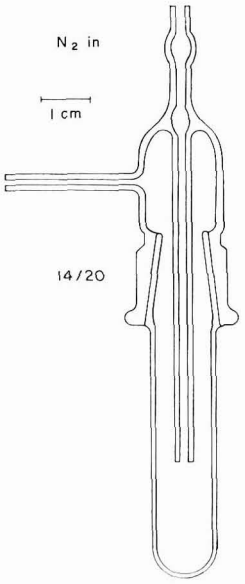

Fig. 3. Sample preparation apparatus.

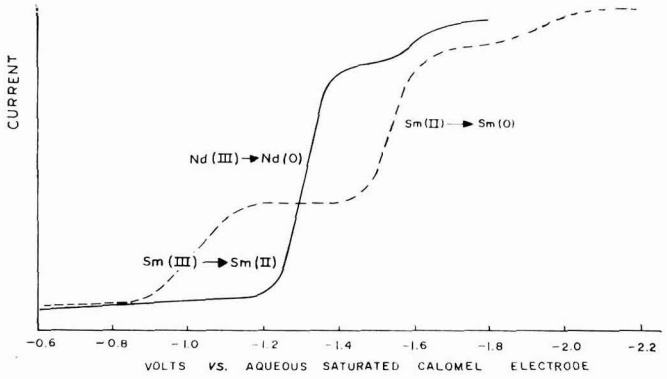

Fig. 4. Reduction wave in 0.100 *M* $TEAClO_4$ of: (—), neodymium; (---), samarium.

Rare-earth nitrates, bromides, and iodides were prepared from the chloride stock solutions in a similar manner by substitution of the appropriate acid for perchloric acid.

Preparation of supporting electrolyte solution

A two-day supply of supporting electrolyte, usually 50–100 ml of 0.100 *M* $TEAClO_4$, was prepared by transferring the appropriate weight of salt to a volumetric flask and diluting to volume with acetonitrile. To prevent contamination of the dry acetonitrile by atmospheric moisture, the volumetric flask was purged with dry nitrogen before filling.

Polarographic measurements

Conventional polarographic techniques were used throughout the investigation.

The potential scan rate was 0.200 V/min. Solutions were de-aerated for 5 min before the polarographic scan was begun. Polarograms were obtained *versus* a silver–silver-ion electrode, the potential of which was afterwards compared to that of an aqueous S.C.E. with the aid of the Fluke differential voltmeter. Only the amount of damping necessary to overcome internal noise in the instrumentation was used in the recording of the polarograms.

RESULTS

Polarography of neodymium perchlorate

A $5.32 \cdot 10^{-4}$ *M* solution of neodymium perchlorate in 0.100 *M* $TEAClO_4$ has a half-wave potential of -1.45 V *vs.* S.C.E. as shown in Fig. 4. The diffusion current was measured by extrapolating the diffusion plateau of the entire wave, not just the first part, back to -1.45 V. At a mercury flow rate of $m = 0.841$ mg/sec and drop time, $t = 5.00$ sec, the diffusion current was 3.93 μA. The observed distortion of the polarogram which yields an apparent double wave is thought to be a result of the presence of an unavoidable trace of a surface-active impurity.

Polarography of samarium perchlorate

The polarographic results for samarium are somewhat at variance with those reported by KOLTHOFF AND COETZEE[2]. These authors found that the diffusion current for the polarographic reduction of samarium(III) to samarium(II) occurs at a half-wave potential of -1.62 V *vs.* S.C.E. and that the diffusion current is proportional to concentration, at least over the range $0.2–2.0 \cdot 10^{-3}$ *M*. They also reported that they were unable to obtain a wave corresponding to the reduction of samarium(II). The value of the half-wave potential of the samarium(III) reduction found in the work reported here is -1.04 V. Another wave, approximately twice the height of that corresponding to the samarium(III) reduction, was found at -1.55 V. This remained after the controlled-potential reduction of samarium(III), and must be assumed to result from the samarium(II)→(O) reduction.

TABLE 1

HALF-WAVE POTENTIAL OF SAMARIUM(III)→(II) AS A FUNCTION OF CONCENTRATION

Sm(III) concn. $\cdot 10^3$ *M*	$E_{\frac{1}{2}}$ *vs. S.C.E., 25°*
0.405	−1.04
0.744	−1.07
1.03	−1.10

The half-wave potential of the samarium(III) reduction becomes more cathodic with increasing samarium concentration, as shown by Table 1.

The samarium waves are shown in Figs. 4 and 5. The addition of a small amount of water to the samarium(III) solutions results in a slight cathodic shift of the half-wave potential.

Although well-formed, easily measurable waves were obtained over a samarium(III) concentration range of $9 \cdot 10^{-6}–1.03 \cdot 10^{-3}$ *M*, the diffusion current obtained was not proportional to the concentration. It is likely that traces of acid, water, or

unremoved oxygen cause enhancement of the wave height by oxidizing samarium(III) as it forms at the dropping electrode. Since it has not been possible to obtain non-aqueous solutions completely free of the above-mentioned substances, the polarographic determination of samarium in acetonitrile appears to be impractical at present.

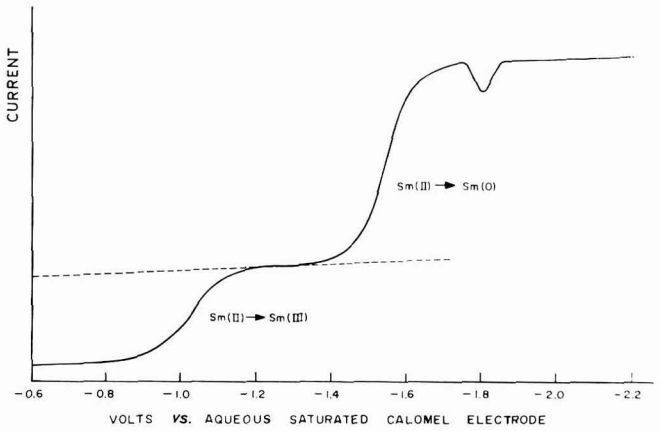

Fig. 5. Samarium oxidation waves in 0.100 M $TEAClO_4$.

Polarography of ytterbium perchlorate

The polarographic reduction of ytterbium occurs in two steps in acetonitrile, as it does in other solvents. The reduction of ytterbium(III) to ytterbium(II) occurs at a half-wave potential of -0.60 V. This wave can be distinguished in the presence of all the other rare earths. The half-wave potential for the reduction of divalent ytterbium, -1.58 V, is too close to those of the remaining rare-earth(III)$\rightarrow$(O) reductions to be of analytical value.

Solutions of ytterbium(III) perchlorate in acetonitrile decompose rapidly, as evidenced by the appearance of a flocculent white precipitate within 1 h. Precipitation could be prevented only by the addition of water and acid to the acetonitrile solutions. When this was done, the resulting partially aqueous solution was unsuitable for the determination of samarium. No practical means of preventing the precipitation of ytterbium in the non-aqueous solution was found that would allow the determination of samarium in the same solution.

Polarography of europium perchlorate

Two waves were found upon polarographic reduction of europium(III) solutions. The half-wave potentials determined in this work are slightly different from those reported by KOLTHOFF AND COETZEE, as shown in Table 2. This discrepancy probably results from our use of a somewhat different method of preparing the anhydrous perchlorates. The addition of small amounts of water resulted in a shift of the half-wave potentials. The europium(III)–(II) reduction wave was affected more than that of the europium(II)–(O) reduction. In addition to the shift of the half-wave potentials, the slopes of the waves decreased, indicating that the presence of water makes the reduction "polarographically irreversible".

Further evidence for a decreased rate of the electrode reaction upon addition of

TABLE 2

SUMMARY OF RARE-EARTH POLAROGRAPHIC HALF-WAVE POTENTIALS IN ACETONITRILE *vs.* AQUEOUS S.C.E.

Reaction	$E_{\frac{1}{2}}$	
	(Kolthoff and Coetzee)	*(this work)*
Eu(III) → Eu(II)	+0.15	+0.10
Eu(II) → Eu(O)	−1.67	−1.62
Yb(III) → Yb(II)	−0.57	−0.60
Yb(II) → Yb(O)	−1.69	−1.58[d]
Sm(III) → Sm(II)	−1.62	−1.04[b,c]
Sm(II) → Sm(O)	[a]	−1.55[b,c]
Nd(III) → Nd(O)	−1.5	−1.45[b]

[a] Not obtained. [b] Split wave, see figs. 4 and 5. [c] Concn. $4.05 \cdot 10^{-4}$ *M*. The half-wave potential shifts cathodically with increasing concn. [d] Split wave.

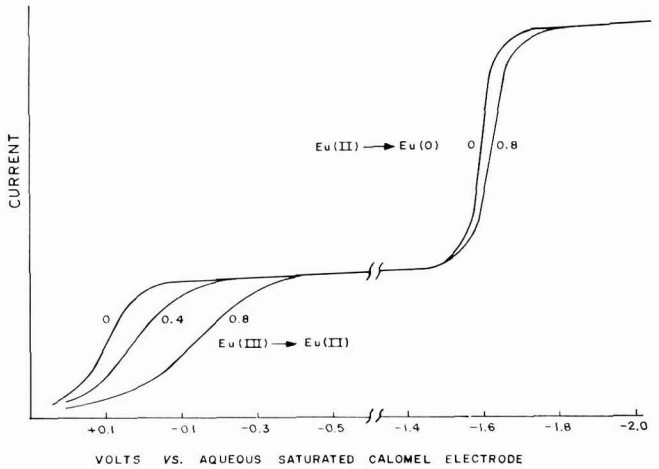

Fig. 6. Europium reduction waves. Numbers on curves refer to per-cent water added to the soln.

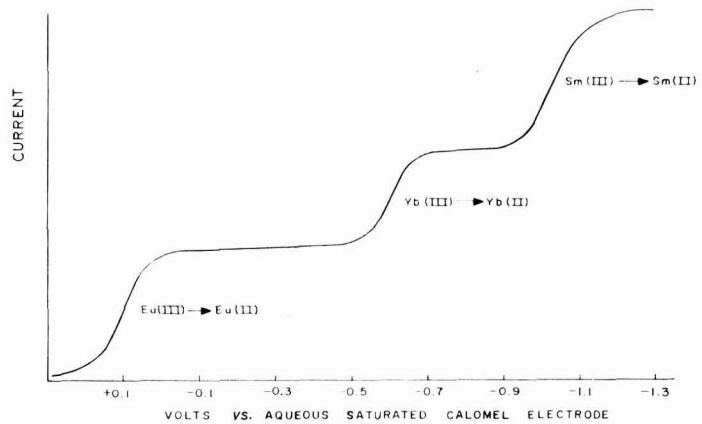

Fig. 7. Polarogram of rare-earth perchlorates.

water was obtained when the europium was reduced at controlled potential. The control potential required for quantitative reduction of europium(III) was shifted cathodically by several tenths of a volt in the solutions containing water.

The appearance of the europium polarographic waves is indicated in Fig. 6.

Polarography of rare-earth perchlorate mixtures

A polarogram of a solution containing approximately 1 μmole of each rare-earth element, as its perchlorate, is shown in Fig. 7. The polarographic behavior of europium, samarium, and ytterbium in solutions of this type is easier than would be expected from the results obtained in the solutions containing only one rare-earth element, since the matrix of non-reducible rare earths has the beneficial effect of decreasing the interference caused by traces of water and oxygen.

DISCUSSION

The results of our work and that of KOLTHOFF AND COETZEE are compared in Table 2. It can be seen that the polarographic determination of these elements is possible under conditions appropriate to an analytical laboratory. However, the method is at present more complicated than polarographic procedure using aqueous solvents because of the sample preparation problem and the necessity of purifying the solvent.

Effects of water on the electrode reactions

Mention was made in a preceding section, of the shifts of half-wave potentials of the ytterbium and samarium waves upon the addition of water to the acetonitrile solutions. Although the magnitude and direction of the shifts are such as to suggest the formation of rare-earth–aquo complex ions prior to reduction, no evidence is available regarding this point. The much larger shift resulting from the addition of water to europium(III) solutions probably arises from a cause other than complexing, although a part of the total effect may be due to aquo-complex formation. It seems more reasonable to assume that in this case the rate of the electrode reaction is affected by the presence of water molecules adsorbed on the mercury-electrode surface. This accounts for the fact that the effect is observed on the positive side of the electrocapillary maximum potential, where the europium is reduced, and not on the negative side. The electrocapillary maximum potential in acetonitrile lies at approximately -0.5 V *vs.* aqueous S.C.E., as judged from the potential of minimum current oscillation on the residual current polarograms.

ACKNOWLEDGEMENT

The financial support of the U. S. Atomic Energy Commission by Contracts AT(11-1)-553 and AT(11-1)-1418 is gratefully acknowledged.

SUMMARY

Europium, samarium, and ytterbium can be determined in rare-earth mixtures

by polarography in specially purified solutions on the perchlorates. The polarographic waves correspond to the reduction of the tripositive ions to dipositive species. Water and traces of acid interfere but their effect can be made negligible by adding an excess of non-reducible rare earths. The half-wave potential of the Sm(II)–(O) polarogram in acetonitrile was found to be -1.55 V *vs.* the aqueous S.C.E.

REFERENCES

1 E. N. WISE AND E. J. COKAL, *Anal. Chem.*, 32 (1960) 1417.
2 I. M. KOLTHOFF AND J. F. COETZEE, *J. Am. Chem. Soc.*, 79 (1957) 1852.
3 J. F. COETZEE, G. P. CUNNINGHAM, D. K. MCGUIRE AND G. R. PADMANABHAN, *Anal. Chem.* 34 (1962) 1139.

FURTHER CONSIDERATIONS ON REDOX TITRATION EQUATIONS

JAMES A. GOLDMAN
Department of Chemistry, Polytechnic Institute of Brooklyn, N.Y. (U.S.A.)
(Received July 10th, 1965)

Over a decade ago[1] it was recognized that, generally, the potential at the equivalence point in a potentiometric redox titration could not be expressed solely in terms of the formal potentials of the two redox couples. This was later explicitly demonstrated by a derivation of an equation[2] which expressed the equivalence point potential as a function of not only the weighted mean of the formal potentials but also the equilibrium constant for the reaction and the initial concentration of one of the participating species.

More recently[3], redox reactions have been classified according to the relationships existing between the stoichiometric coefficients of the reactants and products. For homogeneous and symmetrical reactions, the equivalence-point potential is dependent only upon the weighted mean of the two appropriate formal potentials[1,2,4,5]. BISHOP[1,4] has made some observations upon the form of the equation to be expected for inhomogeneous reactions. Further detailed considerations[5,6] for inhomogeneous reactions have been also undertaken, the conclusions being that the equivalence-point potential, in general, cannot be expressed solely in terms of the formal potentials.

A fundamental difficulty that arises is the impossibility of expressing the concentration ratio [Red]/[Ox]—for $a\mathrm{Ox} + ne \rightleftarrows c\mathrm{Red}$—as a function *only* of the potential and appropriate constants (such as the formal potential, n, etc.). This is explicitly demonstrated by the restrictions necessary in the recent derivation of a general redox titration equation[7]. To some extent, it is this situation which generally makes the equivalence-point potential, E^*, concentration dependent. Nevertheless, it is indeed interesting to note that even when $a \neq c$, E^* will be concentration independent as long[6] as $ad = bc$ (where $d\mathrm{Ox}_2 + n_2e \rightleftarrows b\mathrm{Red}_2$).

Indeed, for symmetrical and homogeneous reactions, it is evident from the general equation[7] that the entire curve is independent of the concentrations of the species participating in the reaction, the potential being dependent only upon the values of the formal potentials and the progress of the titration. Although BISHOP first proposed a rigorous method[8], utilizing reaction deficiences, and formulated in terms of absolute rather than relative concentrations, for the calculation of the entire curve, it was later reformulated[3] so as not to involve the use of absolute concentrations. But it was then readily admitted that the actual calculations based on this method are somewhat more laborious than by the formerly proposed method[8]. Therefore, the most recently proposed equation[7] is particularly advantageous not only because it facilitates the procedure of calculation but also because it explicitly and emphatically shows the entire titration curve to be independent of the concentration of any species.

Presented now, are some further considerations pertaining to the equations

descriptive of redox titration curves. The result of an investigation into the explicit relationship between the equivalence-point potential and the equilibrium constant for the titration reaction is first discussed.

FACTORS UPON WHICH THE EQUIVALENCE-POINT POTENTIAL DEPENDS

In general, the value of some measured property at the equivalence point in any titration is dependent upon the equilibrium constant for the titration reaction and the initial concentration (corrected for dilution which occurs during the titration) of the species being titrated. For precipitation titrations and those of strong acids by strong bases, the potential (as determined by the concentration of an appropriate species) at equivalence depends only upon the value of the equilibrium constant and not upon the initial concentration of any species. However, for the titration of a weak acid (base) with a strong base (acid), the pH at equivalence and therefore, potential, depends also upon the initial concentration of the species to be determined. In potentiometric redox titrations, the equivalence point potential, E^*, is concentration dependent only for some types of inhomogeneous reactions[5,6] but even from the commonly given equations for homogeneous and symmetrical reactions, the explicit dependence of E^* upon the equilibrium constant is not readily evident.

Let us first consider homogeneous and symmetrical reactions. The equation that represents the titration reaction is[3,7]

$$n_2\mathrm{Ox}_1 + n_1\mathrm{Red}_2 \rightleftarrows n_2\mathrm{Red}_1 + n_1\mathrm{Ox}_2 \tag{1}$$

and the Nernst expressions for the corresponding reversible half-reactions are

$$E = E_1^{0'} - \frac{RT}{n_1 F} \ln \frac{[\mathrm{Red}_1]}{[\mathrm{Ox}_1]} \tag{2}$$

and

$$E = E_2^{0'} - \frac{RT}{n_2 F} \ln \frac{[\mathrm{Red}_2]}{[\mathrm{Ox}_2]} \tag{3}$$

The relationship between the equilibrium constant, K, for the reaction represented by eqn. (1), and the formal potentials, is

$$\Delta E^{0'} = E_1^{0'} - E_2^{0'} = \frac{RT}{n_1 n_2 F} \ln K \tag{4}$$

where

$$K = \frac{[\mathrm{Red}_1]^{n_2}[\mathrm{Ox}_2]^{n_1}}{[\mathrm{Ox}_1]^{n_2}[\mathrm{Red}_2]^{n_1}} \tag{5}$$

Throughout the entire titration $[\mathrm{Ox}_2] = (n_1/n_2)[\mathrm{Red}_1]$, so that at equivalence we may write

$$[\mathrm{Ox}_2]^* = (n_1/n_2)[\mathrm{Red}_1]^* \tag{6}$$

where the asterisk denotes the indicated concentration at the equivalence point. However, only at equivalence does

$$[\mathrm{Ox}_1]^* = (n_2/n_1)[\mathrm{Red}_2]^* \tag{7}$$

Substitution into eqn. (5) of expressions for $[Ox_2]^*$ and $[Red_2]^*$, obtained from eqns. (6) and (7), respectively, yields

$$\frac{[Red_1]^*}{[Ox_1]^*} = K^{1/(n_1+n_2)} \tag{8}$$

and substitution into eqn. (5) of expressions for $[Red_1]^*$ and $[Ox_1]^*$ obtained from eqns. (6) and (7), respectively, yields

$$\frac{[Ox_2]^*}{[Red_2]^*} = K^{1/(n_1+n_2)} \tag{9}$$

Substitution of eqn. (8) into eqn. (2), and of eqn. (9) into eqn. (3), results in

$$E^* = E_1{}^{0\prime} - \frac{n_2 RT}{n_1 n_2 (n_1+n_2) F} \ln K \tag{10}$$

and

$$E^* = E_2{}^{0\prime} - \frac{n_1 RT}{n_1 n_2 (n_1+n_2) F} \ln K \tag{11}$$

where E^* represents the potential at the equivalence point.

Addition of eqn. (10) and eqn. (11), followed by solution for E^*, yields

$$E^* = \frac{E_1{}^{0\prime}+E_2{}^{0\prime}}{2} + \frac{(n_1-n_2) RT}{2n_1 n_2 (n_1+n_2) F} \ln K \tag{12}$$

which may be rewritten as

$$E^* = \frac{E_1{}^{0\prime}+E_2{}^{0\prime}}{2} + \frac{(n_1-n_2)}{2(n_1+n_2)} \Delta E^{0\prime} \tag{13}$$

by the use of eqn. (4). Now it is readily seen, by substitution of $E^{0\prime} = E_1{}^{0\prime} - E_2{}^{0\prime}$, that eqn. (13) is equivalent to

$$E^* = \frac{n_1 E_1{}^{0\prime} + n_2 E_2{}^{0\prime}}{n_1+n_2} \tag{14}$$

which is the commonly given expression[3,4]. However, eqn. (13) more explicitly shows the dependence of E^* on the magnitude of $\Delta E^{0\prime}$ (which is determined by the value of K). Equation (13) (and eqn. (14)) may also be written as

$$E^* = E_1{}^{0\prime} - \frac{n_2}{n_1+n_2} \Delta E^{0\prime}$$

which form has been previously used[7]. The customary methods[3,4] of deriving E^* always yield directly eqn. (14) in which the dependence of E^* upon $\Delta E^{0\prime}$ (and therefore K) is somewhat obscured.

For the most general situation, namely inhomogeneous reactions, the titration reaction may be represented as[3,7,8]

$$ax\mathrm{Ox}_1 + by\mathrm{Red}_2 \rightleftarrows cx\mathrm{Red}_1 + dy\mathrm{Ox}_2 \tag{15}$$

where $n_1 x = n_2 y$, and the two appropriate reversible redox systems may be represented as

$$a\mathrm{Ox}_1 + n_1 \varepsilon \rightleftarrows c\mathrm{Red}_1$$

and

$$d\mathrm{Ox}_2 + n_2\varepsilon \rightleftarrows b\mathrm{Red}_2$$

BARD AND SIMONSEN[2] have presented an equation for E^*, which in the present notation may be written as

$$E^* = \frac{n_1 E_1^{0'} + n_2 E_2^{0'}}{n_1 + n_2} - \frac{bRT}{(bn_1 + an_2)F} \ln \left[\left(\frac{cx}{dy}\right)^c \Big/ \left(\frac{ax}{by}\right)^a \right] -$$
$$- \frac{(a-b)RT}{(n_1+n_2)(bn_1+an_2)F} \ln K - \frac{(bc-ad)RT}{(bn_1+an_2)F} \ln [\mathrm{Ox}_2]^* \qquad (16)$$

More recently[7], an equivalent form based upon BRINKMAN'S[6] approach was presented as

$$E^* = \frac{bn_1 E_1^{0'} + an_2 E_2^{0'}}{bn_1 + an_2} + \frac{RT}{(bn_1+an_2)F} \times$$
$$\{(ad-bc) \ln [\mathrm{Red}_1]^* + ad \ln (d/c) - ab \ln (b/a) + a(d-b) \ln (y/x)\} \qquad (17)$$

By use of $[\mathrm{Ox}_2]^* = (dy/cx)[\mathrm{Red}_1]^*$, it is readily proved that eqns. (16) and (17) are equivalent.

The practical utility of eqn. (17) (as compared to eqn. (16)) is that it is then easily seen in what manner the value of E^* depends upon the values of the stoichiometric coefficients and the values of n_1 and n_2. However, eqn. (16) more clearly shows the dependency of E^* upon the value of K. Nevertheless, in view of eqns. (12), (13), and (14), even the first term on the right-hand side of eqn. (16) is itself dependent upon the value of K. Therefore, because eqn. (16) already contains a term dependent upon K, it is convenient to use it in continuing with further considerations.

The relationship between the formal potentials and K is

$$\Delta E^{0'} = E_1^{0'} - E_2^{0'} = \frac{RT}{n_1 n_2 F} \ln K$$

where K is now the *equilibrium constant for the reaction represented by eqn. (15)*. Therefore, we may write

$$\frac{(a-b)RT}{(n_1+n_2)(bn_1+an_2)F} \ln K = \frac{n_1 n_2 (a-b)}{(n_1+n_2)(bn_1+an_2)} \Delta E^{0'} \qquad (18)$$

and because eqn. (13) is equivalent to eqn. (14) we may write:

$$\frac{n_1 E_1^{0'} + n_2 E_2^{0'}}{n_1+n_2} = \frac{E_1^{0'} + E_2^{0'}}{2} + \frac{(n_1-n_2)}{2(n_1+n_2)} \Delta E^{0'} \qquad (19)$$

so that substitution of eqns. (18) and (19) into eqn. (16) gives:

$$E^* = \frac{E_1^{0'} + E_2^{0'}}{2} + \frac{(bn_1-an_2)}{2(bn_1+an_2)} \Delta E^{0'} -$$
$$- \frac{bRT}{(bn_1+an_2)F} \ln \left[\left(\frac{cx}{dy}\right)^c \Big/ \left(\frac{ax}{by}\right)^a \right] - \frac{(bc-ad)RT}{(bn_1+an_2)F} \ln [\mathrm{Ox}_2]^* \qquad (20)$$

If $an_2 = bn_1$, then E^* may be expressed as (because $x/y = n_2/n_1 = b/a$):

$$E^* = \frac{E_1^{0'} + E_2^{0'}}{2} - \frac{cRT}{2n_1F} \ln (bc/ad) - \frac{(cn_2 - dn_1)RT}{2n_1n_2F} \ln [Ox_2]^*$$

i.e., E^* depends upon the average of the formal potentials and is a function also of concentration and the values of the stoichiometric coefficients. Now, E^* will be independent of $[Ox_2]^*$ only if $cn_2 = dn_1$, but it then follows that $ad = bc$, so that we obtain $E^* = (E_1^{0'} + E_2^{0'})/2$.

However, it should be realized that $ad = bc$ is a necessary and sufficient requirement *only* for E^* to be concentration independent. Under these conditions ($ad = bc$), from eqn. (20):

$$E^* = \frac{E_1^{0'} + E_2^{0'}}{2} + \frac{(bn_1 - an_2)}{2(bn_1 + an_2)} \Delta E^{0'} - \frac{b(c-a)RT}{(bn_1 + an_2)F} \ln \frac{an_2}{bn_1} \qquad (21)$$

and $E^* = (E_1^{0'} + E_2^{0'})/2$ is obtained only if $bn_1 = an_2$.

It is evident that the equivalence-point potential, E^*, is never concentration dependent if $E(f)$[+] is concentration independent. However, whenever E^* is concentration dependent then it is most probable that $E(f)$ is also concentration dependent. However, there are situations, such as for inhomogeneous reactions, when $ad = bc$, where E^* is concentration independent but where it is very likely that $E(f)$ is concentration dependent[5,6].

FACTORS DETERMINING THE MAGNITUDE OF $(dE/df)_{f=1}$

In general, for most titrations at equivalence, the magnitude of the slope of the tangent to the titration curve is dependent upon the magnitude of K *and* the initial concentration (corrected for dilution) of the species being titrated.

Because no general equation has yet been presented to describe the relationship between E and f (fraction titrated) for inhomogeneous reactions, we will restrict our discussion to homogeneous and symmetrical reactions. However, it has been shown then that the curve of E *vs.* f is concentration independent so that it may be anticipated that so will be the magnitude of $(dE/df)_{f=1}$.

The general equation, for homogeneous and symmetrical reactions, is[7]

$$f = \frac{1 + k \exp(n_1\psi)}{1 + k \exp(-n_2\psi)} \qquad (22)$$

where f is the fraction titrated (the quantitative measure of the progress of the titration), $\psi = (F/RT)(E - E^*)$, $k = \exp(-n\delta)$, $\delta = (F/RT)\Delta E^{0'}$, and $n = n_1n_2/(n_1 + n_2)$. Using eqn. (22), dE/df may be easily obtained:

$$\frac{dE}{df} = \frac{RT}{F} \frac{[1 + k \exp(-n_2\psi)]^2}{k\{[n_1 \exp(n_1\psi) + n_2 \exp(-n_2\psi)] + k(n_1 + n_2) \exp(n_1 - n_2)\psi\}} \qquad (23)$$

so that

$$\left(\frac{dE}{df}\right)_{f=1} = \frac{RT}{F} \frac{(1+k)}{k(n_1 + n_2)} \qquad (24)$$

because $\psi = 0$ at $f = 1$. It is evident that the greater the magnitude of $\Delta E^{0'}$, the greater will be the magnitude of $(dE/df)_{f=1}$.

[+] $E(f)$ designates the curve represented by a graph of E *vs.* f.

Of interest is the comparison between the values of $(dE/df)_{f=1}$ and those of $\Delta E^{0'}$. For $n_1 = n_2 = 1$, eqn. (24) may be written as

$$\left(\frac{dE}{df}\right)_{f=1} = \frac{RT}{F} \frac{1 + \exp\left(-\frac{F}{2RT}\Delta E^{0'}\right)}{2\exp\left(-\frac{F}{2RT}\Delta E^{0'}\right)} \tag{25}$$

and the results of the calculations utilizing this equation are presented in Table 1 for 25°.

TABLE 1

THE MAGNITUDE OF $(dE/df)_{f=1}$ AT 25°, $n_1 = n_2 = 1$

$\Delta E^{0'}$ (mV)	K	k	$(dE/df)_{f=1}$ (mV)
50	6.99	0.378	46.9
100	48.0	0.143	102.7
150	342	0.0539	251.9
200	$2.39 \cdot 10^3$	0.0204	642.5
250	$1.7 \cdot 10^4$	0.00775	1542
300	$2.0 \cdot 10^5$	0.00291	4433

The magnitude of $(dE/df)_{f=1}$ is a measure of the sharpness of the potential change in the equivalence-point region and the necessity in any practical titration for $\Delta E^{0'} \geq 200$ mV is immediately evident from Table 1.

EVALUATION OF POTENTIAL AT 50% AND 200% TITRATED

The values of f at $E = E_2^{0'}$ and at $E = E_1^{0'}$ have been previously presented[7]. It was concluded that the value of f is always somewhat greater than $\frac{1}{2}$ at $E = E_2^{0'}$, and that the value of f at $E = E_1^{0'}$ is always somewhat less than 2. Nevertheless, in any practical titration, *e.g.*, whenever $\Delta E^{0'} \geq 200$ mV, the difference between the commonly given value and that rigorously calculated is less than 0.1%.

It is however of interest to also inquire into the *actual value* of E at $f = \frac{1}{2}$ and at $f = 2$.

For the region prior to equivalence it is convenient to rewrite the general equation as[7]

$$E - E_2^{0'} = -\frac{RT}{n_2 F} \ln\left\{\frac{1-f}{f} + \frac{1}{f}[\exp(-n_1\delta)]\left[\exp\frac{n_1 F}{RT}(E - E_2^{0'})\right]\right\} \tag{26}$$

which becomes

$$E - E_2^{0'} = -\frac{RT}{n_2 F} \ln\left\{1 + 2[\exp(-n_1\delta)]\left[\exp\frac{n_1 F}{RT}(E - E_2^{0'})\right]\right\} \tag{27}$$

at $f = \frac{1}{2}$.

For the region subsequent to equivalence, the following form is convenient:

$$E - E_1^{0'} = \frac{RT}{n_1 F} \ln\left\{(f-1) + f[\exp(-n_2\delta)]\left[\exp\frac{-n_2 F}{RT}(E - E_1^{0'})\right]\right\} \tag{28}$$

and becomes

$$E-E_1^{0\prime} = \frac{RT}{n_1 F} \ln \left\{1+2[\exp(-n_2\delta)]\left[\exp \frac{-n_2 F}{RT}(E-E_1^{0\prime})\right]\right\} \qquad (29)$$

at $f=2$.

From eqn. (26) it is seen that, prior to equivalence, the rigorously calculated value of E is always less than the common approximately calculated value as was explicitly stated by BISHOP[3]:

"... the true potential is always less than the approximate potential."

However, subsequent to the equivalence point, as is apparent from eqn. (28), the rigorously calculated potential will always be greater in magnitude than the approximate value. This conclusion agrees with the calculated values presented in his earlier discussion[8].

In particular, it is evident from eqn. (27) that $E-E_2^{0\prime}<0$ at $f=\frac{1}{2}$, *i.e.*, at 50% titrated the value of E will always be somewhat less than $E_2^{0\prime}$. From eqn. (29) it is readily seen that $E-E_1^{0\prime}>0$ at $f=2$ so that at 200% titrated the value of E will always be somewhat greater than $E_1^{0\prime}$. The magnitude of the deviation of E from $E_1^{0\prime}$ and from $E_2^{0\prime}$ at these points of interest depends upon the values of n_1, n_2 and δ, *i.e.*, $\Delta E^{0\prime}$, and therefore is readily calculated by the method of successive approximations from eqns. (27) and (29), respectively, for any given set of values. Table 2 presents the results of such calculations at 25° for various values of $\Delta E^{0\prime}$ and for the situation where $n_1=n_2=1$.

TABLE 2

VALUES OF E AT 50% AND 200% TITRATED, $n_1=n_2=1$, AT 25°

$\Delta E^{0\prime}$ (mV)	$-(E-E_2^{0\prime})$ at $f=\frac{1}{2}$ (mV)	$(E-E_1^{0\prime})$ at $f=2$ (mV)
50	5.37	5.37
100	0.989	0.989
150	0.149	0.149
200	0.0215	0.0215
250	0.00309	0.00309
300	0.000440	0.000440

It is evident that the deviation of E from the appropriate $E^{0\prime}$ is less than 0.1 mV for $\Delta E^{0\prime}\geq 200$ mV as would be the case in any practical titration.

For $\Delta E^{0\prime}\geq 150$ mV, we may write eqns. (27) and (29) as

$$E-E_2^{0\prime} = \frac{-RT}{n_2 F} \ln \left\{1+2[\exp(-n_1\delta)]+2[\exp(-n_1\delta)]\left[\frac{n_1 F}{RT}(E-E_2^{0\prime})\right]\right\}$$

and

$$E-E_1^{0\prime} = \frac{RT}{n_1 F} \ln \left\{1+2[\exp(-n_2\delta)]-2[\exp(-n_2\delta)]\left[\frac{n_2 F}{RT}(E-E_1^{0\prime})\right]\right\}$$

with an error of less than 0.1%. Whenever $\Delta E^{0\prime}\geq 250$ mV, an error of less than 0.1% is made if we further transform these equations into:

$$E - E_2^{0'} = \frac{-2RT}{n_2 F} \exp(-n_1 \delta)$$

and

$$E - E_1^{0'} = \frac{2RT}{n_1 F} \exp(-n_2 \delta) ,$$

respectively.

It is evident that the greater the magnitude of $\Delta E^{0'}$ (for a given set of values for n_1 and n_2) or the greater the values of n_1 and n_2 (for a given value of $\Delta E^{0'}$), the smaller will be the deviation of E from the appropriate $E^{0'}$.

APPENDIX

Alternative derivation of eqn. (13)

In the discussion previously presented[7], it was shown that for homogeneous redox reactions:

$$E = E_2^{0'} - \frac{RT}{n_2 F} \ln \left\{ \frac{1-f}{f} + \frac{1}{f} [\exp(-n_1 \delta)] \left[\exp \frac{n_1 F}{RT} (E - E_2^{0'}) \right] \right\}$$

and

$$E = E_1^{0'} + \frac{RT}{n_1 F} \ln \left\{ (f-1) + f[\exp(-n_2 \delta)] \left[\exp - \frac{n_2 F}{RT} (E - E_1^{0'}) \right] \right\}$$

At $f = 1$, these equations then take, respectively, the following forms:

$$E^* - E_2^{0'} = (n_1/n_2)\Delta E^{0'} - (n_1/n_2)(E^* - E_2^{0'})$$

and

$$E^* - E_1^{0'} = -(n_2/n_1)\Delta E^{0'} - (n_2/n_1)(E^* - E_1^{0'})$$

from which are obtained, respectively,

$$E^* = E_2^{0'} + \frac{n_1}{n_1 + n_2} \Delta E^{0'}$$

and

$$E^* = E_1^{0'} - \frac{n_2}{n_1 + n_2} \Delta E^{0'}$$

The addition of these two equations and subsequent solution for E^* yields eqn. (13).

SUMMARY

The results of an investigation into the dependence of the equivalence-point potential upon concentration and upon the equilibrium constant for the general redox reaction are presented. For symmetrical and homogeneous reactions, the equivalence-point potential is always concentration independent. The quantitative evaluation of the magnitude of the slope of the tangent to the titration curve at the equivalence point for homogeneous and symmetrical reactions is discussed as well as the rigorously calculated values of the potential at 50% and 200% titrated.

REFERENCES

1 E. BISHOP, *Anal. Chim. Acta*, 7 (1952) 15.
2 A. J. BARD AND S. H. SIMONSEN, *J. Chem. Educ.*, 37 (1960) 364.
3 E. BISHOP, *Anal. Chim. Acta*, 27 (1962) 253.
4 E. BISHOP, *Theory and Principles of Titrimetric Analysis* in *Comprehensive Analytical Chemistry*, edited by WILSON AND WILSON, Vol. IB, Elsevier, Amsterdam, 1960.
5 J. A. GOLDMAN, *Anal. Chim. Acta*, 33 (1965) 277.
6 U. A. TH. BRINKMAN, *Chem. Weekblad*, 59 (1963) 9
7 J. A. GOLDMAN, *J. Electroanal. Chem.*, 11 (1966) 255.
8 E. BISHOP, *Anal. Chim. Acta*, 26 (1962) 397.

ALTERNATING CURRENT POLAROGRAPHY WITH MULTI-STEP CHARGE TRANSFER

II. THEORY FOR SYSTEMS WITH QUASI-REVERSIBLE TWO-STEP CHARGE TRANSFER

HOYING L. HUNG AND DONALD E. SMITH
Department of Chemistry, North-western University, Evanston, Illinois (U.S.A.)
(Received July 9th, 1965)

INTRODUCTION

The theory of the a.c. polarographic wave with a two-step heterogeneous charge transfer reaction has been discussed for the diffusion-controlled or "reversible" case[1,2]. Of greater interest are situations where the a.c. polarogram manifests kinetic effects of rate processes in addition to mass transfer. To our knowledge, no formulation of the theory for such cases has been presented. This fact, as well as some experimental results obtained in these laboratories[3,4], have suggested to us the desirability of examining this theoretical problem. The present communication is concerned with a theoretical description of the a.c. polarographic wave in which the alternating currents derived from two-step charge transfer are influenced by the kinetics of charge transfer as well as diffusion (the "quasi-reversible" case). Emphasis is placed on presentation of a method of derivation and some of the more interesting and informative aspects of the theoretical predictions. The method of derivation, modelled after MATSUDA's analysis of the single-step quasi-reversible case[5], appears applicable to any multi-step charge transfer scheme involving rate control by diffusion, charge transfer and/or coupled chemical reactions. The equation obtained for the a.c. polarographic wave is examined to ascertain the following: (a) the nature of experimental results predicted for the quasi-reversible two-step mechanism, particularly those that will aid in recognition of the mechanism; (b) the conditions, if any, where it will prove impossible to distinguish between quasi-reversible two-step and single-step mechanisms; (c) the magnitudes of charge transfer rates necessary to effect Nernstian behavior. The large number of parameters (k_h, α, E^0 and n for each charge transfer step) characterizing the quasi-reversible two-step charge transfer scheme and the very cumbersome algebraic forms found in the mathematical description of the a.c. polarographic wave preclude a complete discussion of all aspects of the theoretical predictions. The same factors discourage attempts to formulate a generalized approach for determining all thermodynamic and kinetic parameters associated with the charge transfer steps that is based solely on the a.c. polarographic read-out. However, theoretical results are given sufficient to formulate criteria which enable rough qualitative assessment of the relative values of k_h and α for the two steps. Further, it

appears that methods of calculating rate parameters to fit specific situations can be frequently developed. A method of calculating quantitatively k_h- and α-values for both charge transfer steps is outlined for the special case in which the *d.c.* process is diffusion-controlled.

THEORY

1. *Assumptions*

The majority of assumptions incorporated in the derivation to follow are identical to those described in the theoretical treatment of the diffusion-controlled two-step case[1]. The main difference is found in the replacement of the Nernstian assumption by the assumption of the applicability of absolute rate theory[6] to the charge transfer processes in question. That is, the Nernstian boundary condition is replaced by the relations (a list of notation definitions is given in Appendix 1);

$$\frac{i_1(t)}{n_1 F A k_{h,1}} = f_O C_{O_{x=0}} \exp\left\{\frac{-\alpha_1 n_1 F}{RT}[E(t)-E_1^0]\right\} - f_Y C_{Y_{x=0}} \exp\left\{\frac{(1-\alpha_1)n_1 F}{RT}[E(t)-E_1^0]\right\} \quad (1)$$

$$\frac{i_2(t)}{n_2 F A k_{h,2}} = f_Y C_{Y_{x=0}} \exp\left\{\frac{-\alpha_2 n_2 F}{RT}[E(t)-E_2^0]\right\} - f_R C_{R_{x=0}} \exp\left\{\frac{(1-\alpha_2)n_2 F}{RT}[E(t)-E_2^0]\right\} \quad (2)$$

where

$$i(t) = i_1(t)+i_2(t) \quad (3)$$

Specific double-layer effects are neglected in the derivation to follow. Double-layer corrections of the Frumkin type[7] may be introduced conveniently into the final equations in the usual manner[8].

It should be noted that application of the stationary plane diffusion model as an approximation to the normally employed dropping mercury electrode (D.M.E.) may introduce small but significant error under certain specific conditions. Recent work has indicated[9,10] that the correction for spherical diffusion can be significant, even with reversible systems, when the reduced form of the electroactive couple is in the amalgam state. It has been shown, also, that when the *d.c.* process is influenced kinetically by charge transfer, curvature and motion relative to the solution of the electrode surface may contribute significantly to the magnitude of the a.c. polarographic wave[5,11]. One should keep in mind these effects when examining quantitative aspects of the theoretical predictions. Most qualitative features of the a.c. polarograms are not expected to be grossly altered by the contributions of drop growth and geometry.

2. *Derivation*

For the step-wise electrode reaction

$$O + n_1 e \rightleftarrows Y + n_2 e \rightleftarrows R$$

the set of differential equations, initial and boundary conditions sufficient to obtain expressions for the surface concentrations is given elsewhere[1,2,12]. The surface concentrations may be expressed in the form (assuming only species O present in the bulk);

$$C_{O_{x=0}} = C_O^* - \int_0^t \frac{i_1(t-u)\mathrm{d}u}{n_1 FA(D_O\pi u)^{\frac{1}{2}}} \tag{4}$$

$$C_{Y_{x=0}} = \int_0^t \frac{i_1(t-u)\mathrm{d}u}{n_1 FA(D_Y\pi u)^{\frac{1}{2}}} - \int_0^t \frac{i_2(t-u)\mathrm{d}u}{n_2 FA(D_Y\pi u)^{\frac{1}{2}}} \tag{5}$$

$$C_{R_{x=0}} = \int_0^t \frac{i_2(t-u)\mathrm{d}u}{n_2 FA(D_R\pi u)^{\frac{1}{2}}} \tag{6}$$

Substitution of equations (4), (5) and (6) in eqns. (1) and (2) and algebraic rearrangement yields the integral equations

$$\frac{D_1^{\frac{1}{2}}\psi_1(t)}{f_1 k_{h,1}} = \mathrm{e}^{-\alpha_1 j_1(t)} - (\mathrm{e}^{-\alpha_1 j_1(t)} + \mathrm{e}^{\beta_1 j_1(t)}) \int_0^t \frac{\psi_1(t-u)\mathrm{d}u}{(\pi u)^{\frac{1}{2}}} + \mathrm{e}^{\beta_1 j_1(t)} \int_0^t \frac{\psi_2(t-u)\mathrm{d}u}{(\pi u)^{\frac{1}{2}}} \tag{7}$$

$$\frac{D_2^{\frac{1}{2}}\psi_2(t)}{f_2 k_{h,2}} = \mathrm{e}^{-\alpha_2 j_2(t)} \int_0^t \frac{\psi_1(t-u)\mathrm{d}u}{(\pi u)^{\frac{1}{2}}} - (\mathrm{e}^{-\alpha_2 j_2(t)} + \mathrm{e}^{\beta_2 j_2(t)}) \int_0^t \frac{\psi_2(t-u)\mathrm{d}u}{(\pi u)^{\frac{1}{2}}} \tag{8}$$

where

$$\psi_i(t) = \frac{i_i(t)}{n_i FAC_O^* D_O^{\frac{1}{2}}} \tag{9}$$

$$D_1 = D_O^{\beta_1} D_Y^{\alpha_1} \tag{10a}$$

$$D_2 = D_Y^{\beta_2} D_R^{\alpha_2} \tag{10b}$$

$$f_1 = f_O^{\beta_1} f_Y^{\alpha_1} \tag{11a}$$

$$f_2 = f_Y^{\beta_2} f_R^{\alpha_2} \tag{11b}$$

$$\beta_i = 1 - \alpha_i \tag{12}$$

$$j_i(t) = \frac{n_i F}{RT}[E(t) - E^r_{\frac{1}{2},i}] \tag{13}$$

$$E^r_{\frac{1}{2},1} = E_1^0 - \frac{RT}{n_1 F} \ln\left(\frac{f_Y}{f_O}\right)\left(\frac{D_O}{D_Y}\right)^{\frac{1}{2}} \tag{14}$$

$$E^r_{\frac{1}{2},2} = E_2^0 - \frac{RT}{n_2 F} \ln\left(\frac{f_R}{f_Y}\right)\left(\frac{D_Y}{D_R}\right)^{\frac{1}{2}} \tag{15}$$

Substituting the expression for the applied potential

$$E(t)=E_{\text{d.c.}}-\Delta E \sin \omega t, \tag{16}$$

and the power series

$$\exp\left[\frac{\alpha_i n_i F}{RT}\,\Delta E \sin \omega t\right] = \sum_{p=0}^{\infty} \frac{\alpha_i^p}{p!}\left(\frac{n_i F \Delta E}{RT}\right)^p (\sin \omega t)^p \tag{17}$$

$$\exp\left[\frac{-\beta_i n_i F}{RT}\,\Delta E \sin \omega t\right] = \sum_{p=0}^{\infty} \frac{(-1)^p \beta_i^p}{p!}\left(\frac{n_i F \Delta E}{RT}\right)^p (\sin \omega t)^p \tag{18}$$

$$\psi_i(t) = \sum_{p=0}^{\infty} \psi_{i,p}(t)\left(\frac{n_i F \Delta E}{RT}\right)^p \tag{19}$$

$$p = 0, 1, 2, 3, \ldots . \tag{20}$$

and equating coefficients of equal powers of $n_1 F \Delta E/RT$, yields two sets of integral equations in two unknowns;

$$\begin{aligned}\frac{D_1^{\frac{1}{2}}\psi_{1,p}(t)}{k_{h,1} f_1} = {} & e^{-\alpha_1 j_1}\frac{\alpha_1^p}{p!}(\sin \omega t)^p - \sum_{r=0}^{p}\Bigg[(\alpha_1^r e^{-\alpha_1 j_1} \\ & + (-1)^r \beta_1^r e^{\beta_1 j_1})\frac{(\sin \omega t)^r}{r!}\int_0^t \frac{\psi_{1,p-r}(t-u)\mathrm{d}u}{(\pi u)^{\frac{1}{2}}} \\ & - (-1)^r \beta_1^r e^{\beta_1 j_1}\,\frac{(\sin \omega t)^r}{r!}\left(\frac{n_2}{n_1}\right)^{p-r}\int_0^t \frac{\psi_{2,p-r}(t-u)\mathrm{d}u}{(\pi u)^{\frac{1}{2}}}\Bigg]\end{aligned} \tag{21}$$

$$\begin{aligned}\frac{D_2^{\frac{1}{2}}\psi_{2,p}(t)}{k_{h,2} f_2} = {} & \sum_{r=0}^{p}\Bigg[\alpha_2^r e^{-\alpha_2 j_2}\frac{(\sin \omega t)^r}{r!}\left(\frac{n_1}{n_2}\right)^{p-r}\int_0^t \frac{\psi_{1,p-r}(t-u)\mathrm{d}u}{(\pi u)^{\frac{1}{2}}} \\ & - (\alpha_2^r e^{-\alpha_2 j_2} + (-1)^r \beta_2^r e^{\beta_2 j_2})\frac{(\sin \omega t)^r}{r!}\int_0^t \frac{\psi_{2,p-r}(t-u)\mathrm{d}u}{(\pi u)^{\frac{1}{2}}}\Bigg]\end{aligned} \tag{22}$$

where

$$j_i = \frac{n_i F}{RT}(E_{\text{d.c.}} - E^r_{\frac{1}{2},i}) \tag{23}$$

The small amplitude ($\Delta E \leq 8/n$ mV) fundamental harmonic a.c. polarographic wave equation is derived from the solutions of eqns. (21) and (22) for $p=1$[5] which have the form

$$\begin{aligned}\frac{D_1^{\frac{1}{2}}\psi_{1,1}(t)}{k_{h,1} f_1} = {} & F_1(t)\sin \omega t - (e^{-\alpha_1 j_1} + e^{\beta_1 j_1})\int_0^t \frac{\dot{\psi}_{1,1}(t-u)\mathrm{d}u}{(\pi u)^{\frac{1}{2}}} \\ & + e^{\beta_1 j_1}\left(\frac{n_2}{n_1}\right)\int_0^t \frac{\psi_{2,1}(t-u)\mathrm{d}u}{(\pi u)^{\frac{1}{2}}}\end{aligned} \tag{24}$$

$$\frac{D_2^{\frac{1}{2}}\psi_{2,1}(t)}{k_{h,2}f_2} = F_2(t)\sin\omega t + e^{-\alpha_2 j_2}\left(\frac{n_1}{n_2}\right)\int_0^t \frac{\psi_{1,1}(t-u)du}{(\pi u)^{\frac{1}{2}}} - (e^{-\alpha_2 j_2}+e^{\beta_2 j_2})\int_0^t \frac{\psi_{2,1}(t-u)du}{(\pi u)^{\frac{1}{2}}} \quad (25)$$

where

$$F_1(t) = \alpha_1 e^{-\alpha_1 j_1} - (\alpha_1 e^{-\alpha_1 j_1} - \beta_1 e^{\beta_1 j_1})\int_0^t \frac{\psi_{1,0}(t-u)du}{(\pi u)^{\frac{1}{2}}} - \beta_1 e^{\beta_1 j_1}\int_0^t \frac{\psi_{2,0}(t-u)du}{(\pi u)^{\frac{1}{2}}} \quad (26)$$

$$F_2(t) = \alpha_2 e^{-\alpha_2 j_2}\int_0^t \frac{\psi_{1,0}(t-u)du}{(\pi u)^{\frac{1}{2}}} - (\alpha_2 e^{-\alpha_2 j_2} - \beta_2 e^{\beta_2 j_2})\int_0^t \frac{\psi_{2,0}(t-u)du}{(\pi u)^{\frac{1}{2}}} \quad (27)$$

The solutions to eqns. (24) and (25) contain only fundamental harmonic components and may be expressed as

$$\psi_{1,1}(t) = a\sin\omega t + b\cos\omega t \quad (28)$$

$$\psi_{2,1}(t) = c\sin\omega t + d\cos\omega t \quad (29)$$

As in previous work[5,13,14], the solution of the integral equations is approached by substituting eqns. (28) and (29) in eqns. (24) and (25) and applying the trigonometric identities

$$\sin\omega(t-u) = \sin\omega t\cos\omega u - \cos\omega t\sin\omega u \quad (30)$$

$$\cos\omega(t-u) = \cos\omega t\cos\omega u + \sin\omega t\sin\omega u \quad (31)$$

This yields an expression which is integrable if one neglects the slight time dependence of a, b, c and d[5,13,14], assumes steady state in the a.c. concentration profile[8] and employs the identities[15]

$$\int_0^\infty \frac{\cos\omega u du}{(\pi u)^{\frac{1}{2}}} = \int_0^\infty \frac{\sin\omega u du}{(\pi u)^{\frac{1}{2}}} = \frac{1}{(2\omega)^{\frac{1}{2}}} \quad (32)$$

Equating coefficients of $\sin\omega t$ and $\cos\omega t$ on each side of the resulting equations yields a system of four linear algebraic equations in the four unknowns a, b, c and d. Solution of the system of algebraic equations may be effected using standard techniques of matrix algebra. The solutions for a, b, c and d are related to the fundamental harmonic alternating current by the relationship

$$I(\omega t) = \frac{F^2 A C_O^* D_O^{\frac{1}{2}} \Delta E}{RT}[(n_1^2 a + n_2^2 c)^2 + (n_1^2 b + n_2^2 d)^2]^{\frac{1}{2}}\sin\left[\omega t + \cot^{-1}\frac{n_1^2 a + n_2^2 c}{n_1^2 b + n_2^2 d}\right] \quad (33)$$

which is obtained by applying eqns. (3), (9), (19), (28) and (29) and the expression

$$\delta\sin\omega t + \gamma\cos\omega t = (\delta^2+\gamma^2)^{\frac{1}{2}}\sin\left(\omega t + \cot^{-1}\frac{\delta}{\gamma}\right) \quad (34)$$

Substitution of the solutions for a, b, c and d in eqn. (33) and considerable algebraic rearrangement yields for the small amplitude fundamental harmonic alternating current:

$$I(\omega t) = \frac{2F^2 AC_O^* \Delta E(2\omega D_O)^{\frac{1}{2}}}{RTQ} [Y^2 + Z^2]^{\frac{1}{2}} \sin\left(\omega t + \cot^{-1}\frac{Y}{Z}\right) \tag{35}$$

where

$$Q = 4\left\{\frac{[1-(1+e^{-j_1})(1+e^{j_2})]^2}{(1+e^{-j_1})^2(1+e^{j_2})^2}\right\} + 4(2\omega)^{\frac{1}{2}}\left[\frac{(1+e^{-j_1})(1+e^{j_2})-1}{(1+e^{-j_1})(1+e^{j_2})}\right]\frac{(\lambda_1+\lambda_2)}{\lambda_1\lambda_2}$$
$$+ \frac{4\omega(\lambda_1+\lambda_2)^2}{\lambda_1^2\lambda_2^2} + \frac{2(2\omega)^{\frac{1}{2}}(\lambda_1+\lambda_2)}{\lambda_1^2\lambda_2^2} + \frac{(2\omega)^2}{\lambda_1^2\lambda_2^2} \tag{36}$$

$$Y = n_1^2 G_1(t)\left\{\frac{\left(1+e^{j_2}+\frac{n_2}{n_1}\right)[(1+e^{j_2})(1+e^{-j_1})-1]}{(1+e^{-j_1})(1+e^{j_2})^2}\right.$$
$$+ (2\omega)^{\frac{1}{2}}\left(\frac{\lambda_1+\lambda_2}{\lambda_1\lambda_2}\right)\left[\frac{n_1(1+e^{j_2})+n_2}{n_1(1+e^{j_2})}\right]$$
$$\left.+ \frac{(2\omega)}{\lambda_1\lambda_2^2}\left[\lambda_1+\lambda_2\left(\frac{n_2+2n_1(1+e^{j_2})}{2n_1(1+e^{j_2})}\right)\right] + \frac{(2\omega)^{\frac{3}{2}}}{2\lambda_1\lambda_2^2}\right\}$$
$$+ n_2^2 G_2(t)\left\{\frac{\left(1+e^{-j_1}+\frac{n_1}{n_2}\right)[(1+e^{j_2})(1+e^{-j_1})-1]}{(1+e^{-j_1})^2(1+e^{j_2})}\right.$$
$$+ (2\omega)^{\frac{1}{2}}\left(\frac{\lambda_1+\lambda_2}{\lambda_1\lambda_2}\right)\left[\frac{n_2(1+e^{-j_1})+n_1}{n_2(1+e^{-j_1})}\right]$$
$$\left.+ \frac{2\omega}{\lambda_1^2\lambda_2}\left[\lambda_2+\lambda_1\left(\frac{n_1+2n_2(1+e^{-j_1})}{2n_2(1+e^{-j_1})}\right)\right] + \frac{(2\omega)^{\frac{3}{2}}}{2\lambda_1^2\lambda_2}\right\} \tag{37}$$

$$Z = n_1^2 G_1(t)\left\{\frac{\left(1+e^{j_2}+\frac{n_2}{n_1}\right)[(1+e^{j_2})(1+e^{-j_1})-1]}{(1+e^{-j_1})(1+e^{j_2})^2}\right.$$
$$\left.+ \frac{(2\omega)^{\frac{1}{2}}}{\lambda_2}\left[\frac{(1+e^{j_2})(1+e^{-j_1})-1}{(1+e^{-j_1})(1+e^{j_2})}\right] + \frac{\omega}{\lambda_1\lambda_2^2}\left[\frac{n_1(1+e^{j_2})\lambda_1-n_2\lambda_2}{n_1(1+e^{j_2})}\right]\right\}$$
$$+ n_2^2 G_2(t)\left\{\frac{\left(1+e^{-j_1}+\frac{n_1}{n_2}\right)[(1+e^{j_2})(1+e^{-j_1})-1]}{(1+e^{-j_1})^2(1+e^{j_2})}\right.$$

$$+\frac{(2\omega)^{\frac{1}{2}}}{\lambda_1}\left[\frac{(1+e^{j_2})(1+e^{-j_1})-1}{(1+e^{-j_1})(1+e^{j_2})}\right]+\frac{\omega}{\lambda_1^2\lambda_2}\left[\frac{n_2(1+e^{-j_1})\lambda_2-n_1\lambda_1}{n_2(1+e^{-j_1})}\right]\Bigg\} \tag{38}$$

$$G_1(t)=\frac{1}{(1+e^{-j_2}+e^{j_1})}\left[\frac{1}{(1+e^{-j_1})}+\frac{(1+e^{-j_2})}{\lambda_2(1+e^{-j_1})}\psi_{2,0}(t)\right.$$

$$\left.+\frac{(\alpha_1+\alpha_1e^{-j_2}-\beta_1e^{j_1})}{\lambda_1}\psi_{1,0}(t)\right] \tag{39}$$

$$G_2(t)=\frac{1}{(1+e^{-j_2}+e^{j_1})}\left[\frac{1}{(1+e^{j_2})}-\frac{(1+e^{j_1})}{\lambda_1(1+e^{j_2})}\psi_{1,0}(t)-\frac{(\beta_2+\beta_2e^{j_1}-\alpha_2e^{-j_2})}{\lambda_2}\psi_{2,0}(t)\right] \tag{40}$$

$$\lambda_i=\frac{k_{h,i}f_i}{D_i^{\frac{1}{2}}}(e^{-\alpha_i j_i}+e^{\beta_i j_i}) \tag{41}$$

The solution to the a.c. wave equation is incomplete unless the expression for the d.c. polarographic current is introduced in eqns. (39) and (40). This entails solving eqns. (21) and (22) for $p=0$. While a number of authors have considered special cases of this problem[16–19] involving the combination of reversible and/or irreversible steps, a completely general solution encompassing conditions corresponding to a quasi-reversible d.c. wave has not, to our knowledge, been given. However, the problem is readily solved, as shown in Appendix 2. The solutions obtained are:

$$\psi_{1,0}(t)=\frac{\lambda_1}{(1+e^{j_1})(\chi_--\chi_+)}[(\chi_--\lambda_2)\exp(\chi_-^2\,t)\operatorname{erfc}(\chi_-t^{\frac{1}{2}})$$

$$-(\chi_+-\lambda_2)\exp(\chi_+^2\,t)\operatorname{erfc}(\chi_+t^{\frac{1}{2}})] \tag{42}$$

$$\psi_{2,0}(t)=\frac{\lambda_1\lambda_2}{(\chi_--\chi_+)(1+e^{j_1})(1+e^{j_2})}[\exp(\chi_+^2\,t)\operatorname{erfc}(\chi_+t^{\frac{1}{2}})-\exp(\chi_-^2\,t)\operatorname{erfc}(\chi_-t^{\frac{1}{2}})] \tag{43}$$

where

$$\chi_\pm=\frac{\lambda_1+\lambda_2\pm[(\lambda_1+\lambda_2)^2-4K]^{\frac{1}{2}}}{2} \tag{44}$$

$$K=\lambda_1\lambda_2\left[\frac{e^{j_2}+e^{-j_1}+e^{(j_2-j_1)}}{(1+e^{j_2})(1+e^{-j_1})}\right] \tag{45}$$

Substitution of eqns. (42) and (43) in eqns. (39) and (40) completes the expression for the a.c. polarographic wave.

3. Limiting cases

A necessary condition for the validity of the foregoing expression describing the a.c. polarographic wave is that it reduces to previously derived expressions under

two important sets of limiting conditions: (a) very rapid charge transfer kinetics and/or very low frequency; (b) the second reduction step occurs at much more negative potentials than the first reduction step.

Case a. This corresponds to the diffusion-controlled or reversible two-step wave discussed previously[1,2]. The condition of rapid charge transfer and/or low frequency is impressed by taking the limit of eqn. (35), etc. as $\sqrt{2\omega}/\lambda_1$ and $\sqrt{2\omega}/\lambda_2$ approach zero. An implication of this limit is that $\chi_+ t^{\frac{1}{2}}$ and $\chi_- t^{\frac{1}{2}}$ are very large (greater than about 50). Application of these limits and algebraic rearrangement yields

$$\lim_{\sqrt{(2\omega)}/\lambda_1,\ \sqrt{(2\omega)}/\lambda_2} I(\omega t)$$

$$= \frac{F^2 A C_O^* \Delta E(\omega D_O)^{\frac{1}{2}} [n_1^2 e^{j_1} + n_2^2 e^{-j_2} + (n_1+n_2)^2 e^{(j_1-j_2)}]}{RT(1+e^{-j_2}+e^{j_1})^2} \sin\left(\omega t + \frac{\pi}{4}\right) \qquad (46)$$

Equation (46) is identical to the previously derived expression[1,2] for the diffusion-controlled wave.

Case b. This represents the situation in which the two reduction steps yield two completely resolved a.c. polarographic waves occurring in the vicinity of $E_{\frac{1}{2},1}{}^r$ and $E_{\frac{1}{2},2}{}^r$, respectively. The mathematical condition appropriate to this case is $E_{\frac{1}{2},1}{}^r \gg E_{\frac{1}{2},2}{}^r$. Applying this condition to eqn. (35), etc. one finds for $E_{\text{d.c.}}$ in the vicinity of $E_{\frac{1}{2},1}{}^r$.

$$I(\omega t) = \frac{n_1^2 F^2 A C_O^* \Delta E(\omega D_O)^{\frac{1}{2}}}{4RT \cosh^2 \frac{j_1}{2}} \left[\frac{2}{1+\left(1+\frac{\sqrt{(2\omega)}}{\lambda_1}\right)^2}\right]^{\frac{1}{2}}$$

$$\times [1+(\alpha_1 e^{-j_1}-\beta_1)\exp(\lambda_1^2 t)\,\mathrm{erfc}(\lambda_1 t^{\frac{1}{2}})] \times \sin\left[\omega t + \cot^{-1}\left(1+\frac{\sqrt{(2\omega)}}{\lambda_1}\right)\right] \qquad (47)$$

and for $E_{\text{d.c.}}$ in the vicinity of $E_{\frac{1}{2},2}{}^r$ one obtains an expression identical to eqn. (47) except that the subscript 1 is replaced by the subscript 2. Thus, two completely resolved waves are predicted, each governed by the well-known expression for the single-step quasi-reversible a.c. wave[5,13,20] (for diffusion to a stationary plane). The kinetic and thermodynamic parameters associated with the first and second charge transfer steps apply to the first ($E_{\text{d.c.}} \sim E_{\frac{1}{2},1}{}^r$) and second ($E_{\text{d.c.}} \sim E_{\frac{1}{2},2}{}^r$) waves, respectively. This result for case b is obviously in accord with expectations for $E_{\frac{1}{2},1}{}^r \gg E_{\frac{1}{2},2}{}^r$. The above results obtained for limiting cases a and b show that eqn. (35) is consistent with previously discussed theory for these simplified situations.

With the reversible system, reasonably quantitative statements regarding conditions for the appearance of two peaks or completely resolved waves in the a.c. polarogram can be deduced. However, this is not possible with the quasi-reversible system, as such conditions are complicated functions of the various rate and thermodynamic parameters. Although correct, the statement that $E_{\frac{1}{2},1}{}^r \gg E_{\frac{1}{2},2}{}^r$ is required to observe completely resolved peaks, is hardly quantitative and it hides the fact that differences in $E_{\frac{1}{2},1}{}^r$ and $E_{\frac{1}{2},2}{}^r$ required to produce resolved waves will vary widely, depending on the values of k_h, α and ω.

Expressions for some other limiting cases of interest are worth examining because the simplified forms obtained may frequently be useful and will aid in the

discussion of a.c. polarographic behavior predicted from calculations based on the general form.

Case c. When

$$\chi_+ t^{\frac{1}{2}} \geq 50 \tag{48}$$

$$\chi_- t^{\frac{1}{2}} \geq 50 \tag{49}$$

the functions $G_1(t)$ and $G_2(t)$ reduce to

$$G_1(t) = \frac{1}{(1+e^{-j_1})(1+e^{-j_2}+e^{j_1})} \tag{50}$$

$$G_2(t) = \frac{1}{(1+e^{j_2})(1+e^{-j_2}+e^{j_1})} \tag{51}$$

Equations (48) and (49) define the diffusion-controlled *d.c.* process[5,13,20] so that eqns. (50) and (51) may be employed whenever the charge transfer rates are sufficiently rapid that the d.c. components of the surface concentrations maintain their Nernstian values.

Case d. One obtains when

$$\lambda_1 \gg \lambda_2 \tag{52}$$

$$Q = 4\left\{\frac{[1-(1+e^{-j_1})(1+e^{j_2})]^2}{(1+e^{-j_1})^2(1+e^{j_2})^2}\right\} + \frac{4(2\omega)^{\frac{1}{2}}}{\lambda_2}\left\{\frac{(1+e^{-j_1})(1+e^{j_2})-1}{(1+e^{-j_1})(1+e^{j_2})}\right\} + \frac{4\omega}{\lambda_2^2} + \frac{2(2\omega)^{\frac{3}{2}}}{\lambda_1\lambda_2^2} + \frac{(2\omega)^2}{\lambda_1^2\lambda_2^2} \tag{53}$$

$$Y = n_1^2 G_1(t)\left\{\frac{\left(1+e^{j_2}+\frac{n_2}{n_1}\right)[(1+e^{j_2})(1+e^{-j_1})-1]}{(1+e^{-j_1})(1+e^{j_2})^2} + \frac{(2\omega)^{\frac{1}{2}}}{\lambda_2}\left[\frac{n_1(1+e^{j_2})+n_2}{n_1(1+e^{j_2})}\right] + \frac{2\omega}{\lambda_2^2} + \frac{(2\omega)^{\frac{3}{2}}}{2\lambda_1\lambda_2^2}\right\}$$

$$+ n_2^2 G_2(t)\left\{\frac{\left(1+e^{-j_1}+\frac{n_1}{n_2}\right)[(1+e^{j_2})(1+e^{-j_1})-1]}{(1+e^{-j_1})^2(1+e^{j_2})} + \frac{(2\omega)^{\frac{1}{2}}}{\lambda_2}\left[\frac{n_2(1+e^{-j_1})+n_1}{n_2(1+e^{-j_1})}\right] + \frac{2\omega}{\lambda_1\lambda_2}\left[\frac{n_1+2n_2(1+e^{-j_1})}{2n_2(1+e^{-j_1})}\right] + \frac{(2\omega)^{\frac{3}{2}}}{2\lambda_1^2\lambda_2}\right\} \tag{54}$$

$$Z = n_1^2 G_1(t)\left\{\frac{\left(1+e^{j_2}+\frac{n_2}{n_1}\right)[(1+e^{j_2})(1+e^{-j_1})-1]}{(1+e^{-j_1})(1+e^{j_2})^2}\right.$$
$$\left. + \frac{(2\omega)^{\frac{1}{2}}}{\lambda_2}\left[\frac{(1+e^{j_2})(1+e^{-j_1})-1}{(1+e^{-j_1})(1+e^{j_2})}\right] + \frac{\omega}{\lambda_2^2}\right\}$$
$$+ n_2^2 G_2(t)\left\{\frac{\left(1+e^{-j_1}+\frac{n_1}{n_2}\right)[(1+e^{j_2})(1+e^{-j_1})-1]}{(1+e^{-j_1})^2(1+e^{j_2})}\right.$$
$$\left. + \frac{(2\omega)^{\frac{1}{2}}}{\lambda_1}\left[\frac{(1+e^{j_2})(1+e^{-j_1})-1}{(1+e^{-j_1})(1+e^{j_2})}\right] - \frac{\omega n_1}{\lambda_1\lambda_2 n_2(1+e^{-j_1})}\right\} \tag{55}$$

$$\psi_{1,0}(t) = \frac{1}{(1+e^{j_1})}\left[\frac{\lambda_2}{(1+e^{j_2})(1+e^{-j_1})}\exp(\chi_-^2 t)\operatorname{erfc}(\chi_- t^{\frac{1}{2}})\right.$$
$$\left. + \lambda_1 \exp(\lambda_1^2 t)\operatorname{erfc}(\lambda_1 t^{\frac{1}{2}})\right] \tag{56}$$

$$\psi_{2,0}(t) = \frac{\lambda_2}{(1+e^{j_1})(1+e^{j_2})}\exp(\chi_-^2 t)\operatorname{erfc}(\chi_- t^{\frac{1}{2}}) \tag{57}$$

$$\chi_- = \lambda_2\left[\frac{e^{j_2}+e^{-j_1}+e^{j_2-j_1}}{(1+e^{j_2})(1+e^{-j_1})}\right] \tag{58}$$

Equations (39) and (40) apply to $G_1(t)$ and $G_2(t)$. Equations (52)–(58) apply in any situation where the rate of the first charge transfer step greatly exceeds that of the second step. Further simplification is possible if the first step is so rapid that it exerts no kinetic influence at any frequency of interest. In this case one may apply the relations

$$\frac{(2\omega)^{\frac{1}{2}}}{\lambda_1} \simeq 0 \tag{59}$$

and

$$\lambda_1 \exp(\lambda_1^2 t)\operatorname{erfc}(\lambda_1 t^{\frac{1}{2}}) \simeq 0 \tag{60}$$

to eqns. (53)–(56).

Case e. The situation which is the reverse of case d occurs when

$$\lambda_2 \gg \lambda_1 \tag{61}$$

For this case Q is essentially the same as given in eqn. (53) except that λ_1 is replaced by λ_2 and *vice versa*. The other parameters are given by

$$Y = n_1^2 G_1(t)\left\{\frac{\left(1+e^{j_2}+\frac{n_2}{n_1}\right)[(1+e^{j_2})(1+e^{-j_1})-1]}{(1+e^{-j_1})(1+e^{j_2})^2}\right.$$

$$+\frac{(2\omega)^{\frac{1}{2}}}{\lambda_1}\left[\frac{n_1(1+e^{j_2})+n_2}{n_1(1+e^{j_2})}\right]+\frac{2\omega}{\lambda_1\lambda_2}\left[\frac{n_2+2n_1(1+e^{j_2})}{2n_1(1+e^{j_2})}\right]+\frac{(2\omega)^{\frac{3}{2}}}{2\lambda_1\lambda_2^2}\Bigg\}$$

$$+n_2^2\,G_2(t)\Bigg\{\frac{\left(1+e^{-j_1}+\frac{n_1}{n_2}\right)[(1+e^{j_2})(1+e^{-j_1})-1]}{(1+e^{-j_1})^2(1+e^{j_2})}$$

$$+\frac{(2\omega)^{\frac{1}{2}}}{\lambda_1}\left[\frac{n_2(1+e^{-j_1})+n_1}{n_2(1+e^{-j_1})}\right]+\frac{(2\omega)}{\lambda_1^2}+\frac{(2\omega)^{\frac{3}{2}}}{2\lambda_1^2\lambda_2}\Bigg\} \tag{62}$$

$$Z=n_1^2\,G_1(t)\Bigg\{\frac{\left(1+e^{j_2}+\frac{n_2}{n_1}\right)[(1+e^{j_2})(1+e^{-j_1})-1]}{(1+e^{-j_1})(1+e^{j_2})^2}$$

$$+\frac{(2\omega)^{\frac{1}{2}}}{\lambda_2}\left[\frac{(1+e^{j_2})(1+e^{-j_1})-1}{(1+e^{-j_1})(1+e^{j_2})}\right]-\frac{\omega}{\lambda_1\lambda_2}\left[\frac{n_2}{n_1(1+e^{j_2})}\right]\Bigg\}$$

$$+n_2^2\,G_2(t)\Bigg\{\frac{\left(1+e^{-j_1}+\frac{n_1}{n_2}\right)[(1+e^{j_2})(1+e^{-j_1})-1]}{(1+e^{-j_1})^2(1+e^{j_2})}$$

$$+\frac{(2\omega)^{\frac{1}{2}}}{\lambda_1}\left[\frac{(1+e^{j_2})(1+e^{-j_1})-1}{(1+e^{-j_1})(1+e^{j_2})}\right]+\frac{\omega}{\lambda_1^2}\Bigg\} \tag{63}$$

$$\psi_{1,0}(t)=\frac{\lambda_1}{(1+e^{j_1})}\exp(\chi_-^2\,t)\,\mathrm{erfc}(\chi_-\,t^{\frac{1}{2}}) \tag{64}$$

$$\psi_{2,0}(t)=\frac{\lambda_1}{(1+e^{j_1})(1+e^{j_2})}\exp(\chi_-^2\,t)\,\mathrm{erfc}(\chi_-\,t^{\frac{1}{2}}) \tag{65}$$

$$\chi_-=\lambda_1\left[\frac{e^{j_2}+e^{-j_1}+e^{j_2-j_1}}{(1+e^{j_2})\,(1+e^{-j_1})}\right] \tag{66}$$

Case f. Finally, a limiting case of considerable interest arises when the second reduction step can proceed at much more positive potentials than the first step; *i.e.*, when

$$E^r_{\frac{1}{2},2}\gg E^r_{\frac{1}{2},1} \tag{67}$$

The primary source of interest in this case is that distinction between the single- and two-step mechanisms is not possible under these conditions with reversible systems[1]. Condition (67) implies that

$$e^{j_2},\,e^{-j_1}\ll 1 \tag{68}$$

because the a.c. polarographic wave appears at d.c. potentials intermediate to and

well removed from $E_{\frac{1}{2},2}{}^{r}$ and $E_{\frac{1}{2},1}{}^{r}$. Applying eqn. (68) to eqns. (35), etc. yields

$$Q = 4\left\{(e^{j_2}+e^{-j_1})^2+(2\omega)^{\frac{1}{2}}\frac{(\lambda_1+\lambda_2)}{\lambda_1\lambda_2}(e^{j_2}+e^{-j_1})\right.$$
$$\left.+\frac{\omega(\lambda_1+\lambda_2)^2}{2\lambda_1^2\lambda_2^2}\left[1+\left(1+\frac{\sqrt{2\omega}}{\lambda_1+\lambda_2}\right)^2\right]\right\} \tag{69}$$

$$Y = n_1^2 G_1(t)\left\{\left(\frac{n_1+n_2}{n_1}\right)(e^{j_2}+e^{-j_1})+(2\omega)^{\frac{1}{2}}\left(\frac{\lambda_1+\lambda_2}{\lambda_1\lambda_2}\right)\left(\frac{n_1+n_2}{n_1}\right)\right.$$
$$\left.+\frac{2\omega}{\lambda_1\lambda_2^2}\left[\lambda_1+\lambda_2\left(\frac{n_2+2n_1}{2n_1}\right)\right]+\frac{(2\omega)^{\frac{3}{2}}}{2\lambda_1\lambda_2^2}\right\}$$
$$+ n_2^2 G_2(t)\left\{\left(\frac{n_1+n_2}{n_2}\right)(e^{j_2}+e^{-j_1})+(2\omega)^{\frac{1}{2}}\left(\frac{\lambda_1+\lambda_2}{\lambda_1\lambda_2}\right)\left(\frac{n_1+n_2}{n_2}\right)\right.$$
$$\left.+\frac{2\omega}{\lambda_1^2\lambda_2}\left[\lambda_2+\lambda_1\left(\frac{n_1+2n_2}{2n_2}\right)\right]+\frac{(2\omega)^{\frac{3}{2}}}{2\lambda_1^2\lambda_2}\right\} \tag{70}$$

$$Z = n_1^2 G_1(t)\left\{\left(\frac{n_1+n_2}{n_1}\right)(e^{j_2}+e^{-j_1})\right.$$
$$\left.+\frac{(2\omega)^{\frac{1}{2}}}{\lambda_2}(e^{j_2}+e^{-j_1})+\frac{\omega}{\lambda_1\lambda_2^2}\left(\frac{n_1\lambda_1-n_2\lambda_2}{n_1}\right)\right\}$$
$$+ n_2^2 G_2(t)\left\{\left(\frac{n_2+n_1}{n_2}\right)(e^{j_2}+e^{-j_1})\right.$$
$$\left.+\frac{(2\omega)^{\frac{1}{2}}}{\lambda_1}(e^{j_2}+e^{-j_1})+\frac{\omega}{\lambda_1^2\lambda_2}\left(\frac{n_2\lambda_2-n_1\lambda_1}{n_2}\right)\right\} \tag{71}$$

$$G_1(t) = \frac{1}{[1+e^{(j_1+j_2)}]}\left\{e^{j_2}+\frac{\psi_{2,0}(t)}{\lambda_2}+\frac{[\alpha_1-\beta_1 e^{(j_1+j_2)}]}{\lambda_1}\psi_{1,0}(t)\right\} \tag{72}$$

$$G_2(t) = \frac{1}{[1+e^{(j_1+j_2)}]}\left\{e^{j_2}-\frac{e^{(j_1+j_2)}}{\lambda_1}\psi_{1,0}(t)+\frac{[\alpha_2-\beta_2 e^{(j_1+j_2)}]}{\lambda_2}\psi_{2,0}(t)\right\} \tag{73}$$

$$\psi_{1,0}(t) = \frac{\lambda_1}{(1+e^{j_1})(\lambda_1+\lambda_2)}[\lambda_2\exp(\chi_-^2 t)\operatorname{erfc}(\chi_- t^{\frac{1}{2}})+\lambda_1\exp(\chi_+^2 t)\operatorname{erfc}(\chi_+ t^{\frac{1}{2}})] \tag{74}$$

$$\psi_{2,0}(t) = \frac{\lambda_1\lambda_2}{(\lambda_1+\lambda_2)(1+e^{j_1})(1+e^{j_2})}\exp(\chi_-^2 t)\operatorname{erfc}(\chi_- t^{\frac{1}{2}}) \tag{75}$$

$$\chi_+ = \lambda_1+\lambda_2 \tag{76}$$

$$\chi_- = \frac{\lambda_1 \lambda_2 (e^{j_2} + e^{-j_1})}{\lambda_1 + \lambda_2} \tag{77}$$

$$\lambda_1 = \frac{k_{h,1} f_1}{D_1^{\frac{1}{2}}} e^{\beta_1 j_1} \tag{78}$$

$$\lambda_2 = \frac{k_{h,2} f_2}{D_2^{\frac{1}{2}}} e^{-\alpha_2 j_2} \tag{79}$$

Equations (69)–(79) should prove reasonably accurate when $E_{\frac{1}{2},2}^r \gg E_{\frac{1}{2},1}^r$ except when the charge transfer coefficients have extreme values (*i.e.*, $\alpha_2 \to 0$ and/or $\alpha_1 \to 1$). To obtain eqns. (74)–(77) it should be noted that under these conditions

$$(\lambda_1 + \lambda_2)^2 \gg 4K \tag{80}$$

which permits simplification of eqn. (44) with the aid of the binomial theorem. The above equations for cases c–f will be discussed below.

DISCUSSION OF PREDICTED A. C. POLAROGRAPHIC BEHAVIOR FOR THE QUASI-REVERSIBLE TWO-STEP REDUCTION

The existence of four parameters (α, k_h, n, E^0) characterizing each charge transfer step, and the complexity of the functional relations describing the a.c. polarographic wave make difficult, a simple, complete analysis and discussion of the theoretical predictions. To aid in obtaining detailed insight into these predictions and to answer certain significant questions regarding a.c. polarographic behavior with the quasi-reversible two-step mechanism, numerous calculations encompassing a wide range of conditions have been performed with the aid of the IBM 709 digital computer. A sampling of the results of these calculations, hopefully representative of the most salient aspects of the theory, will be discussed here. A Fortran IV computer program used in these calculations can be obtained from the authors on written request.

Figures 1–21 illustrate the nature of the predictions of eqn. (35). All results shown correspond to the case where $n_1 = n_2 = 1$. This is done to confine considerations to the effects of the relative values of k_h, α, and $E_{\frac{1}{2}}^r$ and because this situation is likely to be the commonest example of the two-step process. It should be recognized in examining these figures that choice of position of the waves on the d.c. potential axis is purely arbitrary and has no effect on the wave characteristics. The magnitude of the separation of $E_{\frac{1}{2}}^r$ values is the parameter of interest.

Despite the many variations in behavior illustrated in Figs. 1–21, it is often possible to establish the source, and qualitatively rationalize, many of the effects predicted, using as a basis the well-known predictions for the single-step mechanism[5,13,21]. This occurs because many of the effects shown are similar to what one would expect for an a.c. wave in which two completely independent, single-step charge transfer processes contribute to the total alternating current (*i.e.*, as with a multicomponent system[12]). The implication of this observation is that, although coupled, the individual charge transfer steps in the step-wise mechanism

$$O + n_1 e \rightleftharpoons Y + n_2 e \rightleftharpoons R \tag{R1}$$

often retain to a significant extent their own identity in contributing to the total alternating current. This is not a surprising result in view of the close relationship between the mechanism involving step-wise charge transfer and one involving two completely independent steps, *i.e.*,

$$O + n_1 e \rightleftharpoons Y$$

$$Z + n_2 e \rightleftharpoons R \qquad (R2)$$

Indeed, when $E_{\frac{1}{2},1}^{r} \gg E_{\frac{1}{2},2}^{r}$, the two mechanisms are mathematically equivalent as exemplified by eqn. (47), and as pointed out elsewhere[12]. If the $E_{\frac{1}{2}}^{r}$-values are more comparable (currents due to the two charge transfer steps overlap), the mathematical equivalence of the two mechanisms is destroyed on a quantitative basis, but many qualitative features remain common to both mechanisms (R1) and (R2), as one might expect. Of course, in the extreme case where $E_{\frac{1}{2},2}^{r} \gg E_{\frac{1}{2},1}^{r}$, the two mechanisms will cease to show even common qualitative characteristics. As will become evident in the discussion to follow (regarding Figs. 19 and 20), when $E_{\frac{1}{2},2}^{r} \gg E_{\frac{1}{2},1}^{r}$, the a.c. polarographic wave for the mechanism of interest (reaction (R1)) is influenced profoundly by coupling of the charge transfer steps, making this the dominant factor. Thus, while one should not be indiscriminate in seeking or expecting analogous qualitative behavior for the mechanisms represented by reactions (R1) and (R2), conditions frequently do exist where qualitative similarities in behavior are to be found. When existent, such similarities may be considered a valid and useful rationale for the predictions of eqn. (35).

Careful study has indicated that, regardless of the situation, the main factors to be taken into account in rationalizing the predictions of eqn. (35) are the relative and/or absolute values of k_h, α, and $E_{\frac{1}{2}}^{r}$ for the two steps, as well as the status of the d.c. process (*i.e.*, whether it is diffusion-controlled or influenced by charge transfer kinetics). Thus, the following discussion will be categorized correspondingly.

(*A*) *Influence of the difference in* $E_{\frac{1}{2}}^{r}$ *values*

The predicted influence of the difference in $E_{\frac{1}{2}}^{r}$-values on the magnitude and shape of the a.c. polarographic wave with a quasi-reversible two-step process, has a number of qualitative similarities to the behavior predicted for the reversible[1] system and a few marked differences. Interpretation of the similar features is the same as for the reversible system so discussion will dwell primarily on the differences.

As with the reversible system, when $E_{\frac{1}{2},1}^{r} \gg E_{\frac{1}{2},2}^{r}$, completely resolved waves are predicted (*cf.*, eqn. (47)) for the quasi-reversible two-step process. For any given set of rate parameters, positive variation of $E_{\frac{1}{2},2}^{r}$ (all other parameters held constant) yields a merging of the resolved waves, eventually into a single peak. Continued positive variation of $E_{\frac{1}{2},2}^{r}$ beyond this point, at first produces an increase in height and decrease in width of the a.c. polarogram, just as observed with the reversible system[1] (compare Figs. 1B and 4B, 2B and 5B or 3B and 6B). However, the predicted magnitude of the wave does not approach an upper limit for $E_{\frac{1}{2},2}^{r} \gg E_{\frac{1}{2},1}^{r}$, as one finds with the reversible system, but passes through a maximum and begins to decrease with additional increase in $E_{\frac{1}{2},2}^{r}$ (*c.f.*, Fig. 19B). In other words, for a given set of rate parameters, the system is predicted to be more subject to the effects of charge transfer kinetics as $E_{\frac{1}{2},2}^{r}$ is made more positive relative to $E_{\frac{1}{2},1}^{r}$. This is reflected also in the

phase angle where deviations of cot ϕ from unity are seen to increase as $E_{\frac{1}{2},2}{}^r$ increases. This may be seen by comparing the figures just cited. The effect is particularly pronounced when $E_{\frac{1}{2},2}{}^r \gg E_{\frac{1}{2},1}{}^r$, as seen in Figs. 19A and 20A. In Fig. 20, k_h-values of 10 cm sec^{-1} produce substantial deviations from reversible behavior (deviations of cot ϕ from unity), even at the relatively low frequency of 143.4 c/sec ($\omega/2\pi$). With the same rate parameters, a single-step mechanism would yield essentially undetectable deviations from reversible behavior (cot $\phi = 1.007$ at peak). It appears that the enhanced influence of charge transfer kinetics with increasing $E_{\frac{1}{2},2}{}^r$, observed in both current amplitude and phase angle data, can be explained on the basis of two effects. First, it is known that the magnitude of alternating current required of each charge transfer step to maintain Nernstian conditions increases as the parameter, $E_{\frac{1}{2},2}{}^r - E_{\frac{1}{2},1}{}^r$ increases[1], producing correspondingly increased demands on each charge transfer step. For this reason, one would expect enhanced deviations from Nernstian behavior to be apparent in the current amplitude and phase angle read-out as $E_{\frac{1}{2},2}{}^r - E_{\frac{1}{2},1}{}^r$ increases, other factors held constant. That still another effect is responsible, in part, for the phenomena in question is suggested by the fact that currents required to maintain Nernstian conditions become constant when $E_{\frac{1}{2},2}{}^r - E_{\frac{1}{2},1}{}^r \geq 0.20$ V[1] (approx.) while positive deviations of $E_{\frac{1}{2},2}{}^r - E_{\frac{1}{2},1}{}^r$ in excess of 0.20 V produce further decrease in wave height and increases in cot ϕ (Figs. 19 and 20). It appears that the origin of the second effect is found in the position of the wave relative to the $E_{\frac{1}{2}}{}^r$-value (or E^0-values), a factor described previously by SMUTEK[19]. When $E_{\frac{1}{2},2}{}^r \gg E_{\frac{1}{2},1}{}^r$, the wave appears at d.c. potentials intermediate to and well-removed from the $E_{\frac{1}{2}}{}^r$-values. Under such conditions, the rate of reduction of the first step and the rate of oxidation of the second step are considerably suppressed due to the very small values of the exponential terms in the rate expressions (eqns. (1) and (2). As $E_{\frac{1}{2},2}{}^r - E_{\frac{1}{2},1}{}^r$ increases, the wave is further removed from the respective $E_{\frac{1}{2}}{}^r$-values and this effect becomes more pronounced. It is apparent that maintenance of alternating currents sufficient to achieve Nernstian conditions is made more difficult by such circumstances, producing greater influence of charge transfer kinetics.

Mathematical expression of these effects is seen in eqns. (69)–(79). In particular, it should be noted that the frequency independent terms in the parameters Q, Y, and Z, which must predominate to achieve reversible conditions, are very small (*cf.*, eqn. (68)). From these expressions, approximate criteria for reversible behavior is found to be given by

$$\frac{(2\omega)^{\frac{1}{2}}(\lambda_1+\lambda_2)}{\lambda_1\lambda_2} \ll e^{j_2}+e^{-j_1} \tag{81}$$

or, for usual experimental uncertainties ($\pm 1\%$ or less), one has

$$\frac{(2\omega)^{\frac{1}{2}}(\lambda_1+\lambda_2)}{\lambda_1\lambda_2} \leq 10^{-2}(e^{j_2}+e^{-j_1}) \tag{82}$$

For the rate parameters given in Fig. 20A and 20B, eqn. (82) becomes, at the peak of the wave,

$$\omega^{\frac{1}{2}} \lesssim 0.125 \tag{83}$$

and

$$\omega^{\frac{1}{2}} \gtrsim 3.2 \tag{84}$$

respectively. Thus, even at the lowest frequencies employed in a.c. polarography ($\sim$10 c/sec), reversible behavior would not be observed for the system depicted in Fig. 20, despite the large values of k_h. The condition for reversibility at the peak of the wave with a single-step reduction involving $\alpha = 0.50$ and $k_h = 10$ cm sec^{-1} is given by

$$\omega^{\frac{1}{2}} \lesssim 45 \tag{85}$$

Contrasting eqn. (85) with eqns. (83) and (84) makes apparent the extreme difference in the condition for reversible behavior associated with single-step and two-step mechanisms when $E_{\frac{1}{2},2}^r \gg E_{\frac{1}{2},1}^r$.

(*B*) *Influence of the charge transfer coefficients*

Figures 1–8 illustrate some interesting predictions in which the relative values of α_1 and α_2 play an important role. In this series of figures, $k_{h,1} = k_{h,2} = 0.100$ cm sec^{-1} so that influence of k_h is held constant and differences arise from variations in the α-values. Comparison of Figs. 1, 2 and 3 shows that when $\alpha_1 > \alpha_2$ (Fig. 2), the a.c. polarogram (current amplitude wave) tends to be narrower than when $\alpha_1 = \alpha_2$ (Fig. 1). On the other hand, the cot ϕ–$E_{d.c.}$ plot shows a wave (phase angle wave) which is wider when $\alpha_1 > \alpha_2$ than when $\alpha_1 = \alpha_2$. The exact opposite effect appears when $\alpha_1 < \alpha_2$ (Fig. 3) with the phase angle wave appearing narrower and the current amplitude wave wider than when $\alpha_1 = \alpha_2$. This dependence of the width of the wave on the relative α-values is made even more apparent by comparing Figs. 4, 5 and 6 which depict conditions where resolved or near-resolved peaks appear. When resolved peaks appear with $\alpha_1 = \alpha_2 = 0.50$ (Fig. 4), the degree of resolution found in the current amplitude and phase angle waves are comparable and nearly independent of frequency. The resolution predicted for the current amplitude wave is roughly the same as would be expected for a reversible wave with the same separation in $E_{\frac{1}{2}}^r$-values. Figure 5 shows that with $\alpha_1 > \alpha_2$, resolution of peaks in the current amplitude wave is reduced, with the effect becoming noticeably more pronounced at higher frequencies. At the same time, resolution of peaks in the phase angle wave is considerably enhanced relative to the situation where $\alpha_1 = \alpha_2 = 0.50$, but is essentially independent of frequency. When $\alpha_1 < \alpha_2$ (Fig. 6), resolution of the current amplitude wave is greater than when $\alpha_1 = \alpha_2 = 0.5$, and the degree of resolution is seen to increase with increasing frequency. Resolution of phase angle peaks is destroyed in this case, and frequency again plays a minor role. It is apparent that the effects illustrated in Figs. 5 and 6 are merely extensions of those shown in Figs. 2 and 3, respectively, with the effect of frequency being readily apparent only in the former. Figure 7 shows that when $\alpha_2 > \alpha_1$, theory predicts the possibility of observing resolved peaks on an a.c. polarogram (at $\omega = 8100$ sec^{-1}) arising from a quasi-reversible two-step process with a separation of $E_{\frac{1}{2}}^r$-values of 50 mV. This separation is considerably smaller than the minimum separation (71 mV for $n_1 = n_2 = 1$) required for resolution of peaks with a reversible two-step wave[1]. When charge transfer coefficients for the two charge transfer steps are equal, but different from one-half, the symmetrical read-out

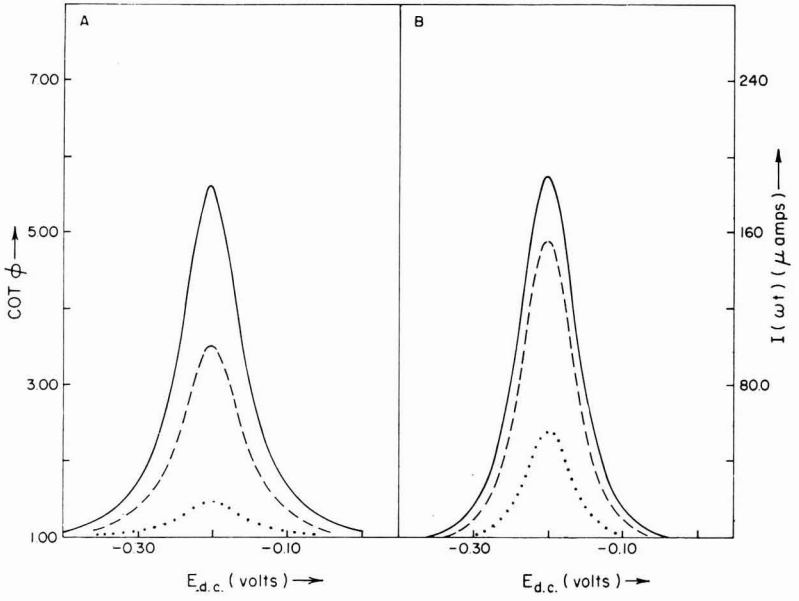

Fig. 1.

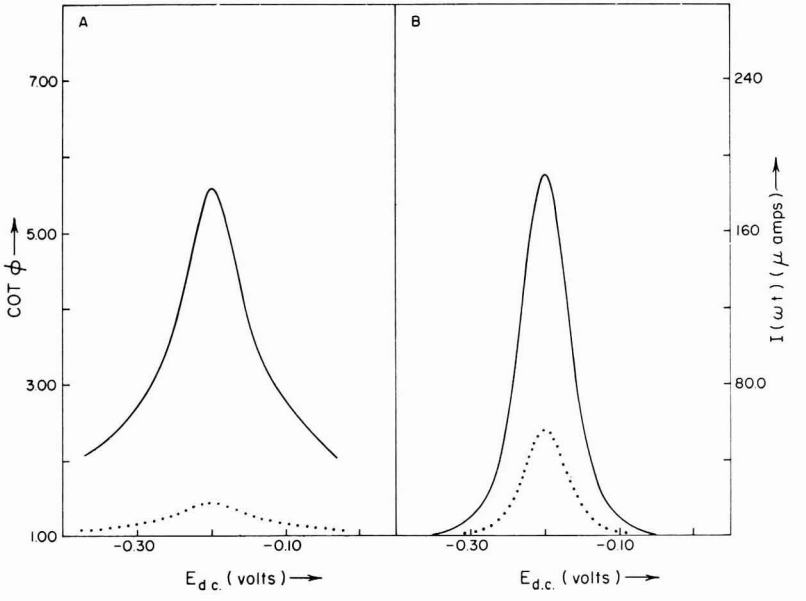

Fig. 2.

Figs. 1–10. Calculated a.c. polarographic current and phase angle with two-step reduction (. . . .), $\omega = 100\ \mathrm{sec}^{-1}$; (— — —), $\omega = 2500\ \mathrm{sec}^{-1}$; (———), $\omega = 8100\ \mathrm{sec}^{-1}$. $n_1 = n_2 = 1$, $T = 298°\mathrm{K}$, $\Delta E = 5.00$ mV, $C_O^* = 5.00 \cdot 10^{-3}\ M$, $A = 3.50 \cdot 10^{-2}\ \mathrm{cm}^2$, $D_O = D_Y = D_R = 1.00 \cdot 10^{-5}\ \mathrm{cm}^2\ \mathrm{sec}^{-1}$. (A), phase angle; (B), current amplitude. Values of k_h, $\varkappa$ and $E_{\frac{1}{2}}{}^r$ are given in the following table:

Fig.	$k_{h,1}$ *(cm sec^{-1})*	$k_{h,2}$ *(cm sec^{-1})*	$\varkappa_1$	$\varkappa_2$	$E_{\frac{1}{2},1}{}^r$ *(V)*	$E_{\frac{1}{2},2}{}^r$ *(V)*
1	0.100	0.100	0.500	0.500	−0.200	−0.200
2	0.100	0.100	0.800	0.200	−0.200	−0.200
3	0.100	0.100	0.200	0.800	−0.200	−0.200
4	0.100	0.100	0.500	0.500	−0.200	−0.300
5	0.100	0.100	0.800	0.200	−0.200	−0.300
6	0.100	0.100	0.200	0.800	−0.200	−0.300
7	0.100	0.100	0.200	0.800	−0.200	−0.250
8	0.100	0.100	0.800	0.800	−0.200	−0.300
9	1.00×10^{-2}	1.00	0.800	0.200	−0.200	−0.300
10	1.00	1.00×10^{-2}	0.800	0.200	−0.200	−0.200

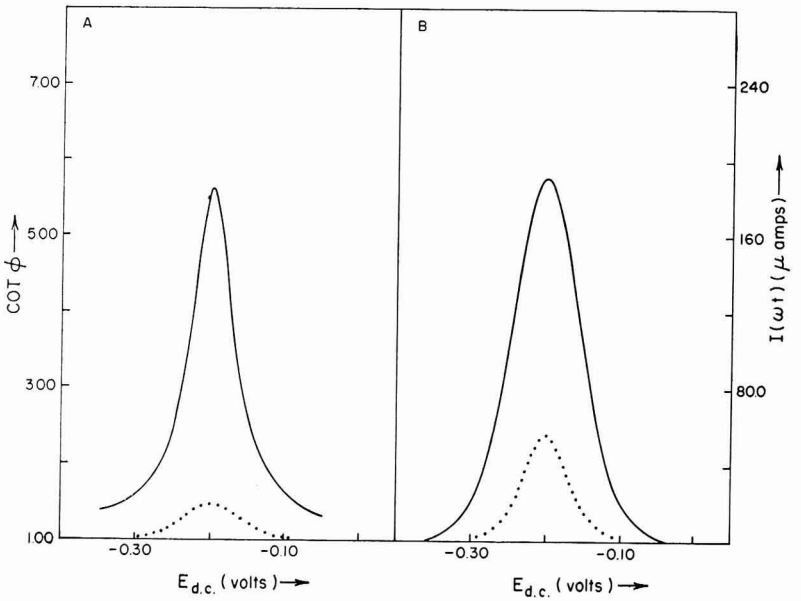
A
B
7.00
5.00
3.00
1.00
240
160
800
COT φ
I(ωt) (μ amps)
-0.30
-0.10
-0.30
-0.10
E d.c. (volts)
E d.c. (volts)

Fig. 3.

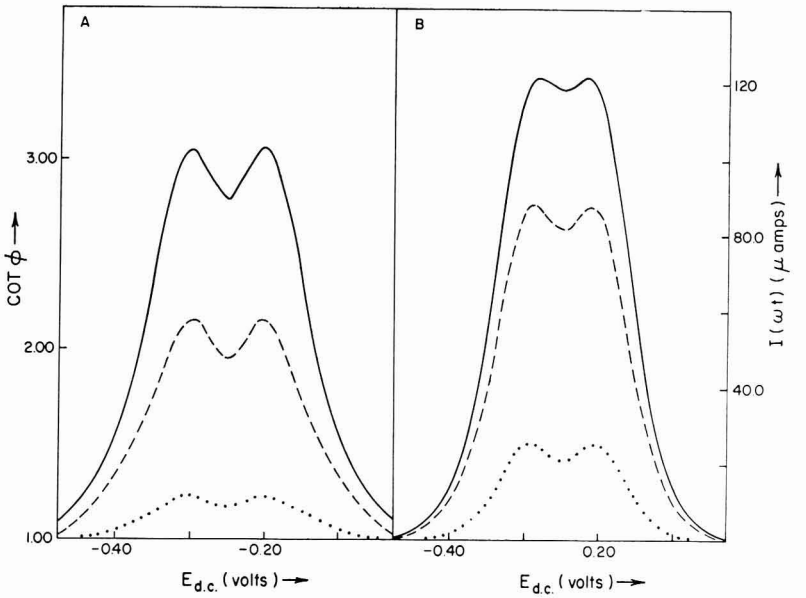
A
B
3.00
2.00
1.00
120
80.0
40.0
COT φ
I(ωt) (μ amps)
-040
-0.20
-0.40
0.20
E d.c. (volts)
E d.c. (volts)

Fig. 4.

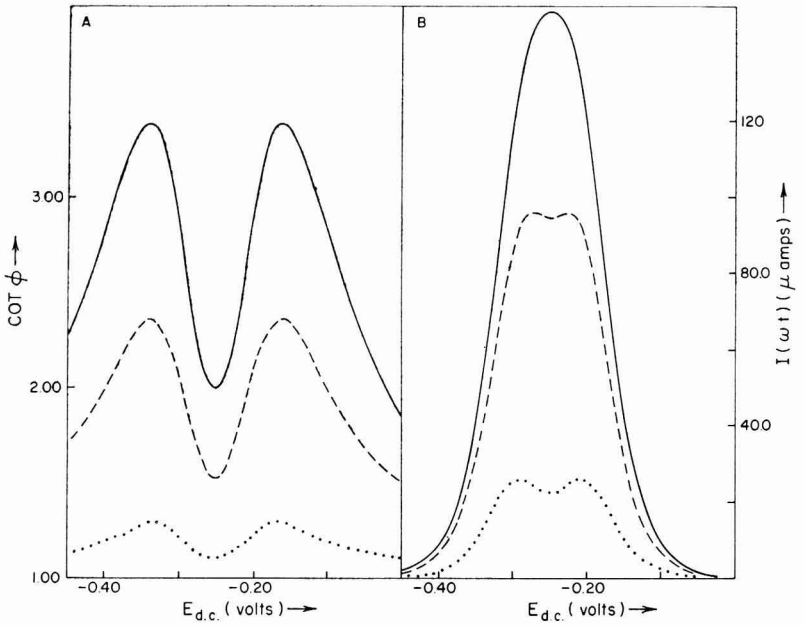
A
B
3.00
2.00
1.00
COT φ
120
80.0
40.0
I(ωt) (μ amps)
-0.40
-0.20
E d.c. (volts)

Fig. 5.

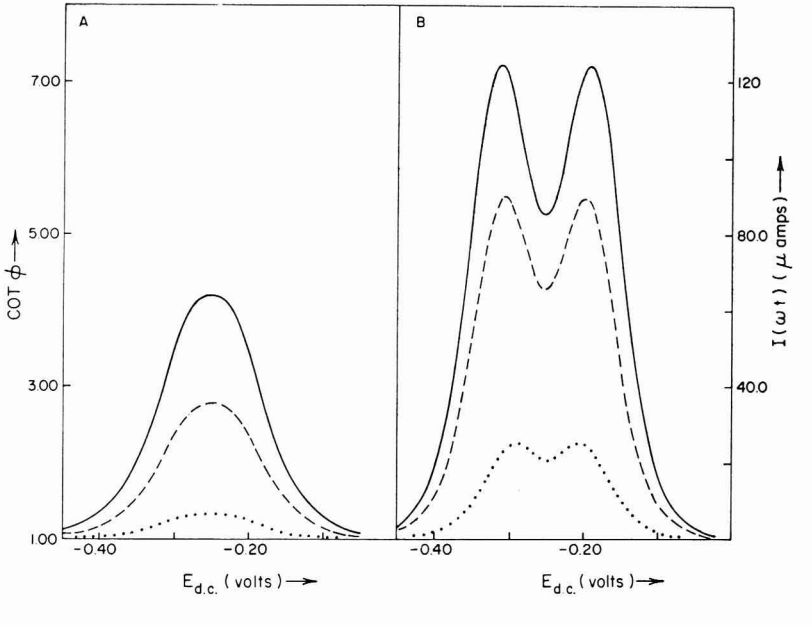
A
B
7.00
5.00
3.00
1.00
COT φ
120
80.0
40.0
I(ωt) (μ amps)
-0.40
-0.20
E d.c. (volts)

Fig. 6.

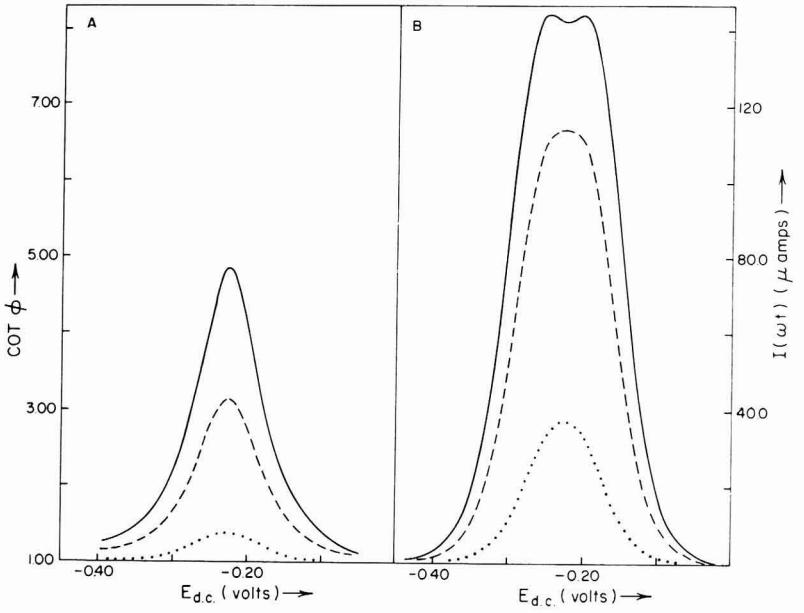
A
B
7.00
5.00
3.00
1.00
COT φ
120
80.0
40.0
I(ωt) (μ amps)
-0.40
-0.20
E d.c. (volts)

Fig. 7.

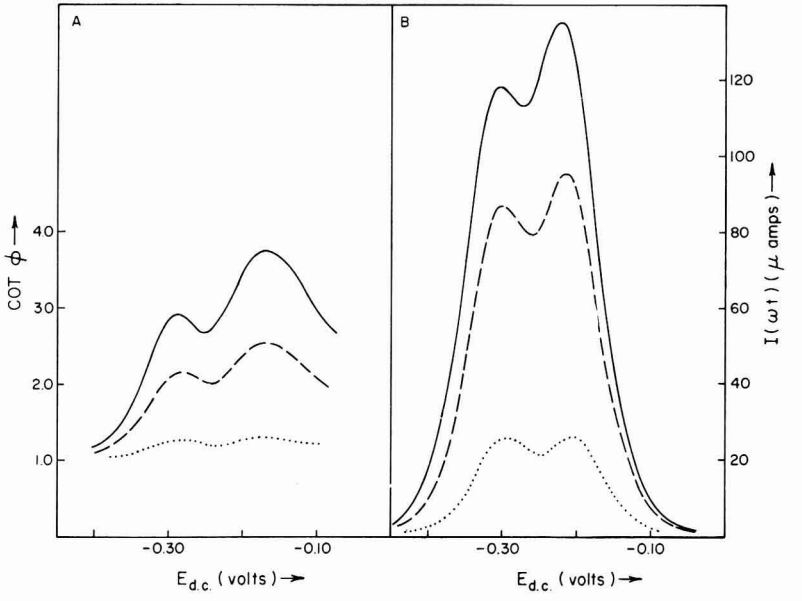
A
B
40
30
20
1.0
COT φ
120
100
80
60
40
20
I(ωt) (μ amps)
-0.30
-0.10
E d.c. (volts)

Fig. 8.

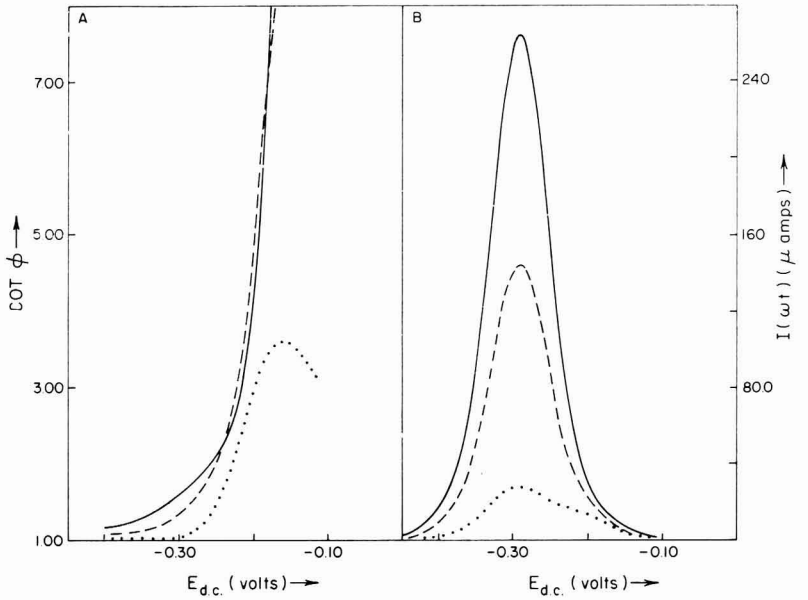
A
B
7.00
5.00
3.00
1.00
240
160
80.0
COT ϕ ⟶
I(ωt) (μ amps) ⟶
-0.30
-0.10
$E_{d.c.}$ (volts) ⟶

Fig. 9.

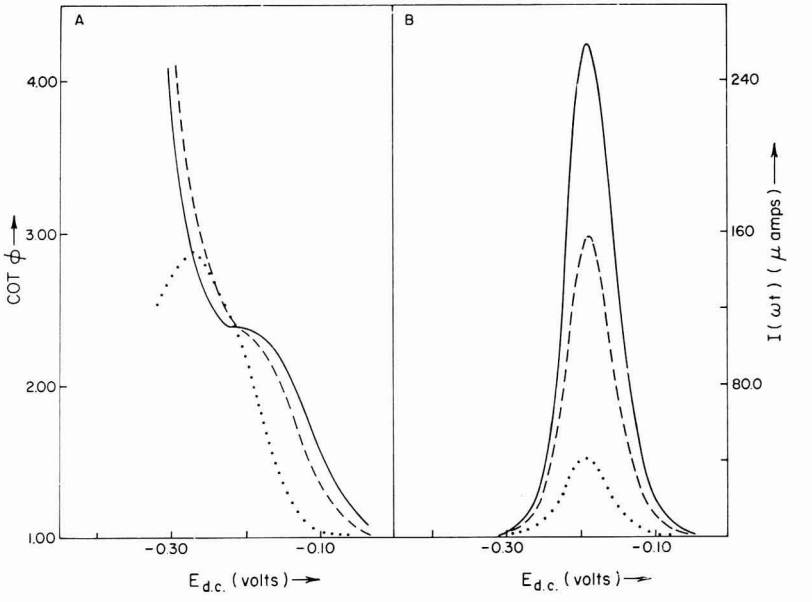
A
B
4.00
3.00
2.00
1.00
240
160
80.0
COT ϕ ⟶
I(ωt) (μ amps) ⟶
-0.30
-0.10
$E_{d.c.}$ (volts) ⟶

Fig. 10.

associated with $\alpha_1=\alpha_2=0.5$ (Figs. 1 and 5) is not predicted. Figure 8 shows results of calculations for $\alpha_1=\alpha_2=0.80$. When $\alpha_1=\alpha_2=0.20$, one obtains essentially mirror images of Figs. 8A and 8B with respect to the abscissa. As when $\alpha_1=\alpha_2=0.50$, Fig. 8 shows roughly comparable resolution in the phase angle- and current amplitude-waves and the influence of frequency on the separation of peaks is relatively minor. However the peak occurring at more positive d.c. potentials grows more rapidly with frequency than the negative peak, yielding an unsymmetrical response at higher frequencies.

The influence of α-values on the characteristics of a.c. polarographic data depicted in Figs. 1–8, as well as effects of k_h-values, etc. shown in the remaining figures, may appear at first glance sufficiently complex as to defy simple intuitive explanation. However, the previously mentioned analogous behavior associated with the mechanism involving step-wise charge transfer and that involving independent charge transfer appears operative in Figs. 1–8, enabling a reasonable explanation of the effects illustrated. One simply recalls the influence of α on the position of maximum current and cot ϕ in a.c. polarographic currents associated with the single-step, quasi-reversible wave[5,13,21] and assumes these effects remain qualitatively operative with regard to the individual charge transfer steps in the step-wise mechanism. The influence of α on the characteristics of the single-step wave are summarized in Table 1 for convenience. Thus, the tendency of the a.c. polarogram arising from a quasi-reversible two-step mechanism to yield narrower waves and/or less resolved peaks when $\alpha_1=0.80$ and $\alpha_2=0.20$ than when $\alpha_1=\alpha_2=0.50$ (or when the wave is reversible[1,2]), can be interpreted as arising from the fact that the peak current due to the first step is shifted to negative potentials by large values of α, while the small values of α produce the opposite effect with the second step (*c.f.*, Table 1). Thus the faradaic alternating current is confined to a narrower region of d.c. potential when $\alpha_1=0.80$ and $\alpha_2=0.20$. Because these shifts in position of maximum current due to the individual charge transfer steps are enhanced by increasing frequency, the two-step wave

TABLE 1

INFLUENCE OF CHARGE TRANSFER COEFFICIENTS ON POSITION OF PEAK CURRENT AMPLITUDE AND COT ϕ

For $k_h > 10^{-2}$ cm sec^{-1}, *i.e.*, diffusion-controlled d.c. processes.

Value of α	*D.c. potential corresponding to peak current amplitude*	*D.c. potential corresponding to peak cot* ϕ
0.5	peak potential $= E_{\frac{1}{4}}{}^r$ at all frequencies	peak potential $= E_{\frac{1}{4}}{}^r$ at all frequencies
>0.5	peak potential $< E_{\frac{1}{4}}{}^r$; deviations from $E_{\frac{1}{4}}{}^r$ increase with increasing frequency, approaching a limiting value at high frequencies given by $[E_{d.c.}]_{peak} = E_{\frac{1}{4}}{}^r + \frac{RT}{nF} \ln \frac{1-\alpha}{\alpha}$	peak potential $> E_{\frac{1}{4}}{}^r$; value of peak potential is independent of frequency.
<0.5	peak potential $> E_{\frac{1}{4}}{}^r$; deviations from $E_{\frac{1}{4}}{}^r$ increasing with increasing frequency. High frequency limit defined by same equation as above.	peak potential $< E_{\frac{1}{4}}{}^r$; value of peak potential is independent of frequency.

becomes narrower (Fig. 2) and/or exhibits less resolved peaks (Fig. 5) as frequency increases. The broader and/or highly resolved peaks in the phase angle wave with the same combination of α-values appear to manifest the fact that the shift in the d.c. potential of maximum cot ϕ associated with the individual charge transfer steps is in direct opposition to the corresponding shift in the current amplitude wave for large ($\alpha > 0.5$) or small ($\alpha < 0.5$) values of the charge transfer coefficient. Thus, a narrowing in the current amplitude wave is associated with a broadening in the phase angle wave when the source of the effect is found in the values of α. The frequency independence of the position of the phase angle peak with a single charge transfer step appears to lead to the relative frequency insensitivity of the width and resolution of the phase angle waves due to the two-step mechanism. Similar arguments may be used to explain the differences between Figs. 1 and 3 or Figs. 4 and 6. Table 1 indicates that the combination, $\alpha_1 = 0.20$ and $\alpha_2 = 0.80$, should lead to increased width and/or resolution in the current amplitude wave and the opposite effect in the phase angle wave, as is observed in Figs. 3 and 6.

Theory for the single-step wave suggests that equal values of α and k_h would lead to no shift ($\alpha_1 = \alpha_2 = 0.5$) or equal shifts ($\alpha_1 = \alpha_2 \neq 0.5$) in the position of maximum current and cot ϕ relative to $E_{\frac{1}{2}}{}^r$ for the alternating currents due to the individual charge transfer steps in the two-step mechanism. Calculations seem to confirm this expectation as seen in Figs. 4 and 8. Like the other effects discussed above, the asymmetry of the waves in Fig. 8 would be expected for an a.c. polarogram arising from two independent charge transfer processes (mechanism R(2)). It manifests the asymmetry in the alternating current–d.c. potential behavior associated with independent, single-step charge transfer processes[5,13,21]. Figure 8 seems to indicate that this effect remains operative with coupled charge transfer steps. However, the difference in peak heights depicted in Fig. 8 is larger than predicted for two independent charge transfer steps[4]. The origin of this enhancement of asymmetry probably lies in the coupling of the charge transfer steps.

These contributions of the charge transfer coefficient to the form of the a.c. polarographic read-out, as illustrated in Figs. 1–8, are likely existent in all the results shown. However, they are frequently difficult to discern because of the importance of other effects such as non-Nernstian d.c. surface concentrations, etc.

(C) Influence of k_h values

The effect of k_h-values on characteristics of the a.c. polarogram predicted by eqn. (35) are both varied and interesting, but also predictable in terms of the simplified qualitative model employed above. When $k_{h,1}$ and $k_{h,2}$ are nearly equal, one would expect alteration of the magnitude of the wave to be the main effect of variation of k_h. Other characteristics, such as width of wave (amplitude or phase angle), resolution, etc., should be somewhat insensitive to the absolute magnitude of the k_h-values, except when k_h becomes so small that non-Nernstian conditions in the d.c. process become important (see below). On the other hand, when k_h-values differ significantly, the influence of charge transfer kinetics will cause substantial alteration in resolution, dependence of wave characteristics on frequency, etc. One would expect this to occur because in such situations the contribution of the slower of the two steps to the total alternating current will be relatively small. This will tend to destroy resolution and/or reduce the width of the wave, if all other factors remain unchanged. While the a.c.

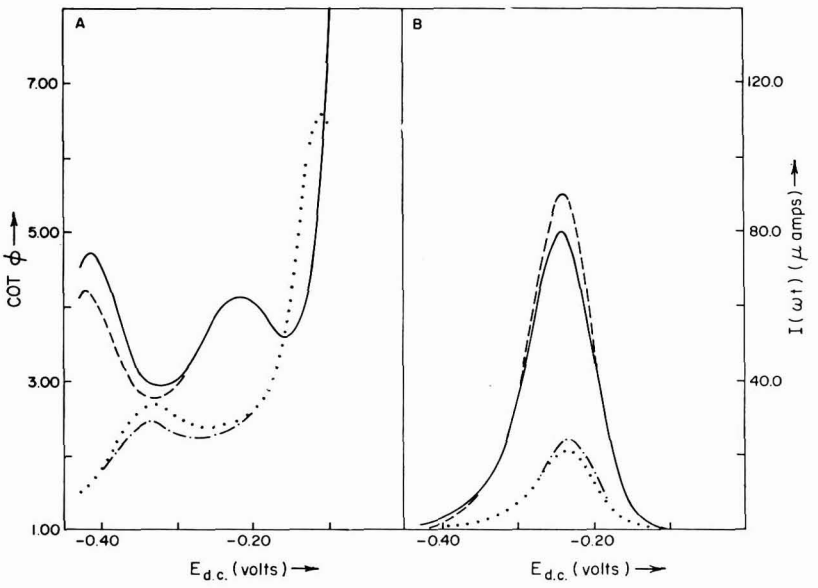

Fig. 11.

Figs. 11–17. Calculated a.c. polarographic current and phase angle with two-step reduction: (———), $\omega = 8100$ sec^{-1}, $\tau = 4.00$ sec; (— — —), $\omega = 8100$ sec^{-1}, $\tau = 9.00$ sec; (. . . . .), $\omega = 100$ sec^{-1}, $\tau = 4.00$ sec; (·–·–·), $\omega = 100$ sec^{-1}, $\tau = 9.00$ sec (τ = drop life). $n_1 = n_2 = 1$, $T = 298$°K, $\Delta E = 5.00$ mV, $C_O^* = 5.00 \cdot 10^{-3}$ M, $A = 3.50 \cdot 10^{-2}$ cm^2, $D_O = D_Y = D_R = 1.00 \cdot 10^{-5}$ cm^2 sec^{-1}. (A), phase angle; (B), current amplitude. Values of k_h, α and $E_{\frac{1}{4}}^r$ are given in the following table:

Fig.	$k_{h,1}$ *(cm sec^{-1})*	$k_{h,2}$ *(cm sec^{-1})*	α_1	α_2	$E_{\frac{1}{4},1}^r$ *(V)*	$E_{\frac{1}{4},2}^r$ *(V)*
11	1.00×10^{-3}	0.100	0.500	0.500	−0.200	−0.220
12	1.00×10^{-2}	1.00×10^{-3}	0.500	0.500	−0.200	−0.300
13	1.00×10^{-2}	1.00	0.500	0.500	−0.300	−0.200
14	1.00×10^{-2}	1.00	0.800	0.200	−0.300	−0.200
15	1.00	1.00×10^{-2}	0.800	0.200	−0.300	−0.200
16	1.00×10^{-3}	1.00×10^{-3}	0.500	0.500	−0.200	−0.300
17	1.00×10^{-2}	1.00×10^{-2}	0.500	0.500	−0.200	−0.400

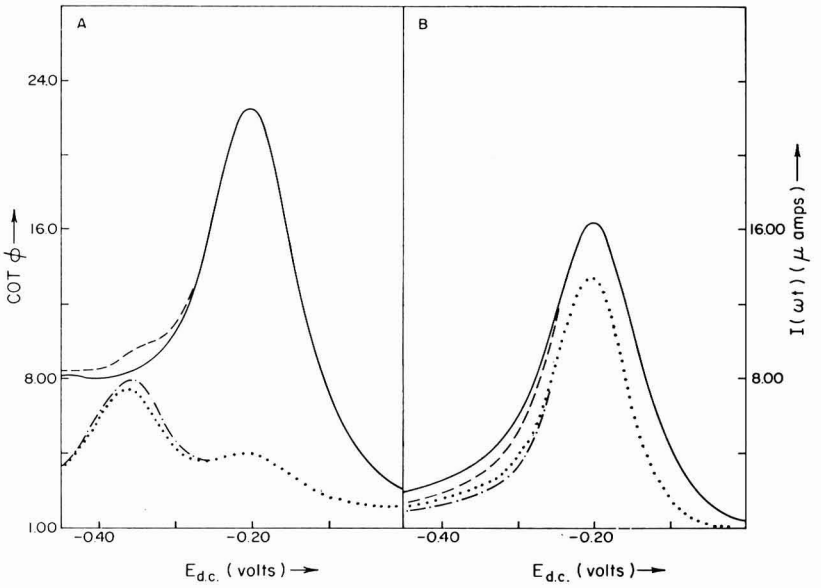
A
B
24.0
16.0
8.00
1.00
COT ϕ ⟶
I(ωt) (μ amps) ⟶
16.00
8.00
-0.40
-0.20
$E_{d.c.}$ (volts) ⟶

Fig. 12.

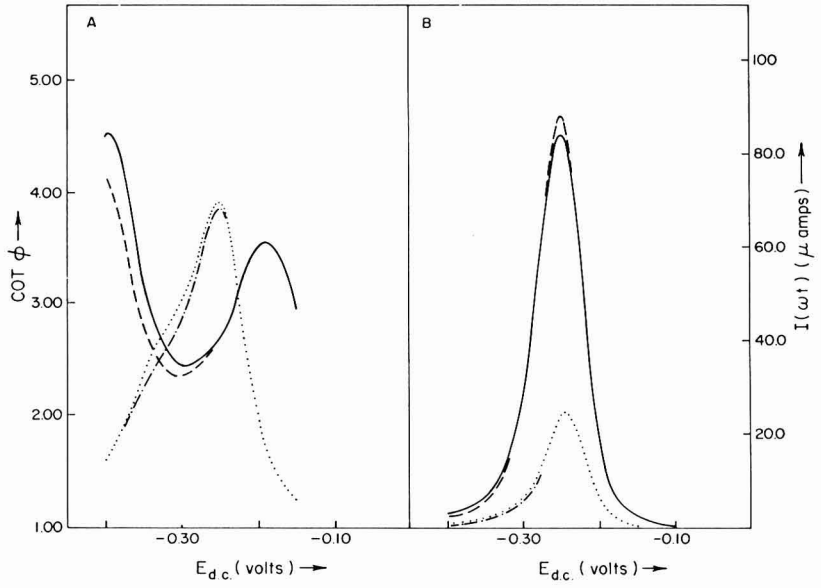
A
B
5.00
4.00
3.00
2.00
1.00
COT ϕ ⟶
I(ωt) (μ amps) ⟶
100
80.0
60.0
40.0
20.0
-0.30
-0.10
$E_{d.c.}$ (volts) ⟶

Fig. 13.

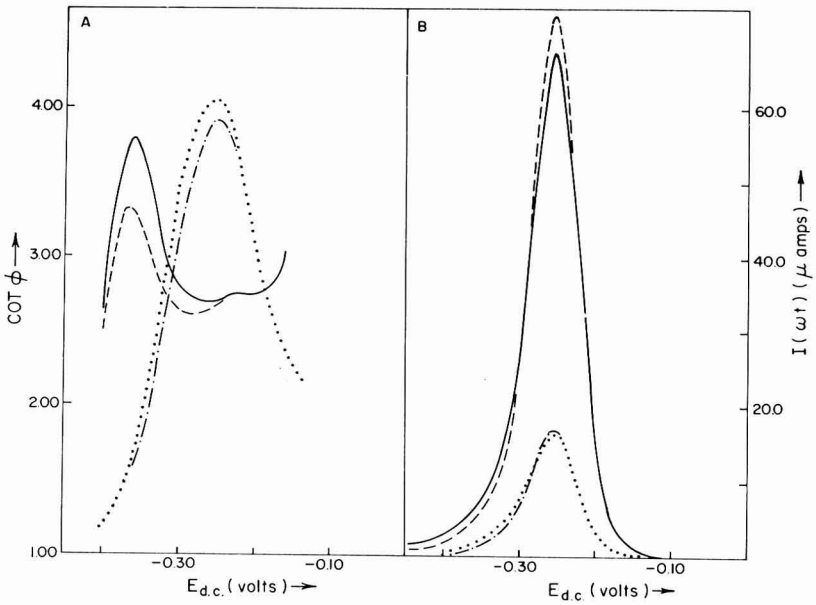
A
B
4.00
3.00
2.00
1.00
COT φ
60.0
40.0
20.0
I (ωt) (μ amps)
-0.30
-0.10
E d.c. (volts)

Fig. 14.

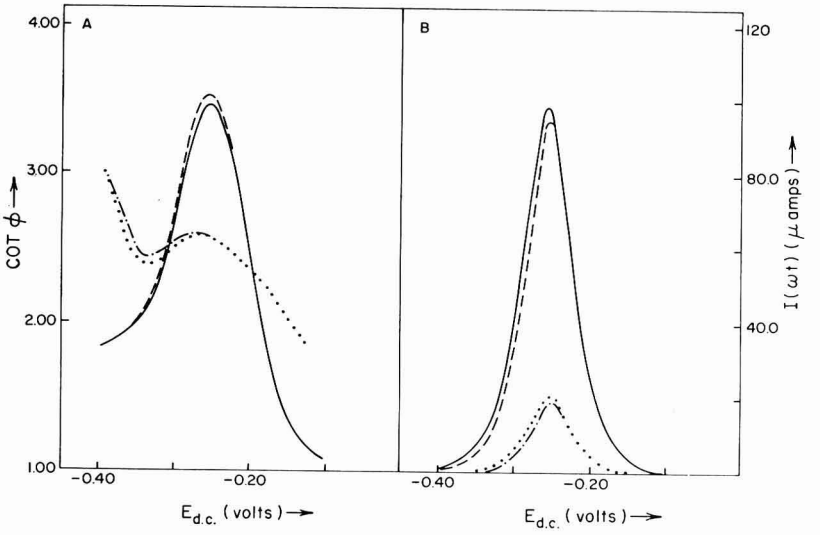
A
B
4.00
3.00
2.00
1.00
COT φ
120
80.0
40.0
I (ωt) (μ amps)
-0.40
-0.20
E d.c. (volts)

Fig. 15.

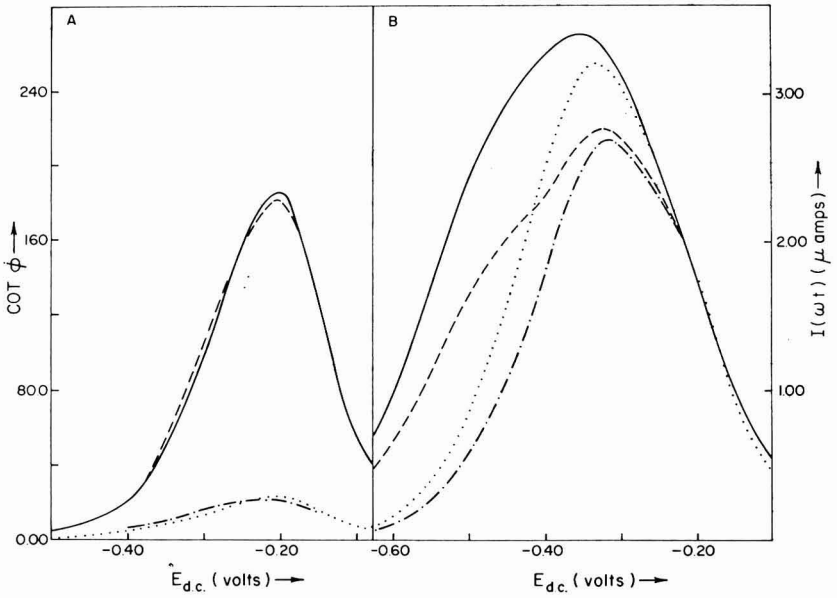
A
B
240
160
80.0
0.00
3.00
2.00
1.00
COT φ
I(ωt) (μ amps)
-0.40
-0.20
-0.60
-0.40
-0.20
E d.c. (volts)
E d.c. (volts)

Fig. 16.

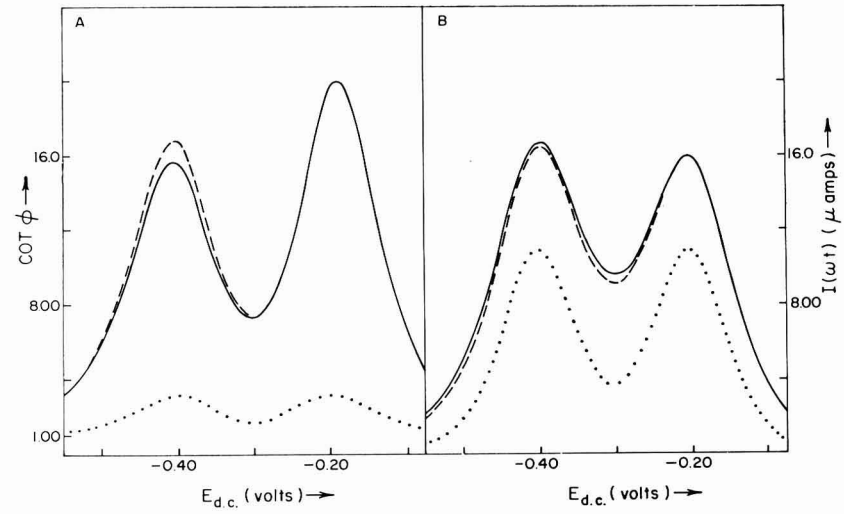
A
B
16.0
8.00
1.00
16.0
8.00
COT φ
I(ωt) (μ amps)
-0.40
-0.20
-0.40
-0.20
E d.c. (volts)
E d.c. (volts)

Fig. 17.

polarogram (current amplitude) may manifest primarily the fast step under such conditions, the appearance of the phase angle wave might be expected to be influenced considerably by the slow step because slow charge transfer yields large cot ϕ-values. Calculations support these intuitive expectations as illustrated for example in Figs. 9 and 10. Equations (52)–(66), which are applicable to such conditions, also predict such behavior as careful perusal indicates. In Fig. 9, where the first step is slow, one finds the predicted a.c. polarogram centered about the standard potential for the second charge transfer step, indicating that the major fraction of the alternating current is due to the second (faster) step. In this example, the separation of E^0-values would have been sufficient to produce resolved peaks in the a.c. polarogram, if diffusion were the sole rate-controlling step. However, the influence of widely differing charge transfer rates leads to the appearance of a single-peak, although an ill-defined shoulder is predicted for the lowest frequency ($\omega = 100$) where the effects of charge transfer kinetics are minimized. On the other hand, effects due to the slow step predominate in the phase angle plot (Fig. 9A), as evidenced by the rapid increase in cot ϕ as $E_{\text{d.c.}}$ becomes more positive. When the second step is the slowest, as in Fig. 10, the effect of d.c. potential is roughly reversed as one would expect. Thus, for example, the largest values of cot ϕ appear at more negative potentials where the second step is more important. Figure 10 also illustrates that the gross asymmetry in the phase angle wave occurs without the necessity that $E_{\frac{1}{2},1} \gg E_{\frac{1}{2},2}$ (as in Fig. 9). The relative k_h-values can also have a profound influence on the frequency dependence of the a.c. polarographic read-out as would be expected. The variation in cot ϕ with frequency is particularly susceptible to differences in $k_{h,1}$ and $k_{h,2}$. When the charge transfer rate constants are comparable, a plot of cot ϕ *vs.* $\omega^{\frac{1}{2}}$ is predicted to be normally a simple, monotonically varying curve, often exhibiting only slight deviations from linearity. However, when the k_h-values differ significantly, the cot ϕ–$\omega^{\frac{1}{2}}$ plot is predicted to assume a more complicated form, as shown in Fig. 21A. At the same time, the current amplitude–$\omega^{\frac{1}{2}}$ plot tends to be less informative from a qualitative viewpoint (Fig. 21B). As before, one can qualitatively interpret these predictions by considering the a.c. polarographic signal as the resultant of contributions of two nearly independent charge transfer steps. It is known[5,13,21] that the quasi-reversible single-step mechanism produces a linear dependence of cot ϕ on $\omega^{\frac{1}{2}}$. If currents due to individual charge transfer steps in the two-step mechanism follow this pattern, a system with comparable $k_{h,1}$ and $k_{h,2}$-values should yield a simple, nearly linear cot ϕ–$\omega^{\frac{1}{2}}$ dependence. This is to be expected because with such a system, the magnitudes of the alternating currents associated with each step are comparable and the relative magnitudes are nearly independent of frequency. However, a system with very different k_h-values is expected to exhibit a markedly different sort of behavior because the relative magnitudes of the alternating currents associated with the individual charge transfer steps will depend significantly on frequency. At low frequencies, the slow step will contribute a much larger fraction of the total alternating current, than at higher frequencies. Thus, ∂ cot $\phi/\partial\omega^{\frac{1}{2}}$ may be large at low frequencies, manifesting the significant contribution of the slow step, but small at high frequencies where alternating current due to the fast step predominates.

(*D*) *Influence of a quasi-reversible d.c. process*

Figures 11–17 depict predictions of eqn. (35) for values of k_h which are suffi-

ciently small that the d.c. polarographic process is influenced by charge transfer kinetics, *i.e.*, the d.c. components of the surface concentrations do not obey the Nernst equation. Perhaps the most obvious manifestation of this effect is the appearance of time-dependent alternating current amplitude and phase angle. This is a result of time-dependence of d.c. surface concentrations induced by non-Nernstian conditions[3,13,20,22–24]. Significant time-dependence is not predicted by eqn. (35) for larger values of k_h (Figs. 1–8) where d.c. surface concentrations obey the Nernst equation. (*c.f.*, eqns. (48)–(51)) The appearance of time-dependent currents is predicted for other electrode reaction mechanisms when non-equilibrium conditions exist with respect to either the electrode reaction or coupled chemical reactions in the d.c. process. However, the time-dependence shown in Figs. 11–17 is somewhat unique in that it appears in both current amplitude and phase angle and its magnitude and dependence on d.c. potential are functions of frequency. With a majority of electrode reaction mechanisms, including the closely related single-step charge transfer, theory predicts a time-dependence which is independent of frequency and which appears *only* in current amplitude[3,4,13,20,24]. However, these unique features of the time-dependence associated with the two-step quasi-reversible charge transfer are not surprising if one considers the result of vectorial addition of two individual alternating current components with charge transfer steps exhibiting time-dependent characteristics associated with the simple, single-step, quasi-reversible process (frequency independent time-dependence of current amplitude; phase angle independent of time). It is apparent that the resultant current (vectorial sum) can readily exhibit a time-dependence which is influenced by frequency and which appears in both phase angle and amplitude. The effect of frequency will appear provided frequency characteristics of the a.c. components due to the individual steps differ, while a phase angle time-dependence requires different phase relations to be associated with the individual a.c. components. In general, these requirements imply that k_h-, α- and/or $E_{\frac{1}{2}}{}^r$-values associated with the two-steps must differ. Thus, for example, phase angle time-dependence would be enhanced by large differences in $k_{h,1}$ and $k_{h,2}$, and *vice versa*. This is readily seen by comparing Figs. 13 and 16. In Fig. 16, k_h-values are very small, but equal. This leads to a very large dependence of current amplitude on time, but phase angle is nearly independent of time. The slight time-dependence of phase angle and the effect of frequency on this phenomenon presumably arises, despite the fact that $k_{h,1}=k_{h,2}$ and $\alpha_1=\alpha_2$, because the $E_{\frac{1}{2}}{}^r$-values differ. In Fig. 13, etc., where kinetic parameters are more divergent, time-dependence of phase angle is much larger.

A number of other effects which are attributable to influence of non-Nernstian d.c. behavior are worth noting. In general, the waves are broadened considerably by this influence (in particular, note Fig. 16), a result which is expected because it also occurs with a single-step mechanism[5,11]. Similarly, when all other factors would suggest the appearance of a symmetrical read-out as a function of d.c. potential, the non-Nernstian d.c. process tends to destroy this symmetry (*cf.*, *e.g.*, Figs. 16 and 17), an effect which also occurs with a single-step mechanism. Finally, the form of the phase angle read-out as a function of d.c. potential is rendered unusually complex, particularly when k_h-values differ substantially. Much of this would appear to arise because alternating currents due to the slow step occur over a wide range of d.c. potential, while the fast step is expected to contribute over a narrower range. Thus, it appears plausible that in such circumstances, alternating currents near the peak of

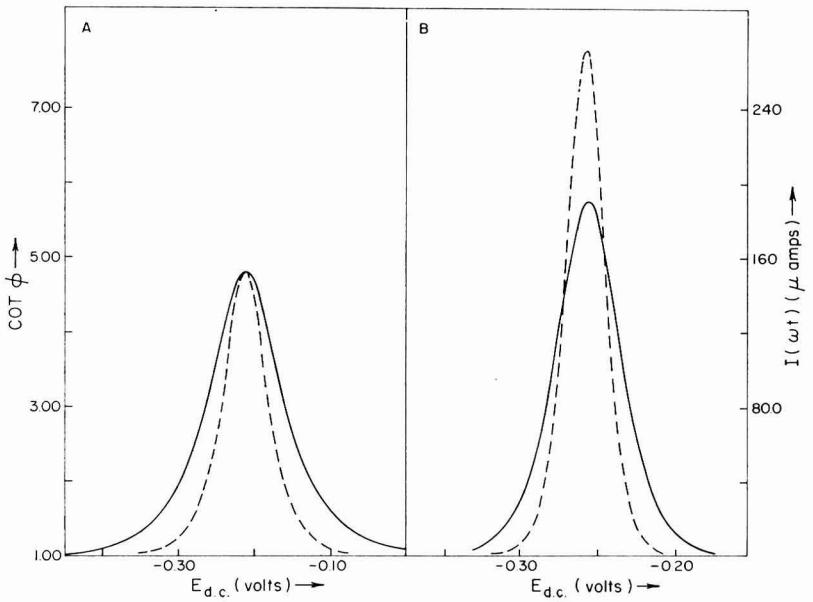
A
B
7.00
5.00
3.00
1.00
COT ϕ
240
160
80.0
I(ωt) (μ amps)
-0.30
-0.10
-0.20
E d.c. (volts)

Fig. 18.

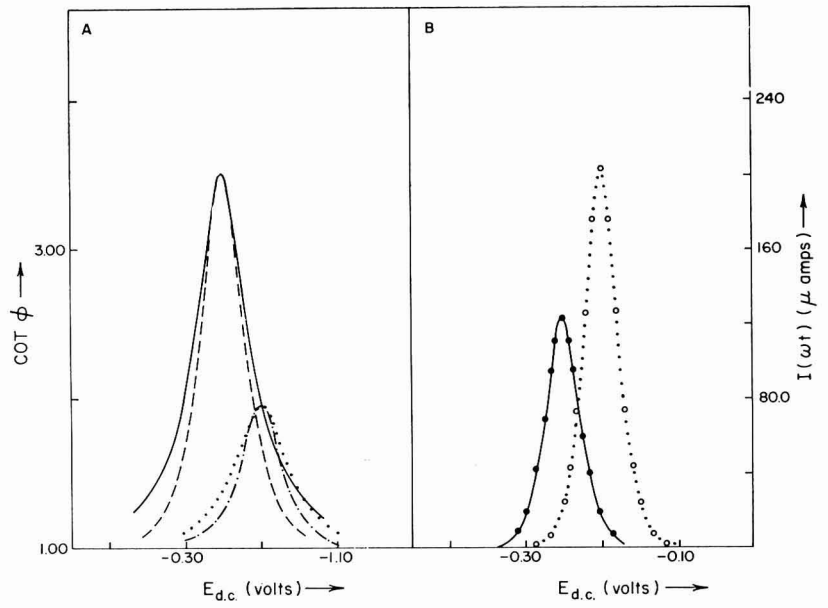
A
B
3.00
1.00
COT ϕ
240
160
80.0
I(ωt) (μ amps)
-0.30
-1.10
-0.10
E d.c. (volts)

Fig. 19.

the a.c. polarogram are due primarily to the fast step (small cot ϕ) while at one or both extremities of the wave the current due to the slow step (large cot ϕ) might become more significant. One can qualitatively explain complicated phase angle predictions such as shown in Fig. 11 with such considerations.

(*E*) *Distinctions between single-step and two-step mechanisms*

An important question the answer to which was one of the original main objectives of this study, is whether conditions can exist where the quasi-reversible two-step mechanism is indistinguishable from the quasi-reversible single-step mechanism on the basis of a.c. polarographic data. It is apparent from Figs. 1–21 and the foregoing discussion that profound differences in a.c. polarographic behavior are

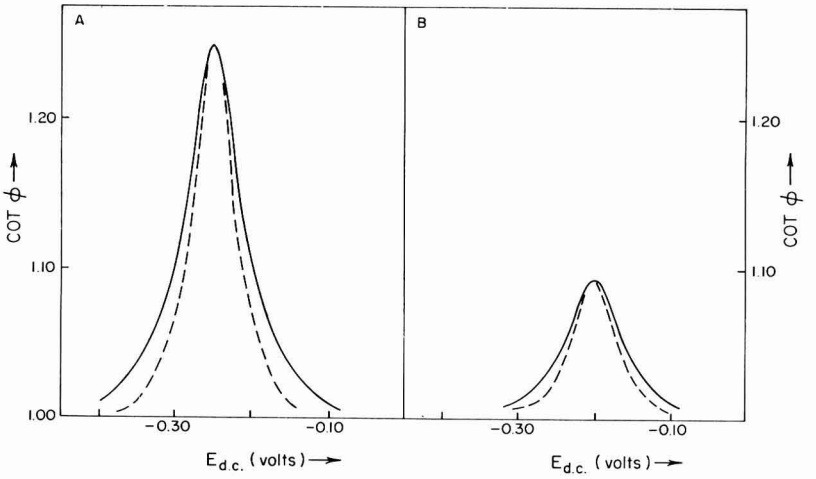

Fig. 20.

Figs. 18–20. Comparison of calculated a.c. polarographic current and phase angle for two-step and single-step reduction. $T = 298°K$, $\frac{1}{2}\Delta E = 5.00$ mV, $C_0^* = 5.00 \cdot 10^{-3}$ M, $A = 3.50 \cdot 10^{-2}$ cm^2, $D_O = D_Y = D_R = 1.00 \cdot 10^{-5}$ cm^2 sec^{-1}, $n_1 = n_2 = 1$ (two-step), $n = 2$ (single-step), $\alpha_1 = \alpha_2 = 0.500$ (two-step), $\alpha = 0.500$ (single-step). Notation definition and other parameters are given in the following table:

Fig.	*Notation*	ω *(sec^{-1})*	$k_{h,1}$ *(two-step)* *(cm sec^{-1})*	$k_{h,2}$ *(two-step)* *(cm sec^{-1})*	k_h *(single-step)*	$E_{\frac{1}{4},1}^r$ *(two-step)* *(V)*	$E_{\frac{1}{4},2}^r$ *(V)*	$E_{\frac{1}{4}}^r$ *(single-step)*
18	———	8100	0.100	0.100		−0.200	−0.220	
18	- - - - -	8100			5.29×10^{-2}			−0.210
19	———	900	1.00	1.00		−0.400	−0.100	
19	. . . . .	900	1.00	1.00		−0.300	−0.100	
19	● and — — —	900			2.70×10^{-2}			−0.250
19	○ and —·—·—	900			7.13×10^{-2}			−0.200
20	———	900	10.0	10.0		−0.400(A) −0.300(B)	−0.100	
20	- - - - -	900			0.270(A) 0.714(B)			−0.25(A) −0.20(B)

predicted for a wide range of conditions, so that ambiguity is highly unlikely. For example, when observable, unique features of the time-dependence such as time-dependent phase angle would be strongly suggestive of the two-step mechanism. The only other mechanisms in which such behavior is likely are those involving adsorption or second- (or higher)-order coupled chemical reactions[20]. Because the latter processes will yield normally an admittance dependent on depolarizer concentration, whereas multi-step charge transfer does not, distinction between these mechanisms is readily achieved. It should be recognized that more complicated mechanisms involving multi-step charge transfer, such as those involving coupled chemical reactions, can also produce a time-dependent phase angle, etc. However, the observation of a time-dependent phase angle will often, at least, permit the classification of the process under investigation as one involving multi-step charge transfer. Criteria for distinction between the simple process of interest in the present work and more complicated processes involving multi-step charge transfer awaits further theoretical investigation. Of course, time-dependence is only one of many observables which might be employed to effect distinction between the two-step and single-step processes. Width of wave, frequency dependence, etc., all may be informative. For most conditions, careful experimental measurements involving examination of both phase angle and amplitude data as a function of frequency and d.c. potential will clearly indicate the presence of the two-step mechanism. Typical of the quantitative distinctions which might be observed between single-step and two-step mechanisms in a situation where qualitative aspects of the read-out suggest nothing unusual, is shown in Fig. 18 where theoretical polarograms for single-step and two-step processes are compared. Values of k_h, α and $E_{\frac{1}{2}}^r$ for the single-step process were selected so that the position and magnitude of the

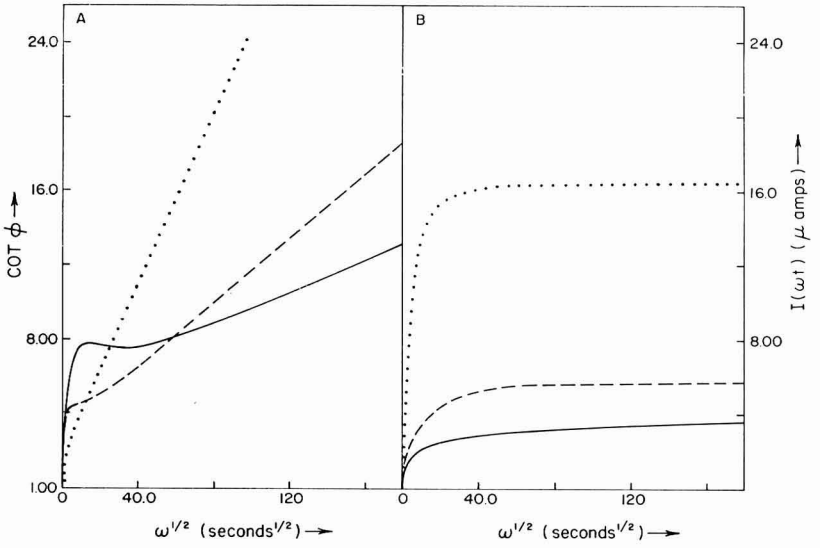

Fig. 21. Calculated frequency dependence of a.c. polarographic current and phase angle for two-step reduction. (———) $E_{d.c.} = 0.350$ V; (- - - -), $E_{d.c.} = -0.300$ V; (. . . .), $E_{d.c.} = -0.200$ V. $n_1 = n_2 = 1$, $T = 298°K$, $\Delta E = 5.00$ mV, $C_O^* = 5.00 \times 10^{-3}$ M, $A = 3.50 \times 10^{-2}$ cm^2, $D_O = D_Y = D_R = 1.00 \times 10^{-5}$ cm^2 sec^{-1}, $k_{h,1} = 1.00 \times 10^{-2}$ cm sec^{-1}, $k_{h,2} = 1.00 \times 10^{-3}$ cm sec^{-1}, $\alpha_1 = \alpha_2 = 0.500$, $E_{\frac{1}{2},1}^r = -0.200$ V, $E_{\frac{1}{2},2}^r = -0.300$ V.

maximum in the cot ϕ–$E_{d.c.}$ plot are identical for both mechanisms (measurement of position and magnitude of peak cot ϕ has been suggested for the evaluation of k_h and α with the single-step mechanism[25]). Perusal of Fig. 18 makes obvious the fact that distinction between the single-step and two-step mechanisms could be effected without difficulty in this situation. A more stringent set of conditions will occur when $E_{\frac{1}{2},2}{}^r \gg E_{\frac{1}{2},1}{}^r$. Under the latter conditions, the reversible two-step mechanism is predicted to be indistinguishable from the single-step process[1]. Thus, one would expect distinctions between the two mechanisms under quasi-reversible conditions to be smallest when $E_{\frac{1}{2},2}{}^r \gg E_{\frac{1}{2},1}{}^r$, if any distinctions exist at all. Figures 19 and 20 show results of some calculations for such conditions. Values of k_h, α and $E_{\frac{1}{2}}{}^r$ for the single-step mechanism again were selected so that peaks on the phase angle plots agree for both mechanisms. One finds that this choice of rate parameters yields a current amplitude wave for the single-step process that is indistinguishable from the wave predicted for the two-step process. However, the phase angle waves differ somewhat, with the single-step mechanism yielding a slightly narrower wave. Thus, a small, but definite distinction is found between the a.c. polarographic read-out predicted for the single-step and two-step mechanisms when $E_{\frac{1}{2},2}{}^r \gg E_{\frac{1}{2},1}{}^r$. As a result, we can state that, at least in principle, no example of ambiguity between theory for the quasi-reversible single-step and two-step mechanisms has been found. In some cases distinction will rely on careful, detailed study of the d.c. potential dependence of the faradaic impedance. The question remains unanswered as to whether the average worker, on obtaining phase angle data following the solid curves in Figs. 19 or 20, would consider significant the observed deviations from the theory for the single-step mechanism (dashed curves). It should be stated that the differences predicted in Figs. 19 and 20 exceed experimental uncertainty obtainable with precision instrumentation. Perhaps the knowledge that such small differences can be mechanistically significant would lead one to take such observations more seriously than would otherwise be the case.

(*F*) *Evaluation of rate parameters from experimental data*

The cumbersome nature of the theoretical expressions for the a.c. wave with the two-step charge transfer mechanism renders difficult the evaluation of rate parameters from experimental data when the existence of this mechanism is established. Difficulties associated with calculation of rate parameters will vary considerably, depending on whether the d.c. process is diffusion-controlled or not and on how much information is available from sources other than a.c. polarography. A complete evaluation of this problem has not been accomplished, but preliminary considerations indicate that the rate and thermodynamic parameters will be calculable readily from a.c. polarographic data in many situations. One example will be discussed here.

If one has a system exhibiting the two-step charge transfer mechanism in which charge transfer rates are sufficiently rapid that the d.c. process is Nernstian, and if the $E_{\frac{1}{2}}{}^r$-values for the system are known (*e.g.*, from d.c. polarographic measurements or from a.c. measurements at low frequencies), the following procedure may be employed. By substituting the known $E_{\frac{1}{2}}{}^r$-values in eqn. (35), etc., two unknowns, λ_1 and λ_2, remain in the a.c. wave equation. It is apparent for any given value of $E_{d.c.}$ and ω, that two independent experimental observables exist (*e.g.*, current amplitude and phase angle) that will enable evaluation of λ_1 and λ_2. That is, two independent equations are available for assessment of the two unknowns. The complexities of the

algebraic expressions relating λ_1 and λ_2 to current amplitude and phase angle may preclude solving for λ_1 and λ_2 with standard algebraic methods. If this is the case, graphical methods, use of appropriate working curves, or trial-and-error methods with the aid of high-speed digital computers can be used to effect solution. The evaluation of λ_1 and λ_2 is repeated over a range of d.c. potentials along the a.c. polarographic wave (frequency constant). These values of λ_1 and λ_2 are then plotted as a function of $E_{\text{d.c.}}$. Such plots should exhibit a minimum defined by

$$(E_{\text{d.c.}})_{\text{min.}} = E_{\frac{1}{2}}^{r} + \frac{RT}{nF} \ln\left(\frac{\alpha}{\beta}\right) \tag{86}$$

$$\lambda_{\text{min.}} = \frac{k_h f}{D^{\frac{1}{2}}}\left[\left(\frac{\alpha}{\beta}\right)^{-\alpha} + \left(\frac{\alpha}{\beta}\right)^{\beta}\right] \tag{87}$$

where $\lambda_{\text{min.}}$ is the magnitude of λ at the minima and $(E_{\text{d.c.}})_{\text{min.}}$ is the d.c. potential corresponding to the minima. Equations (86) and (87) are then used to calculate α and k_h for each charge transfer step. Thus, one concludes that it is possible to evaluate the four kinetic parameters $k_{h,1}$, $k_{h,2}$, α_1 and α_2 from a.c. polarographic data at a single frequency, provided that the system in question definitely involves a rate process which obeys the simple two-step mechanism, that the effects of charge transfer are significant at the frequency employed and that the foregoing assumptions regarding the status of the d.c. process and the availability of $E_{\frac{1}{2}}{}^{r}$-values are applicable. Because the frequency dependence of the a.c. polarographic data was not required for calculation of rate parameters in this example, we believe that rate parameters may still be calculable in less ideal situations (*e.g.*, when $E_{\frac{1}{2}}{}^{r}$'s are unknown or when the d.c. process is quasi-reversible) by making use of the frequency dependence of the a.c. data.

APPENDIX I

Notation definitions

A	= electrode area.
f_i	= activity coefficient of species i.
C_i	= concentration of species i.
C_i^*	= initial concentration of species i.
$C_{i_{x=0}}$	= surface concentration of species i.
D_i	= diffusion coefficient of species i.
$i(t)$	= total faradaic current (cathodic current positive).
$i_1(t)$, $i_2(t)$	= faradaic current due to first and second charge transfer steps, respectively.
$I(\omega t)$	= faradaic fundamental harmonic alternating current.
$i_{\text{d.c.}}(t)$	= d.c. faradaic current.
n_1, n_2	= number of electrons transferred in first and second charge transfer steps, respectively.
$k_{h,1}$, $k_{h,2}$	= standard heterogeneous rate constants for the first and second charge transfer steps, respectively (at $E_1{}^0$ and $E_2{}^0$).

α_1, α_2 = charge transfer coefficients for first and second charge transfer steps, respectively.
E_1^0, E_2^0 = standard redox potentials in the European convention for the first and second charge transfer steps, respectively.
$E_{\frac{1}{2},1}^r, E_{\frac{1}{2},2}^r$ = reversible polarographic half-wave potentials (planar diffusion model) for first and second charge transfer steps, respectively.
$E(t)$ = applied potential.
$E_{d.c.}$ = d.c. component of applied potential.
ΔE = amplitude of applied alternating potential.
F = Faraday's constant.
R = ideal gas constant.
T = absolute temperature.
ω = angular frequency.
t = time.
u = auxiliary variable of integration.
x = distance from electrode surface.
ϕ = phase angle of fundamental harmonic alternating current relative to applied alternating potential.
s = Laplace transform variable.

APPENDIX 2

Derivation of d.c. polarographic current expression

The integral equations defining the d.c. polarographic current are given by (eqns. (21) and (22) for $p=0$).

$$\frac{D_1^{\frac{1}{2}}\psi_{1,0}(t)}{k_{h,1}f_1} = e^{-\alpha_1 j_1} - (e^{-\alpha_1 j_1} + e^{\beta_1 j_1})\int_0^t \frac{\psi_{1,0}(t-u)du}{(\pi u)^{\frac{1}{2}}} + e^{\beta_1 j_1}\int_0^t \frac{\psi_{2,0}(t-u)du}{(\pi u)^{\frac{1}{2}}} \tag{A1}$$

$$\frac{D_2^{\frac{1}{2}}\psi_{2,0}(t)}{k_{h,2}f_2} = e^{-\alpha_2 j_2}\int_0^t \frac{\psi_{1,0}(t-u)du}{(\pi u)^{\frac{1}{2}}} - (e^{-\alpha_2 j_2} + e^{\beta_2 j_2})\int_0^t \frac{\psi_{2,0}(t-u)du}{(\pi u)^{\frac{1}{2}}} \tag{A2}$$

Taking the Laplace Transform of eqns. (A1) and (A2), solving the resulting system of two algebraic equations for $\psi_{1,0}(t)$ and $\psi_{2,0}(t)$ and algebraic rearrangement, yields

$$\psi_{1,0}(s) = \frac{\lambda_1}{(1+e^{j_1})}\left[\frac{s^{\frac{1}{2}}+\lambda_2}{s^{\frac{1}{2}}(s^{\frac{1}{2}}+\chi_-)(s^{\frac{1}{2}}+\chi_+)}\right] \tag{A3}$$

$$\psi_{2,0}(s) = \frac{\lambda_1\lambda_2}{(1+e^{j_1})(1+e^{j_2})}\left[\frac{1}{s^{\frac{1}{2}}(s^{\frac{1}{2}}+\chi_-)(s^{\frac{1}{2}}+\chi_+)}\right] \tag{A4}$$

where

$$\chi_\pm = \frac{\lambda_1+\lambda_2 \pm [(\lambda_1+\lambda_2)^2-4K]^{\frac{1}{2}}}{2} \tag{A5}$$

$$K = \lambda_1 \lambda_2 \left[\frac{e^{j_2} + e^{-j_1} + e^{(j_2 - j_1)}}{(1 + e^{j_2})(1 + e^{-j_1})} \right] \tag{A6}$$

Expansion of eqns. (A3) and (A4) by partial fractions and inverse transformation yields eqns. (42) and (43). The d.c. polarographic current is obtained from eqns. (42) and (43) with the aid of the relation

$$i_{d.c.}(t) = FAC_O^* D_O^{\frac{1}{2}} [n_1 \psi_{1,0}(t) + n_2 \psi_{2,0}(t)] \tag{A7}$$

which follows from eqns. (3), (9) and (19).

ACKNOWLEDGEMENT

The authors are indebted to the National Science Foundation for support of this work and to the North-western University Computing Center for generous donation of computer time.

SUMMARY

A theory is presented for the a.c. polarographic wave arising from a two-step charge transfer process in which rate control is exerted by diffusion and charge transfer. Predictions of the theory are examined in detail. It is found that: (a) conditions for pure diffusion control depend markedly on the relative values of the standard potentials associated with the two charge transfer steps; (b) many features potentially useful in mechanistic diagnosis are predicted for the a.c. polarographic read-out and ambiguity between single-step and two-step mechanisms is highly unlikely; (c) as one would expect, relative and absolute values of the rate and thermodynamic parameters associated with the charge transfer steps have a profound influence on the predicted a.c. polarographic behavior; (d) despite the complexities and variety of behavior predicted, simple rationalization of many of the predictions is possible; (e) the problem of evaluating rate parameters from experimental data appears amenable to solution.

REFERENCES

1 H. L. HUNG AND D. E. SMITH, *J. Electroanal. Chem.*, 11 (1966) 237.
2 J. M. HALE, *J. Electroanal. Chem.*, 8 (1964) 408.
3 G. H. AYLWARD, J. W. HAYES, D. E. SMITH AND H. L. HUNG, *Anal. Chem.*, 36 (1964) 2218.
4 H. L. HUNG AND D. E. SMITH, unpublished work.
5 H. MATSUDA, *Z. Elektrochem.*, 62 (1958) 977.
6 S. GLASSTONE, K. J. LAIDLER AND H. EYRING, *The Theory of Rate Processes*, McGraw-Hill, New York, 1941, pp. 575–77.
7 A. N. FRUMKIN, *Z. Elektrochem.*, 59 (1955) 807.
8 P. DELAHAY, *Advances in Electrochemistry and Electrochemical Engineering*, edited by P. DELAHAY AND C. W. TOBIAS, Vol. 1, Interscience Publishers Inc., New York, 1961, chap. 5.
9 J. R. DELMASTRO AND D. E. SMITH, unpublished work.
10 T. BIEGLER AND H. A. LAITINEN, *Anal. Chem.*, 37 (1965) 572.
11 J. R. DELMASTRO AND D. E. SMITH, *J. Electroanal. Chem.*, 9 (1965) 192.
12 H. B. HERMAN AND A. J. BARD, *Anal. Chem.*, 36 (1964) 971.
13 D. E. SMITH, *Advances in Electroanalytical Chemistry*, edited by A. J. BARD, Vol. 1, M. Dekker, Inc., New York, in press.
14 D. E. SMITH, *Anal. Chem.*, 35 (1963) 602.

15 C. D. HODGMAN, editor, *Handbook of Chemistry and Physics*, 41st ed., Chemical Rubber Publishing Co., Cleveland, 1959, p. 275.
16 T. BERZINS AND P. DELAHAY, *J. Am. Chem. Soc.*, 75 (1953) 5716.
17 K. EBATA, *Tohoku University Science Reports*, 47 (1964) 191.
18 J. M. HALE, *J. Electroanal. Chem.*, 8 (1964) 181.
19 M. SMUTEK, *Collection Czech. Chem. Commun.*, 18 (1953) 171.
20 H. L. HUNG AND D. E. SMITH, *Anal. Chem.*, 36 (1964) 922.
21 B. BREYER AND H. H. BAUER, *Chemical Analysis*, edited by P. J. ELVING AND I. M. KOLTHOFF, Vol. 13, Interscience, New York, 1963, chap. 2.
22 M. SENDA, *Kagaku No Ryoiki, Zokan*, (1962) 15.
23 G. H. AYLWARD AND J. W. HAYES, *J. Electroanal. Chem.*, 8 (1964) 442.
24 G. H. AYLWARD, J. W. HAYES AND R. TAMAMUSHI, *Proceedings of the First Australian Conference on Electrochemistry, 1963*, edited by J. A. FRIEND AND F. GUTMANN, Pergamon Press, Oxford, 1964.
25 R. TAMAMUSHI AND N. TANAKA, *Z. Physik. Chem. N. F.*, 21 (1959) 89.

CONSECUTIVE ELECTROCHEMICAL PROCESSES IN CONTROLLED POTENTIAL ELECTROLYSIS
THE ISOLATION OF INTERMEDIATES

JOHN G. MASON
Department of Chemistry, Virginia Polytechnic Institute, Blacksburg, Virginia (U.S.A.)
(Received July 26th, 1965)

INTRODUCTION

Electrochemical reductions of organic compounds frequently involve consecutive electrode processes with the possibility of chemical reactions intervening at one or more stages. Extensive treatments of the theoretical current–time and coulomb–time characteristics of controlled potential electrolyses have been developed for many reaction mechanisms by BARD[1,2,3] and MEITES[4,5,6] for reductions performed in the mass transport limiting current region. From these treatments it is generally possible to make trivial manipulation and obtain the product distribution as a function of time. MEITES[7] has considered the nature of both reversible and irreversible reductions as a function of potential at potentials below the mass transport region. Our interest in utilizing controlled potential electrolysis to produce isolatable intermediates has led to a re-examination of the general reaction scheme of two consecutive irreversible electrochemical reactions without intervening chemical reactions. This scheme has been discussed in some detail previously by GELB[8] and MEITES. They conclude that for the scheme for electrolysis performed in the limiting current region,

$$A + n_1 e \rightarrow B$$

$$B + n_2 e \rightarrow C$$

deviations of log i *vs.* t plots from linearity are attributable to differences in the mass transport coefficients of A and B. The discussion here leads to conclusions contrary to those of GELB and MEITES.

RESULTS

Mathematical developments

The primary assumptions involved in the development are that steady-state conditions will always be maintained at the electrode surface, that the Nernst diffusion layer treatment is applicable, and that the electrode reactions are totally irreversible. Since the effect of stirring is not being studied as such, it is felt that the simple Nernst treatment will not lead to incorrect qualitative conclusions.

The following symbols will be used:

C_A^0 = initial concentration of species A in the bulk of the solution. C_A^b, C_B^b and C_C^b represent the concentrations of species A, B, and C in the bulk, respectively.

C_A^s, C_B^s and C_C^s represent the concentrations of species A, B and C at the electrode surface. β_A, β_B and β_C represent the mass transport coefficients of species A, B and C with the units sec^{-1}.

β_1^* and β_2^* represent the potential-dependent rate constants for the two consecutive electrochemical reactions with the units sec^{-1}.

The reaction scheme being considered is

$$A + n_1 e \rightarrow B \tag{1}$$

$$B + n_2 e \rightarrow C \tag{2}$$

The overall reaction process involves transport of A from the bulk of solution to the electrode surface, reduction to B, reduction of B to C at the electrode, and competitive transport of B to the bulk of the solution:

$$A^b \underset{\beta_A}{\rightleftharpoons} A^s \qquad \text{(mass transport)} \tag{3}$$

$$A^s \xrightarrow[n_1 e]{\beta_1^*} B^s \qquad \text{(electrochemical)} \tag{4}$$

$$B^s \underset{\beta_B}{\rightleftharpoons} B^b \qquad \text{(mass transport)} \tag{5}$$

$$B^s \xrightarrow[n_2 e]{\beta_2^*} C^s \qquad \text{(electrochemical)} \tag{6}$$

$$C^s \underset{\beta_C}{\rightleftharpoons} C^b \qquad \text{(mass transport)} \tag{7}$$

Rate of change in bulk concentrations

$$\frac{dC_A^b}{dt} = -\beta_A C_A^b + \beta_A C_A^s \tag{8}$$

$$\frac{dC_B^b}{dt} = \beta_B C_B^s - \beta_B C_B^b \tag{9}$$

$$\frac{dC_C^b}{dt} = \beta_C C_C^s - \beta_C C_C^b \tag{10}$$

$$\frac{dC_A^b}{dt} + \frac{dC_B^b}{dt} + \frac{dC_C^b}{dt} = 0 \tag{11}$$

Steady-state equations at the electrode surface

$$\frac{dC_A^s}{dt} = 0 = \beta_A C_A^b - (\beta_A + \beta_1^*) C_A^s \; ; \tag{12}$$

$$C_A^s = \frac{\beta_A C_A^b}{(\beta_A + \beta_1^*)} \tag{12a}$$

$$\frac{dC_B^s}{dt} = 0 = \beta_1^* C_A^s + \beta_B C_B^b - (\beta_B + \beta_2^*) C_B^s \tag{13}$$

$$C_B^s = \frac{\beta_1^* C_A^s}{(\beta_B + \beta_2^*)} + \frac{\beta_B C_B^b}{(\beta_B + \beta_2^*)} = \frac{\beta_1^* \beta_A C_A^b}{(\beta_A + \beta_1^*)(\beta_B + \beta_2^*)} + \frac{\beta_B C_B^b}{(\beta_A + \beta_2^*)} \tag{13a}$$

$$\frac{dC_C^s}{dt} = \beta_C C_C^b + \beta_2^* C_B^s - \beta_C C_C^s \; ; \tag{14}$$

$$C_C^s = C_C^b + \beta_2^* C_B^s \tag{14a}$$

Evaluation of changes of the bulk concentrations of A, B and C

Substitution of eqn. (12a) into eqn. (8) yields

$$\frac{dC_A^b}{dt} = \frac{-\beta_1^* \beta_A}{(\beta_1^* + \beta_A)} C_A^b \tag{15}$$

Substitution of eqns. (12a), (13a), and (14a) into eqn. (10) yields,

$$\frac{dC_C^b}{dt} = \beta_2^* C_B^s = \frac{\beta_2^* \beta_1^* \beta_A C_A^b}{(\beta_1^* + \beta_A)(\beta_B + \beta_2^*)} + \frac{\beta_2^* \beta_B C_B^b}{(\beta_B + \beta_2^*)} \tag{16}$$

Substitution of eqns. (15) and (16) into eqn. (11) yields

$$\frac{dC_B^b}{dt} = \frac{\beta_1^* \beta_A C_A^b}{(\beta_1^* + \beta_A)} - \frac{\beta_1^* \beta_2^* \beta_A C_A^b}{(\beta_1^* + \beta_A)(\beta_B + \beta_2^*)} - \frac{\beta_2^* \beta_B C_B^b}{(\beta_B + \beta_2^*)} \tag{17}$$

which reduces to

$$\frac{dC_B^b}{dt} = \frac{\beta_1^* \beta_A \beta_B C_A^b}{(\beta_1^* + \beta_A)(\beta_B + \beta_2^*)} - \frac{C_B^b \beta_B \beta_2^*}{(\beta_B + \beta_2^*)} \tag{18}$$

For simplicity, let

$$\frac{\beta_1^* \beta_A}{(\beta_1^* + \beta_A)} = \beta_1' ; \quad \frac{\beta_B \beta_2^*}{(\beta_B + \beta_2^*)} = \beta_2' ; \quad \frac{\beta_B}{\beta_B + \beta_2^*} = \frac{\beta_2'}{\beta_2^*} . \tag{19}$$

Since $C_A^b = C_A^0 \exp -\beta_1' t$

$$\frac{dC_B^b}{dt} = \frac{\beta_1' \beta_2'}{\beta_2^*} C_A^0 \exp(-\beta_1' t) - \beta_2' C_B^b \tag{20}$$

Integrating and setting $C_B^b = 0$ at $t = 0$ results in

$$C_B^b = \frac{\beta_1' \beta_2' C_A^0}{\beta_2^* (\beta_2' - \beta_1')} \left[e^{-\beta_1' t} - e^{-\beta_2' t} \right] \tag{21}$$

In the mass transport region (*i.e.*, the region where $\beta_1^* \gg \beta_A$ and $\beta_2^* \gg \beta_B$), eqn. (21) reduces to

$$C_B^b = \frac{\beta_A \beta_B}{\beta_2^* (\beta_B - \beta_A)} C_A^0 \left[e^{-\beta_A t} - e^{-\beta_B t} \right] \tag{22}$$

DISCUSSION

The comparable result to eqn. (22) derived by GELB AND MEITES (their eqn. (10)) is

$$C_B = \frac{\beta_A C_A^0}{\beta_B - \beta_A}\left(e^{-\beta_A t} - e^{-\beta_B t}\right)^{\dagger}$$

The only difference between the two results is the multiplier, β_B/β_2^*, which measures the extent to which B will be reduced at the electrode surface before transport away from the electrode occurs. It seems in order to comment upon the validity of the steady-state treatment to this particular problem. The key equation in this respect is eqn. (14a).

$$C_B^s = \frac{\beta_1^* \beta_A C_A^b}{(\beta_A + \beta_1^*)(\beta_B + \beta_2^*)} + \frac{\beta_B C_B^b}{(\beta_B + \beta_2^*)} \qquad (14a)$$

The conditions for the steady-state approximation to apply, are two-fold, $dC_B^s/dt = 0$ and C_B^s (the steady-state concentration) must be small relative to C_B^b, C_A^b and C_C^b. In order that C_B^s be small, β_1^* and β_2^* must be much larger than β_A and β_B. Under these conditions eqn. (14a) becomes

$$C_B^s = \frac{\beta_A C_A^b}{\beta_2^*} + \frac{\beta_B C_B^b}{\beta_2^*}$$

These are precisely the conditions necessary for mass transport control. For values of β_1^* and β_2^* approximately equal to β_A and β_B, C_B^s would not be small and the steady-state assumptions would perhaps be invalid and the distinction between surface and bulk concentrations of B, specious.

Equation (22) shows the dependence of C_B^b on the ratio β_B/β_2^*, which means that in the true mass transport region, the concentration, C_B^b, is vanishingly small and never reaches concentrations suitable for isolation. For the isolation of B, it is evident that β_2^* must be small in order that B can accumulate in the solution bulk.

For electrolyses performed at potentials on the rising portion of the current–potential curve, it is evident that in order to isolate B in reasonable concentration, β_2^* must be smaller than β_1^* (see eqn. (21)). If β_2^* is much smaller than β_1^*, the current–voltage curve would show separation into two steps: the first corresponding to the reduction of A to B, the second, B to C. For this situation, the isolation of B is obviously easy. However, significant amounts of B can be obtained under less obviously favorable conditions. From the results of BERZINS AND DELAHAY[9], wave separation becomes obvious for ratios of $\beta_1^*/\beta_2^* > 10$. Therefore, isolation of B in consecutive reactions, is feasible only under two conditions when no obvious wave separation occurs:

$$10 > \frac{\beta_1^*}{\beta_2^*} > 5^{\dagger\dagger}$$

† β_A and β_B in the original equation are, respectively, β_1 and β_2.

††The number 5 was arbitrarily chosen as a limit for isolation of B. Crude calculations indicate that the maximum concentration of B at potentials corresponding to 0.1 of the total wave height would be in the range of 50% of total, possible and suitable for isolation.

and the electrolyses are conducted at potentials toward the foot of the current–voltage curve. The ratio, β_1^*/β_2^*, will be independent of potential provided the αn-values for the two stages are approximately the same. Deviations from linearity of log i *vs.* t plots of the type reported by GELB AND MEITES should show a potential-dependence which disappears in the mass transport region.

One danger in the use of polarographic data for defining the conditions for the controlled potential electrolysis of irreversible reactions, has been indicated by DELAHAY[10], who pointed out that the voltammetric half-wave potential for an irreversible reaction is a function of the thickness of the Nernst layer. The significance of this result to controlled potential electrolysis involving irreversible reductions is simply that it is necessary to use a potential significantly more negative than the rising portion of the polarographic wave to ensure mass transport control, since stirring causes a significant decrease in δ.† If this is experimentally not possible, then if the β_1^*/β_2^* ratio is in the appropriate range, segmented log i *vs.* t plots will be observed of the type reported by GELB AND MEITES. For observable curvature of the log i *vs.* t plots, β_2^* does not have to be smaller than β_1^*, such a condition is necessary only if B is to be isolated in reasonable yield.

SUMMARY

The fundamental relations pertaining to the controlled potential electrolysis of a reaction path which involves two consecutive irreversible electrochemical reactions have been derived. The results show that in the true mass transport limiting current region, the conditions are such that no intermediates appear and plots of log i *vs.* t should be linear. This result is contrary to previous findings. The conditions necessary for the isolation of intermediates are discussed.

REFERENCES

1 D. H. GESKE AND A. J. BARD, *J. Phys. Chem.*, 63 (1959) 1057.
2 A. J. BARD AND J. S. MAYELL, *J. Phys. Chem.*, 66 (1962) 2173.
3 A. J. BARD AND E. SOLON, *J. Phys. Chem.*, 67 (1963) 2326.
4 L. MEITES AND S. MOROS, *Anal. Chem.*, 31 (1959) 23.
5 S. A. MOROS AND L. MEITES, *J. Electroanal. Chem.*, 5 (1963) 103.
6 L. MEITES, *J. Electroanal. Chem.*, 5 (1963) 270.
7 L. MEITES, *J. Electroanal. Chem.*, 7 (1964) 337.
8 R. I. GELB AND L. MEITES, *J. Phys. Chem.*, 68 (1964) 630.
9 T. BERZINS AND P. DELAHAY, *J. Am. Chem. Soc.*, 75 (1953) 5716.
10 P. DELAHAY, *New Instrumental Methods in Electrochemistry*, Interscience Publishers Inc., New York, 1954, p. 225.

† β_i, mass transport coefficient of species i, is related to δ by $\beta_i = D_i A/V\delta$, where D_i is the diffusion coefficient of i (cm^2/sec), A is the electrode area (cm^2), V is the solution volume (l) and δ is the layer thickness (cm).

SHORT COMMUNICATION

Electrometric studies on potassium aquopentacyano iron(II) Part II. The reduction of the nitrosobenzene complex at the dropping mercury electrode

The substitution of one of the cyanide groups in the hexacyano compounds of iron by water, ammonia, amine, nitro- or nitroso-groups is a well-established fact. The different substituted groups of these complexes are also known to undergo exchange reactions under suitable conditions. Thus, nitrosobenzene may be introduced into the compound, potassium aquopentacyano iron(II), by replacing H_2O, resulting in the formation of a violet-coloured compound. Such a reaction is also observed when potassium ferrocyanide solution containing small amounts of mercuric chloride is mixed with nitrosobenzene[1-3]. The nature and composition of the complex was studied by electrometric methods. The present communication deals with the polarographic reduction of the complex at the dropping mercury electrode (D.M.E.).

Experimental

Nitrosobenzene was prepared by the method of COLEMAN *et al.*[4]. Potassium aquopentacyano iron(II) was obtained in the form of brownish-yellow crystals by the method described in Part I[5]. All other reagents were A.R. quality. The solutions were prepared in twice-distilled water.

A Toshniwal manual polarograph Type CLO-2 (India) was employed, using a Pye Scalamp Galvanometer in the external circuit. The polarographic cell and the reference electrode (S.C.E.) were kept immersed in a water thermostat maintained at $30 \pm 0.1°$. Purified hydrogen was used for de-aeration. A Fischer capillary with a drop-time of 3.4 sec (open circuit) was used for the D.M.E., the capillary constant $m^{2/3}t^{1/6}$ being 2.877. Potassium chloride with suitable buffers was used as the supporting electrolyte. Polarograms of the various mixtures were taken 24 h after mixing the reactants. No maximum suppressor was required in the present studies.

To determine the effect of pH on the polarographic reduction of the violet complex, solutions containing $6.6 \cdot 10^{-4}$ *M* nitrosobenzene, $6.6 \cdot 10^{-4}$ *M* aquopentacyano iron(II) and $6.6 \cdot 10^{-2}$ *M* KCl were prepared in buffers, ranging from pH 1.15 to 12.5. Polarograms of nitrosobenzene alone in potassium chloride and various buffers were also taken for comparison.

To demonstrate the effect of the ratio of concentrations of nitrosobenzene and aquopentacyano iron(II), the concentration of the latter was varied between $3.3 \cdot 10^{-4}$ *M* and $2 \cdot 10^{-3}$ *M* keeping the concentration of nitrosobenzene at $2 \cdot 10^{-3}$ *M*, and *vice versa*, in buffer pH 4 (shown as optimum from the study of the pH-dependence) containing $6.6 \cdot 10^{-2}$ *M* KCl.

In order to study the relationship between i_d and concentration of the complex, solutions containing equimolecular quantities of both reactants in concentrations ranging between $3.3 \cdot 10^{-4}$ and $2 \cdot 10^{-3}$ *M* were prepared in a phosphate buffer, pH 4.0, containing $6.6 \cdot 10^{-2}$ *M* KCl.

TABLE 1

$E_{\frac{1}{2}}$- AND i_d-VALUES OF POTASSIUM AQUOPENTACYANO IRON(II)–NITROSOBENZENE COMPLEX AND NITROSOBENZENE AT DIFFERENT pH-VALUES

pH	*1.1*	*2.0*	*3.0*	*4.0*	*5.0*	*6.0*	*6.6*	*8.3*	*8.8*	*9.5*	*10.6*	*11.0*
Complex												
$(E_{\frac{1}{2}})_I$ (V *vs.* S.C.E.)	−0.10	−0.15	−0.22	−0.30	−0.06	−0.10	−0.16	−0.24	−0.26	−0.26	−0.29	—
$(i_d)_I$ (μA)	3.0	4.7	4.9	5.3	0.50	0.50	0.50	0.50	0.49	0.50	0.50	—
$(E_{\frac{1}{2}})_{II}$ (V *vs.* S.C.E.)	−0.56	−0.70	−0.83	—	−0.83	−0.46	−0.56	−0.58	−0.59	−0.60	−0.65	−0.70
$(i_d)_{II}$ (μA)	1.2	0.70	0.50	0.20	0.24	0.12	0.6	0.40	0.40	0.45	0.50	1.1
Nitroso-benzene												
$(E_{\frac{1}{2}})_I$ (V *vs.* S.C.E.)	−0.63	−0.70	−0.82	−0.06	−0.08	−0.10	−0.12	−0.14	−0.10	−0.10	−0.10	—
$(E_{\frac{1}{2}})_{II}$ (V *vs.* S.C.E.)	—	—	—	—	−0.36	−0.94	−1.0	−1.1	−1.1	−1.1	−0.70	−0.70

Subscripts I and II refer to second and third steps, respectively.

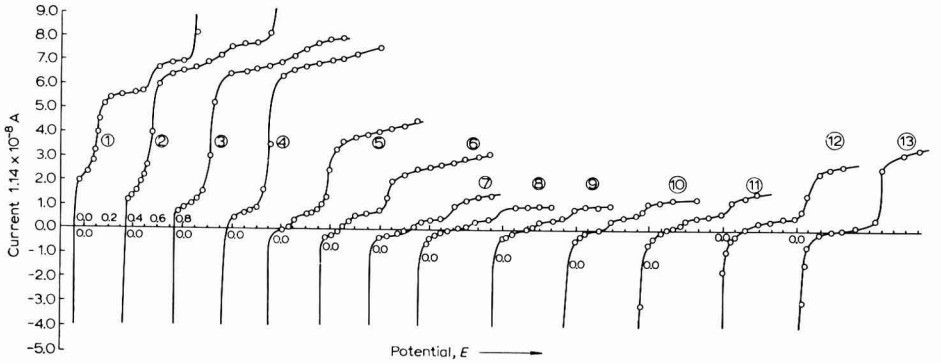

Fig. 1. Polarograms of complex at different pH-values: (1), 1.15; (2), 2; (3), 3; (4), 4; (5), 5; (6), 6; (7), 6.6; (8), 8.3; (9), 8.85; (10), 9.5; (11), 10.6; (12), 11.0; (13), 12.4.
0.0 is the origin for each curve.

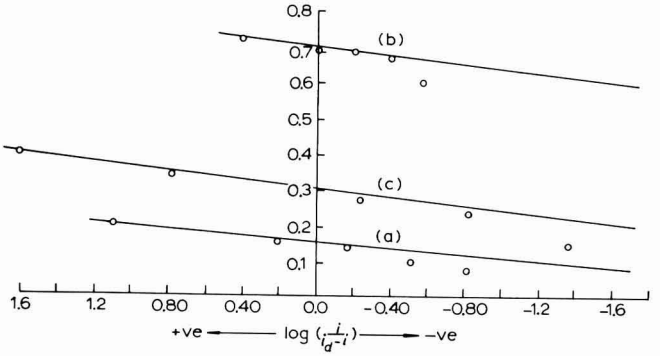

Fig. 2. Plots of log $(i/i_d - i)$ *vs.* E: (a), pH 2 for 1st wave; (b), pH 2 for 2nd wave; (c), pH 4.

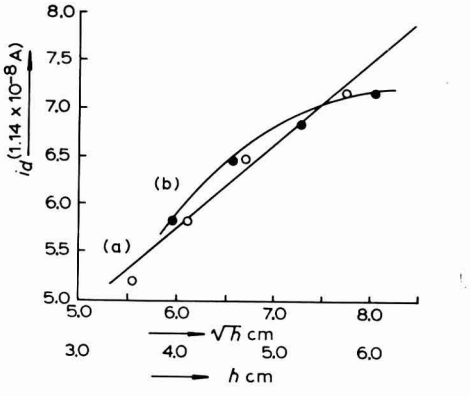

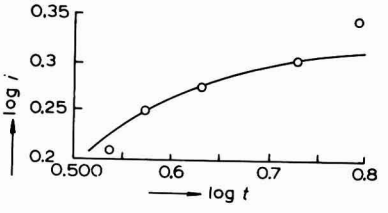

Fig. 3. (a), Plot of i_d *vs.* $\sqrt{h}$; (b), plot of i_d *vs.* h.

Fig. 4. Plot of log i *vs.* log t for the complex at pH 4.

Results and discussion

The reduction of the nitrosobenzene complex of potassium aquopentacyano iron(II) is dependent on the pH of the medium. Three pH-regions can be distinguished:

(i) From pH 1.0–4.0, reduction takes place in three waves. The first, rising directly from the dissolution of mercury decreases, as does the third most negative wave, whereas the second increases. The total wave-height remains practically constant (Fig. 1, curves 1–4). The half-wave potential of the second wave was shifted from −0.10 V at pH 1.15 to −0.30 V at pH 4, whereas that of the third wave was shifted from −0.56 V at pH 1.15 to −0.83 V at pH 3.0.

(ii) At pH > 5, the height of the second wave decreases (Fig. 1, curves 5–10). Another more positive wave appears (at −0.06 V at pH 5.0), the height of which is practically pH-independent.

(iii) At pH > 10.6, the height of the second wave increases again. The half-wave potential, −0.7 V, is identical with that of free nitrosobenzene (Fig. 1, curves 11–13). The results are summarised in Table 1.

In the pH-range 1–4, the polarographic behaviour of the complex is quite different from that of nitrosobenzene; the complex is reduced at a more negative potential than nitrosobenzene (Table 1). Logarithmic analysis[6] of the second and third waves at pH 2.0 is linear (Fig. 2), but since the height of the second wave diminishes with increase in pH, without changing the total height, it appears that some kinetic factor is involved in the pH-range 1–3.

The simplest curve is observed at pH 4.0 where the limiting current of the single wave observed is diffusion-controlled as verified by the effect of mercury pressure (Fig. 3). Also, the plot of log i against log t (Fig. 4) provides evidence for a diffusion-controlled, two-electron transfer process. The wave-height is also a linear function of the concentration of the complex.

The waves obtained with mixtures containing a fixed amount of the aquopentacyano iron(II) and varying amounts of nitrosobenzene and those for mixtures prepared in the reverse order, have i_d-values that increase with increase in the concentration of reactants (nitrosobenzene or aquopentacyano iron(II)); but the values become constant at a combining ratio of 1:1.

The following scheme for the formation and subsequent reduction of the violet complex is suggested:

$$(Fe^{II}(CN)_5H_2O) + C_6H_5NO = (Fe^{II}(CN)_5C_6H_5NO) + H_2O$$

$$(Fe^{II}(CN)_5C_6H_5NO) + 2\,H^+ + 2\,e = (Fe^{II}(CN)_5C_6H_5NHOH) \quad \text{2nd wave}$$

$$(Fe^{II}(CN)_5C_6H_5NHOH) + 2\,H^+ + 2\,e = (Fe^{II}(CN)_5C_6H_5NH_2) \quad \text{3rd wave}$$

This scheme is in agreement with the reported polarographic reduction of nitrosobenzene[7] and N-phenylhydroxylamine[7] in this pH-range.

From the data obtained in the alkaline pH-range, it may be concluded that the complex starts decomposing beyond pH 6.0 and becomes quite unstable at pH 11.0.

Chemical Laboratories,
University of Roorkee,
Roorkee (India)

WAHID U. MALIK
HARI OM

1 T. PINTER, *Chem. Zentr.*, 1 (1941) 1708.
2 S. AŠPERGER, I. MURATI AND O. ČUPAHIN, *J. Chem. Soc.*, (1953) 1041.
3 S. AŠPERGER, I. MURATI AND O. ČUPAHIN, *Acta Pharm., Jugoslav.*, 3 (1953) 20.
4 G. H. COLEMAN, C. M. MCCLOSKEY AND F. A. STUART, *Org. Syn.*, 25 (1945) 80.
5 W. U. MALIK AND H. OM, *Indian J. Appl. Chem.*, in press.
6 J. TOMES, *Collection Czech. Chem. Commun.*, 9 (1937) 12.
7 J. W. SMITH AND J. G. WALLER, *Trans. Faraday Soc.*, 46 (1950) 290.

Received November 20th, 1964; revised August 8th, 1965

J. Electroanal. Chem., 11 (1966) 467–471

ERRATA

K. F. BLURTON AND A. C. RIDDIFORD, Shapes of Practical Rotating Disc Electrodes, *J. Electroanal. Chem.*, 10 (1965) 457–464.

Table I, last column should be headed: $i_{LIM(obs.)}/i_{LIM(calc.)}$.

B. LOVREČEK AND D. CIPRIŠ, Electrochemical studies of quinoline and isoquinoline, *J. Electroanal. Chem.*, 11 (1965) 44–53.

The equation on p. 51 should read: $\frac{c}{c_{\theta=0.5}} = \frac{\theta}{1-\theta} \exp\left[\alpha(1-2\theta)\right]$

J. Electroanal. Chem., 11 (1966) 471

BOOK REVIEW

Electrons and Chemical Bond by HARRY B. GRAY, W. A. Benjamin, Inc., New York and Amsterdam, 1964, xvi + 224 pages, $8.80 ($4.35 paper-back).

This book, based on lectures given by the author to undergraduates at Columbia, is concerned mainly with the application of the molecular orbital theory to the description of certain families of molecules. This is done without the use of formal group-theoretical methods. Diatomic, linear triatomic, trigonal planar, tetrahedral, trigonal pyramidal and angular triatomic molecules are discussed, a chapter being devoted to each type. In addition, there is a chapter on organic molecules and one on transition-metal complexes.

The author discusses the relative molecular orbital energies in the various molecules more thoroughly than has been done in most text books up to date. He has also related the molecular orbital description to published experimental data on bond-dissociation energies, bond lengths, dipole movements and bond angles, where relevant. A brief comparison with the valence bond approach is included for each type of molecule.

The first chapter contains a short historical introduction to the theory of atomic structure, beginning with the Bohr theory. It comprises seventeen sections, examples being one on the properties of the hydrogen atomic wave functions and another on the method of calculating the Russell–Saunders terms. Most chapters contain problems with worked-out solutions.

The last chapter in the book contains a molecular orbital description of some tetrahedral, square planar and octahedral transition-metal complexes. The relationship of the molecular orbital treatment to the valence bond and crystal field theories is discussed. There is also a very brief but useful section on the electronic spectra of octahedral complexes and in this, group-theoretical symbols are introduced but without any detailed explanation of their origin.

This is a very readable book, written in clear English and in a good literary style apart from the occasional split infinitive. There are numerous diagrams illustrating both the shapes and the symmetries of the various molecular orbitals and their relative energies. An attempt has been made to convey the three-dimensional nature of the boundary surfaces of the atomic and molecular orbitals by the use of small dots and there is a note of warning in the preface that the drawings are not intended to be charge-cloud pictures. It might possibly have been better either to use a different method of representing these three-dimensional figures or to have attempted to make them represent an approximate electronic charge density. The procedure that has been adopted can at times be confusing, particularly since overlap appears to have been indicated by addition of the dot densities.

This book would be useful as a supplementary text to an undergraduate course in inorganic chemistry.

K. W. DUNNING, Department of Inorganic Chemistry, University of Bristol

JOURNAL OF ELECTROANALYTICAL CHEMISTRY, VOL. 11 (1966)

AUTHOR INDEX

JOURNAL OF ELECTROANALYTICAL CHEMISTRY, VOL. 11 (1966)

SUBJECT INDEX

CONTENTS

SPOT TESTS IN ORGANIC ANALYSIS

Seventh English Edition, completely revised and enlarged

by FRITZ FEIGL in collaboration with VINZENZ ANGER

6 x 9″, xxiii + 772 pages, 18 tables, over 2000 lit.refs., 1966, Dfl. 85.00, £8.10.0, $30.00

This 7th edition has involved complete revision and reorganisation of the subject in order to present a still clearer picture of the multitudinous applications open to organic spot test analysis. The amount of new work which is appearing has certainly necessitated expansion, but the author has kept this to a minimum by omitting the chapter on spot test techniques (which are covered in the companion volume *Spot Tests in Inorganic Analysis*) and by limiting the number of tables and structural formulae.
Comparison with the 6th edition reveals the following differences:

	Number in 6th Edn.	7th Edn.
Preliminary tests	32	45
Functional group tests	70	109
Individual compound tests	133	148
Detection of particular structures and types of compounds	0	74
Differentiation of isomers etc.	0	54
Applications in the testing of materials etc.	111	131

In total the book now gives in 561 sections information on more than 900 tests compared with 600 tests in 346 sections in the preceding edition.

An important feature is the inclusion of a large number of recently developed tests and comments which have not hitherto been published in any form.

It is the author's hope that this work will help to correct the widespread impression that physical instrumentation is always superior to chemical methods for solving analytical problems. Each of the chapters presents instances of problems for which no solutions by physical means have yet been developed, or for which the rapid spot tests are equal or superior to the expensive instrumental procedure.

CONTENTS: 1. Development, present state and prospects of organic spot test analysis. 2. Preliminary (exploratory) tests. 3. Detection of characteristic functional groups in organic compounds. 4. Detection of structures and certain types of organic compounds. 5. Identification of individual organic compounds. 6. Application of spot tests in the differentiation of isomers and homologous compounds. Determination of constitutions. 7. Application of spot reactions in the testing of materials, examinations of purity, characterization of pharmaceutical products, etc... Appendix: Individual compounds and products examined. Author index. Subject index.

FROM REVIEWS OF THE SIXTH EDITION

... This new book, like its author, is unquestionably a giant on the analytical scene...
Journal of the Royal Institute of Chemistry

... Die Tatsache, dass Feigls klassisch gewordenes Werk, welches überall mit Begeisterung aufgenommen wurde, bereits in 6. Auflage erscheint, ist an sich Empfehlung genug... Es ist also eine wahre Fundgrube für neue Experimentaluntersuchungen...
Chimia

... Even in these days of physical instrumentation there is ample room for the techniques described in this book which were originated and largely developed by Prof. Feigl. They are mostly very quick and very economical on materials. They sometimes present solutions to problems so far insoluble by expensive physical methods...
Laboratory Practice

ELSEVIER PUBLISHING COMPANY
AMSTERDAM LONDON NEW YORK